132755

GENERAL ELECTRIC

GENERAL ELECTRIC COMPANY
CORPORATE RESEARCH AND DEVELOPMENT
Schenectady, N.Y.

FINAL REPORT ON PHASE 3

ATS RANGING AND POSITION FIXING EXPERIMENT

19 March 1971 - 1 December 1972

Contract No.: NAS5-11634

Prepared by

GENERAL ELECTRIC COMPANY
Corporate Research and Development
Schenectady, New York

for

Goddard Space Flight Center
Greenbelt, Maryland

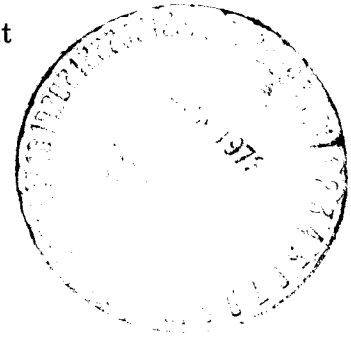

SRD-73-062

114 pg

FINAL REPORT ON PHASE 3
ATS RANGING AND POSITION FIXING EXPERIMENT

19 March 1971 - 1 December 1972

Contract No.: NAS5-11634

Goddard Space Flight Center

Contracting Officer: C. W. Trotter
Technical Monitor: C. N. Smith

Prepared by

GENERAL ELECTRIC COMPANY
Corporate Research and Development
Schenectady, New York

Project Manager: Roy E. Anderson

for

Goddard Space Flight Center
Greenbelt, Maryland

TABLE OF CONTENTS

1.0	INTRODUCTION AND SUMMARY	1-1
2.0	OBJECTIVES	2-1
3.0	EQUIPMENT DEVELOPMENT	3-1
3.1	Factors Affecting Choice of Ranging Parameters	3-1
3.2	Tone-Code Ranging Techniques	3-4
3.3	ATS-5 L-band Signal Characteristics	3-6
3.4	Analysis of L-band Ranging Precision	3-10
3.5	L-band/VHF Transponder Arrangement	3-12
3.6	L-band 300 Watt Solid-State Power Amplifier	3-16
3.7	L-band Receiver	3-24
4.0	EXPERIMENTAL PROCEDURES	4-1
5.0	EXPERIMENTAL RESULTS	5-1
5.1	Data Recording Format	5-1
5.2	Comparison of VHF and L-band Range Measurement Standard Deviations	5-8
5.3	L-band Standard Deviations	5-10
5.4	VHF Standard Deviations	5-16
5.5	Twenty-four Hour Position Fixing Experiment	5-18
5.6	Ionosphere Effects at VHF	5-24
5.7	Satellite Location Experiment	5-41
6.0	CONCLUSIONS	6-1
7.0	RECOMMENDATIONS	7-1
8.0	NEW TECHNOLOGY; PUBLICATIONS	8-1

APPENDIX I: MEMORANDUM - TONE-CODE RANGING PRECISION

LIST OF FIGURES

1.	Tone-Code Ranging Waveform	3-5
2.	Basic Tone-Code Transponder	3-5
3.	Recording of the Beacon Signal Transmitted from the Satellite	3-7
4.	Major Components of L-band/VHF Transponder	3-13
5.	Block Diagram - L-band Portion of the Transponder	3-15
6.	Amplifier Assembly - Front View	3-18
7.	Amplifier Assembly - Side View	3-19
8.	Amplifier Assembly - Internal Front View	3-20
9.	Completed Module; Typical Gain and Match Characteristics	3-21
10.	300 Watt CW L-band Transmitter Block Diagram	3-23
11.	L-band Receiver Block Diagram	3-26
12.	Radio-Optical Observatory	4-2
13.	Equipment Configuration for Experiment	4-3
14.	L-band Signal Return from Spinning ATS-5 Satellite	4-4
15.	Reproduction of the Code as Received from the Satellite and Demodulated	4-6
16.	Format of Data Recorded on Punched Tape	4-7
17.	L-band Range Measurements - 24 August 1972	4-8
18-23.	Histograms of Standard Deviation	5-2 - 5-7
24.	Print-out of Raw Data	5-11
25.	L-band Tone-Code Range Measurement Distribution	5-13
26.	Sample of a Punched Tape Record	5-14
27.	L-band Range Measurement Scatter	5-15
28.	Slant Range and Latitude Precision Versus Power Transmitted from Kings Point	5-17
29.	All the Two Satellite Fixes Made in Twenty-four Hour Test	5-21

30. Diurnal Pattern of Fix Errors 5-22

31. Cause of Diurnal Change in Difference Between Computed and Measured Slant Ranges 5-23

32. Estimated Errors in Slant Range Vectors Due to Satellite Prediction Errors and Estimated Equipment Delay Bias Errors 5-25

33. POSFIX Model Ionosphere Versus Actual on Two Days, Approximately 2 1/2 Years Apart 5-27

34. Difference in Fixes - Actual Ionosphere Versus Model 5-29

35. Scatter of Position Fixes 5-30

36. Scatter of Position Fixes 5-31

37. Comparison of Differences, Measured Minus Computed Slant Ranges at VHF, ATS-3 to Each Transponder 5-33

38. Comparison of Differences, Measured Minus Computed Slant Ranges at VHF, ATS-3 to Transponder at Buenos Aires 5-34

39. Comparison of Differences, Measured Minus Computed Slant Ranges at VHF, ATS-3 to Transponder at Shannon 5-35

40. Comparison of Differences, Measured Minus Computed Slant Ranges at VHF, ATS-3 to Transponder at Reykjavik 5-36

41. Comparison of Differences, Measured Minus Computed Slant Ranges at VHF, ATS-3 to Transponder at Seattle 5-37

42. Comparison of Differences, Measured Minus Computed Slant Ranges at VHF, ATS-3 to L-band/VHF Transponder at Schenectady 5-38

43. Comparison of Differences, Measured Minus Computed Slant Ranges at VHF, ATS-3 to VHF Transponder at Schenectady 5-39

44. Comparison of Differences, Measured Minus Computed Slant Ranges at VHF, ATS-3 to Transponder at Kings Point 5-40

45. Plot of Difference (Two-Way Range, μs) Between Calculated Range and Actual Measured Range - Buenos Aires 5-42

46. Plot of Difference (Two-Way Range, μs) Between Calculated Range and Actual Measured Range - Shannon 5-43

47. Plot of Difference (Two-Way Range, μs) Between Calculated Range and Actual Measured Range - Reykjavik 5-44

48. Plot of Difference (Two-Way Range, μs) Between Calculated Range and Actual Measured Range - Seattle 5-45

49. Plot of Difference (Two-Way Range, μs) Between Calculated Range and Actual Measured Range - Schenectady 5-46

50-53. Satellite Position as Determined by Computation from GE Measurements Using Various Triads of Transponders 5-47 - 5-50

54. Differences - NASA and GE Satellite Locations 5-51

LIST OF TABLES

1.	Theoretical and Measured Precision (L-band)	1-2
2.	Ranging Parameter Selection	3-3
3.	Power Budget	3-9
4.	Theoretical Ranging Resolution at L-band	3-11
5.	300 Watt CW L-band Transmitter	3-16
6.	Junction Temperature for Various Power Outputs	3-17
7.	L-band Receiver Component Descriptions	3-25
8.	Standard Deviations, μs, ~101 Sequential Responses	5-9
9.	Theoretical and Measured Precision	5-10
10.	Summary of Twenty-four Hour Test Results	5-19

ACKNOWLEDGEMENTS

The support and cooperation of the National Aeronautics and Space Administration in making possible the experiments described in this report are gratefully acknowledged. In particular, Mr. Charles N. Smith, NASA Technical Monitor, and his colleagues were especially helpful in the program guidance and coordination. The experimental time on the ATS-3 and ATS-5 satellites was provided by NASA's ATS Operations and Control organization whose assistance and cooperation were extremely valued.

We must also express our appreciation to the domestic and overseas organizations which have graciously acted as hosts for the remote transponders in the General Electric Company experimental network. The host organizations housed and activated the transponders so that ranging data could be recorded for synoptic propagation analyses, and so that satellite location techniques could be demonstrated. These organizations are:

Organization:	Transponder Location:
Argentina Air Force	Buenos Aires, Argentina
Boeing Company	Seattle, Washington
Iceland Civil Aviation Administration	Reykjavik, Iceland
Irish Department of Posts & Telegraphs	Shannon, Ireland
US Merchant Marine Academy, National Maritime Research Center	Kings Point, New York

In addition, we wish to acknowledge the interest and support of General Electric's Heavy Military Electronic Systems Department, Syracuse, New York which designed and built the L-band solid-state power amplifier for the transponder.

SECTION 1

INTRODUCTION AND SUMMARY

The National Aeronautics and Space Administration has sponsored a series of experiments by the General Electric Company to test the use of satellites in aeronautical and marine applications. The Applications Technology Satellites have been used by General Electric since 1968 to test the concept of position location by range measurements from pairs of satellites, to measure the factors that affect position fix accuracy, including the propagation delays in the ionosphere, and to test the reliability of voice and digital communications between ground terminals and mobile craft. The work during the first two phases was restricted to the use of the VHF transponders on ATS-1 and ATS-3. The work is described in the report entitled "Final Report on Phases 1 and 2 - VHF Ranging and Position Fixing Experiments Using ATS Satellites". This report covers the third phase of the series of experiments.

Phase 3 extended the work to L-band using the ATS-5 satellite. An automatic tone-code ranging transponder was designed, constructed, and used to compare ranging measurements and communications reliability at VHF and L-band, and to measure the performance of the tone-code technique at L-band. A contribution to practical implementation of L-band was made by the development of a solid-state RF power amplifier and receiver. The transponder is equipped for voice communications through the VHF satellite. Voice transmissions, like the tone-code signals, employ narrow band frequency modulation.

The L-band/VHF automatic transponder was used in experiments with the ATS-5 and ATS-3 satellites in January and early February and from June through November of 1972. The L-band receiver of the ATS-5 satellite did not function between February and June 1972.

The transponder was located at General Electric's Radio-Optical Observatory during the test period. Tone-code interrogations were transmitted at VHF from the Observatory through the ATS-3 satellite and back to the transponder. The transponder responded on VHF through ATS-3 and on L-band through ATS-5.

Other VHF-only transponders of the General Electric widespread network were also interrogated and responded to collect data for synoptic observations of ionosphere delay and for locating the ATS-3 satellite by trilateration. The transponders of the network are located at Shannon, Ireland; Reykjavik, Iceland; Kings Point, New York; Seattle, Washington; and Buenos Aires, Argentina.

Results of the ranging experiments confirmed that ranging resolution measured in tens or hundreds of feet may be achieved at VHF and L-band within the radio frequency bandwidths used for communications with simple, inexpensive, automatic equipment. The ranging signals can be compatible with communications and the range measurements can be accomplished in a time that is negligibly short compared to the signal durations used for communications.

The comparison of VHF and L-band ranging was impaired by the necessity for ranging through two separate satellites whose positions could not be known exactly. Uncertainty in the satellite positions was larger than the differential delays due to propagation effects in the ionosphere, and therefore range errors due to propagation delay in the ionosphere could not be completely separated from apparent range errors due to satellite position prediction uncertainty. A comparison of the diurnal changes in propagation delay through the ionosphere was obtained by ranging continuously at both frequencies throughout a twenty-four hour period.

Better techniques for locating the satellites will be available in the future and the transponder will be available for making better comparisons of VHF and L-band propagation delays.

One method of locating the satellites accurately was tested in a parallel General Electric funded experiment using a widespread network of VHF tone-code ranging transponders. The experiment is described in this report. It is anticipated that the ATS-F satellite will be located accurately by several means so that the L-band transponder on that satellite will be useful for propagation studies using the L-band/VHF transponder developed under this program.

Standard deviations for sets of 101 measurements were determined by computing a "best fit" quadratic curve to the set of measurements, then computing the standard deviations with respect to the best fit curve. Measured precision at L-band was compared with the theoretical precision for the ranging parameters that were used. The results, as a function of signal-to-noise ratio in the 60 kHz RF bandwidth are as follows:

TABLE 1

THEORETICAL AND MEASURED PRECISION (L-BAND)

Theoretical Precision		Measured Precision	
S/N	1 Sigma Precision	S+N / N	1 Sigma Precision
6 dB	.092 μs	6.0 dB	.24 μs
10 dB	.056 μs	11.0 dB	.14 μs
15 dB	.032 μs	14.5 dB	.10 μs

where 0.1 μs represents 50 feet ranging precision in two-way ranging.

Standard deviations were found to improve as the square root of the increase in integration time during the phase matching process. The integration time was increased by averaging ten or 100 measurements, and computing the standard deviations of the averaged values. L-band standard deviations for ten measurement averages was approximately 0.03 μs, representing a precision of ~15 feet in two-way ranging.

Standard deviations of the VHF measurements were approximately 0.33 μs for single measurements, and approximately 0.12 μs for ten measurement averages when the signal-plus-noise-to-noise ratio was 10-13 dB. The 3 dB range was due to spin modulation on ATS-3.

An important contribution to the use of satellites by aircraft and ships was the development of the solid-state L-band power amplifier by General Electric. An engineering prototype of the amplifier was constructed as part of the Phase 3 experimental program. The amplifier offers high reliability. It was used throughout the L-band experiments. It offers a graceful degradation; should some modular components of the amplifier fail, the power would be reduced in proportion to the number of the components. The output of the amplifier is conservatively rated at 300 Watts and its DC to RF efficiency is approximately 35%. It is potentially lower in cost than tube type amplifiers and versions for ship and aircraft use can be small in size and light in weight.

A 60 Watt version of the amplifier was constructed under a separate program as a prototype for spacecraft use. The DC to RF efficiency of the amplifier was greater than 40% and its three pound weight, 1/2 x 12 x 7 inch dimensions, reliable design, and rugged construction make it attractive for spacecraft applications.

Phase 3 of the Ranging and Position Fixing Experiments has resulted in the development of a unique instrument for ionospheric propagation measurements and for the comparison of ranging and position fixing experiments at VHF and L-band as well as for the development of techniques for the applications of satellites to communications, position surveillance and navigation.

SECTION 2

OBJECTIVES

The objectives of Phase 3 were:

- To build an automatic tone-code ranging transponder that receives a tone-code interrogation at VHF and responds coherently at VHF and L-band. An interrogation with one user code will cause the transponder to respond a single time simultaneously at VHF and L-band. The ranging tones at both frequencies are derived from a single oscillator and are therefore coherent. The duration of the response at L-band shall be shorter than the 50 ms period when the ATS-5 antenna is pointed toward the earth during each 780 ms spin period of the satellite. An interrogation with a different user code will cause the transponder to respond 100 times simultaneously at VHF and L-band. The responses shall be adjustable in timing and in rate so that they can match the spin period of ATS-5 and be timed to arrive at the satellite when the antenna is pointed at the earth.

- Measure propagation effects at VHF and L-band for a direct comparison of the effects on ranging precision and accuracy. Simultaneous ranging measurements at VHF through the ATS-3 satellite and at L-band through the ATS-5 satellite will be made on a number of different days and at frequent intervals through a 24 hour period. Standard deviations of the measurements will be computed for comparison of ranging resolutions at VHF and L-band. Measured changes in range through the 24 hour period will be examined to determine the difference in the diurnal propagation delays at VHF and L-band. It is recognized that the validity of the comparison may be affected by uncertainty in the knowledge of the satellite locations.

- Determine relative reliability of the communication links. Observations will be made of signal-to-noise ratios, day-to-day variability and signal characteristics. Limited observations will be made of the digital error rates in the address code received at the two frequencies. The relative performance reliability of the VHF and the L-band equipments will be observed.

- Build and test an L-band solid-state power amplifier. A 300 Watt all solid-state L-band power amplifier will be developed and incorporated as a part of the VHF/L-band transponder. Its performance characteristics will be measured during the data collection portion of Phase 3. The amplifier will be operated a sufficient number of hours to provide an indication of its reliability.

- Build and test an L-band receiver. An all solid-state L-band receiver will be designed and built to provide a complete independent L-band capability in addition to the complete independent VHF capability of the transponder. Essential characteristics of the receiver will be measured and recorded.

SECTION 3

EQUIPMENT DEVELOPMENT

3.1 Factors Affecting Choice of Ranging Parameters

Tests during Phases 1 and 2 of the contract indicated that the tone-code ranging technique meets commercial surveillance needs. Development of the technique was continued through Phase 3. The ranging parameters of Phases 1 and 2 at VHF were retained. The basic equipment designs were also retained except for improvement in the phase matching technique.

Ranging parameters at L-band were selected to yield high range resolution and thus take advantage of the smaller ionosphere delay at that band. The L-band parameters provide digital data rates that may be adequate for digital voice, and for high digital data rates but with an option for lower data rates. They allow the use of techniques that may provide secure transmission for message privacy.

Equipment developments at L-band were aimed towards improvement in the critical area of L-band power generation. An important objective was the achievement of high reliability at a cost acceptable for commercial applications.

The tests through Phase 3 continued to confirm that the tone-code ranging technique has the following characteristics:

- Useful accuracy can be achieved within the modulation and radio frequency bandwidths of present-day mobile communications.

- The technique can be used with wide bandwidth for high accuracy.

- It requires only one channel for range measurement, receiving and transmitting in the simplex mode if desired without need for an antenna diplexer.

- The time required for a range measurement is a fraction of a second so that it can time-share a communication channel with little additional time usage of the channel.

- It can be implemented by the addition of an inexpensive, solid-state responder unit attached to a communication receiver-transmitter.

- It can, but need not, employ digital or digitized voice transmissions to provide synchronizing of the user responder, thereby further increasing the efficiency of channel usage.

- There are no "lane" ambiguities in the range measurements.

- User identification is simple and is confirmed in the return signal.

One of the uses of the VHF/L-band tone-code ranging transponder is the comparison of propagation characteristics in the two radio frequency bands. The choice of signalling parameters and the design of the equipment must be such that the range measurement resolution is adequate to resolve the variability in the propagation characteristics.

The signalling parameters that were used at VHF through Phases 1 and 2 of the contract were adequate for measuring propagation characteristics at VHF. The same VHF signalling parameters were retained in the new transponder. An improvement in the design of the phase matching circuit was incorporated.

Signalling parameters at L-band were selected with two objectives: first, to insure that the bandwidth would be adequate to resolve the small changes in propagation delay expected at L-band; and second, to test signalling parameters that might be optimum for a narrow bandwidth L-band communications and position fixing system.

The ATS-5 satellite is capable of relaying signals to the earth for only about 50 ms each 780 ms because of its spin and the directivity of its L-band antenna. The useful duration of the "window" depends on signal-to-noise ratio. The period between the times when the received signal is -3 dB below the maximum received signal is 50 ms. This characteristic of the satellite did not affect the choice of the tone-code ranging signal parameters because the recommended duration of a tone-code signal is approximately 30 ms. As a consequence, the spinning of the ATS-5 satellite was not a basic handicap to the test of the tone-code ranging system at L-band. The spin does place a restriction on the timing of the interrogations and it was necessary to synchronize the interrogation rates to the spin rate of the satellite thus requiring inclusion of some timing circuits in the transponder that would not be necessary if the satellite were not spinning. The spinning also modified the method for evaluation of longer interrogation times. Rather than transmit and average the phase measurement over a long continuous tone signal, it was necessary to average a series of shorter measurements. Both techniques would produce the same result. Therefore, the measurements were not handicapped by the spin of the satellite. Table 2 summarizes the signalling parameters selected at VHF and L-band.

The VHF signalling parameters are compatible with all of the other tone-code ranging transponders in the General Electric network, and with those used on aircraft, ships, a buoy, and a land mobile vehicle, as described in the final report on Phases 1 and 2. The VHF/L-band transponder can thus be integrated into the network and used with the other transponders for synoptic measurements of ionospheric propagation characteristics. It is different from the other transponders in that it can respond in two modes. An interrogation with user code 11 initiates a single response like the other transponders, but interrogation with user code 12 causes it to respond 101 times. The VHF phase matcher has an improved design, fully compatible with the other transponders.

TABLE 2

RANGING PARAMETER SELECTION

	VHF	L-BAND
TONE FREQUENCY	2.4414 kHz	9.7656 kHz
NUMBER OF TONE CYCLES IN PHASE MEASUREMENT	256	256
TONE DURATION FOR PHASE MEASUREMENT	~ 105 ms	~ 26 ms
NUMBER OF BITS IN ADDRESS CODE	30	30
FORMATION OF DIGITAL "1"	Transmission of One Tone Cycle	Transmission of One Tone Cycle
FORMATION OF DIGITAL "0"	Suppression of One Tone Cycle	Suppression of One Tone Cycle
DURATION OF ADDRESS CODE	~ 12 ms	~ 3 ms
MODULATION	Narrow-band Frequency Modulation ± 5 kHz	Narrow-band Frequency Modulation ± 20 kHz
RADIO FREQUENCY BANDWIDTH	15 kHz	60 kHz

3.2 Tone-Code Ranging Techniques

Range measurements from satellites are made by measuring the propagation time of a radio signal from the satellite to a transponder and return. The propagation time can then be converted to a range measurement by relating it to the known propagation velocity of the radio signals. Atmospheric propagation delay is determined by computing the time it would take the signal to travel from the satellite to the transponder at the velocity of light in free space, then subtracting the computed travel time from the measured propagation time. Propagation time is measured by placing a time marker in the form of a "tone-code" interrogation (Figure 1) on the transmitted signal and observing the time for the tone-code to go to the user and return. As used in the experiment, the interrogation signal is a short audio frequency tone followed by a digital address code in which audio cycles are inhibited for zeros, transmitted for ones. Improved performance would result from the use of phase shift keying. The simpler format was chosen early in the experiment for convenience, and was not changed as its performance fulfilled the test requirements.

Each transponder is assigned a unique digital address code. When the propagation time to a transponder is to be determined, the tone burst followed by the transponder address code is transmitted by the Observatory to a geostationary satellite that repeats it. All of the transponders in line-of-sight receive the satellite transmission, but the one that is addressed recognizes the address code automatically, and after a precise delay, retransmits the tone-code. The satellite repeats the signal. The Observatory measures the intervals from the initial transmission to the first repetition by the interrogating satellite and to the time of the transponder signal via the satellite.

The transponder receives the tone cycles from the satellite on its receiver (Figure 2). All of the tone cycles received from the satellite, even though they may be interrogations from other craft, are applied to a phase matching circuit. A locally generated tone of the same frequency is also applied to the phase matcher, which adjusts the phase of the locally generated tone so that it corresponds to the phase of the received tone. The local tone is generated at the same frequency as the ground terminal tone within an accuracy of one part in 10^6 or better, an accuracy achievable from a moderately priced oscillator. The phase matcher accomplishes the phase match by averaging over 256 received cycles in establishing the timing of the locally generated phase. The averaging process improves the timing accuracy by the square root of the number of cycles averaged.

At VHF, the tone is at 2.4414 kHz. It is frequency modulated on a carrier at the uplink frequency of 149.22, 149.245, or 149.195 MHz with an RF bandwidth of 15 kHz. The signal is received from the satellite on 135.6, 135.625, or 135.575 MHz.

The demodulated tone is passed through a tuned circuit of approximately 120 Hz bandwidth before its phase is compared with the locally generated 2.4414 kHz tone. The locally generated tone phase is shifted to match the phase of the received tone.

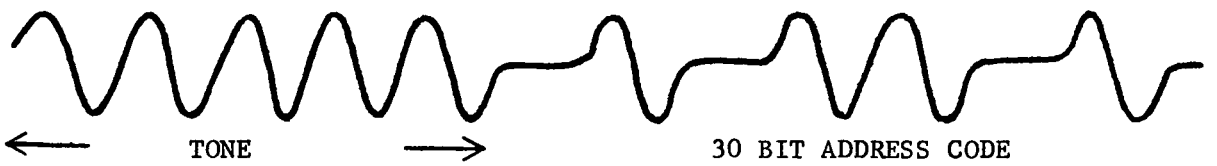

FIGURE 1. TONE-CODE RANGING WAVEFORM

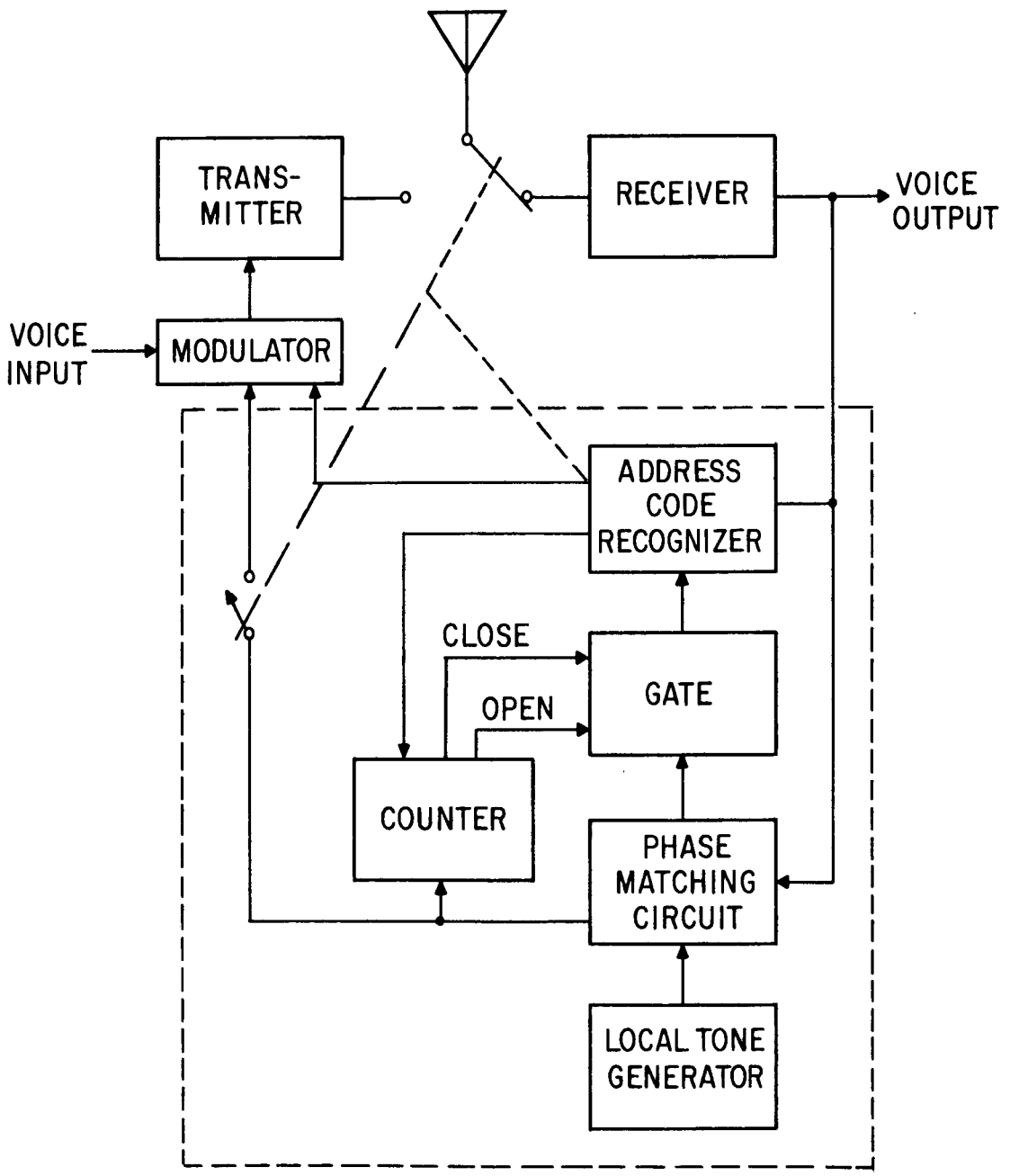

FIGURE 2. BASIC TONE-CODE TRANSPONDER

The locally generated tone is used to generate clock pulses that clock the received interrogation signal into an address code recognizer that consists of a shift register with summing circuits prewired to correspond to the digital address code of the transponder. When the sequence of pulses representing the transponder address code is clocked into the recognizer, it produces a single output clock pulse that opens a gate to interrupt the locally generated pulses that are clocking the shift register. The duration of the interruption is precisely controlled by a pulse counter. During the interval in which the clock pulses are interrupted, the transponder is activated and the antenna is switched from the receiver to the transmitter. When the switching is completed, the locally generated 2.4414 kHz tone is transmitted until the end of the precisely measured interval. Clock pulses are then reapplied to the shift register and the address code is clocked out to key the audio tone to the transmitter and return the address code back through the satellite to the ground station. Introduction of the delay while the antenna is switched eliminates the need for a diplexer in the transponder. It also enables reception and retransmission to occur on the same frequency.

At the Radio-Optical Observatory, the receiver output is applied to an address code recognizer similar to that in the transponder. Prior to the interrogation of an individual transponder, the taps of the summing circuit are switched to correspond to the code of the one that is addressed. When the address code is received from a satellite, a single output clock pulse occurs at the output of the summing circuit.

At L-band, the tone frequency is 9.7656 kHz and frequency modulated on a 1651 MHz carrier with an RF bandwidth of 60 kHz. The signal is received from the satellite on 1550 MHz. The demodulated signal is passed through a 470 Hz bandpass filter. Phase matching and correlation are accomplished in the manner described for the VHF signal to produce the time-of-arrival pulse.

3.3 ATS-5 L-band Signal Characteristics

The ATS-5 satellite was designed to be stabilized so that its L-band antenna would point toward the earth. A malfunction when the satellite was placed in orbit caused it to spin about an axis parallel with the earth's axis at a rate of approximately 77 revolutions per minute. The L-band antenna is fixed to the body of the spacecraft. Its $\sim$ 25 degree wide beam rotates with the satellite like a search light beam so that it points at the earth for approximately 50 ms during each 780 ms rotation period. The satellite is capable of relaying L-band signals only during the time when the antenna beam is pointed toward the earth. The period when it is capable of relaying the signals has been termed the satellite's "window". Figure 3 is a recording of the beacon signal transmitted from the satellite. It shows the antenna pattern as it sweeps past General Electric's Radio-Optical Observatory. The side lobes of the satellite antenna are nominally 15 dB below the peak of the main beam.

The spinning of the satellite resulting in the limitation of its use to the narrow "windows" will not be a characteristic of an operational system. The satellite's receiver bandwidth characteristics and

FIGURE 3. RECORDING OF THE BEACON SIGNAL TRANSMITTED FROM THE SATELLITE

EIRP may not be typical of an operational L-band satellite. These special characteristics of ATS-5 however did not affect the choice of the tone-code ranging parameters. The duration of the signals anticipated for operational systems is short and the capability for operating at low signal-to-noise ratios is such that the tone-code ranging technique could be tested through the ATS-5 satellite without degradation to its special characteristics.

The spin of the satellite made it necessary to provide timing circuits at the Radio-Optical Observatory and on the transponder so that the relay of the tone-code ranging signals is accomplished during the satellite windows. The timing circuits of the platform would not be necessary if the satellite were capable of transmitting signals continuously. The timing circuits of the Observatory are similar to the time sequencing circuits that will be used in polling many users in an operational system.

The L-band transponder of the satellite can operate in narrow band and wide band frequency translation modes. It is operated in the narrow band mode when used with the VHF/L-band transponder. It receives signals in that bandwidth centered at 1550 MHz. The L-band transponder has two traveling wave tubes in its amplifier. Most of the experiments with the VHF/L-band transponder have been in the half power mode using one TWT with 12 Watts RF output. When the satellite transmits with both TWT's in the full power mode its power output is 24 Watts. The peak effective isotropic radiated power (EIRP) is the product of net antenna gain and RF output power, or 190 Watts, 22.8 dBW in the half-power mode, and 380 Watts, 25.8 dBW in the full power mode.

The noise temperature of the satellite receiver system was 32.5 $dB^{o}K$ when the satellite was first placed in orbit. When used in the narrow band frequency translation mode, the receiver noise power at the input to its transponder was -132 dBW. The uplink space loss at 1650 MHz is 188.4 dB. With the satellite net antenna gain of 12.7 dB, the EIRP of a transmitter on the earth would have to be 43.7 dBW in order to equal the receiver noise. A signal approximately 20 dB stronger than the satellite receiver noise input will capture virtually all of the satellite transmitted power. A further increase in received signal power will not increase the output power. The satellite is then said to be saturated.

When the signal into the satellite is much below saturation, the signal relay may be uplink limited. The signal received by the satellite and the satellite's receiver noise add together to become the signal that is transmitted by the satellite. The use of a large ground terminal antenna and a low noise preamplifier will not insure a high signal-to-noise ratio because this is determined at the satellite receiver.

The ATS-5 satellite L-band receiver has had intermittent operation. It may function for a period of months, then suddenly cease to function for a period of months. Tests were made with the VHF transponder in February 1972, shortly before the satellite ceased to function. It became functional again in early June 1972.

Transmission signal parameters were selected to be efficient. Transmitted power at L-band was set between 200 and 300 Watts using the engineering prototype of the solid-state L-band power amplifier. A six foot diameter antenna was selected to permit observations at various signal-to-noise ratios.

Reception of the signal from the satellite at the ground terminal was through a 30 foot antenna. The L-band feed was off-set from prime focus and partially blocked by another feed structure, reducing the gain so that it was approximately that of a 10 foot antenna. During the initial tests in February a transistor preamplifier was used in the Observatory receiver. In later tests starting in June, a parametric amplifier was used. The ground terminal receiving system is representative of proposed ground terminals for aeronautical and maritime use. The signal-to-noise ratio was determined by the up-link. The power budgets are tabulated in Table 3.

TABLE 3

POWER BUDGET

UPLINK:	
Transmitter Power (300 Watts)	54.8 dBm
Antenna Gain - Linear (6' Dish)	24.0 dB
Circuit Loss	-2.0 dB
EIRP	76.8 dBm
Space Loss	-188.4 dB
S/C Antenna Gain	15.0 dB
Circuit Loss	-2.3 dB
Off-beam Loss (Diurnal at 2.5° Inclination)	-3.0 dB max.
Total Received Power	-101.9 dBm
Receiver NPD (32.5 dB°K	-166.1 dBm/Hz
C/NPD	64.2 dB/Hz
C/N in 2.5 MHz Bandwidth	0.2 dB
DOWNLINK:	
S/C Transmitter Power, 1 TWT	40.4 dBm
Antenna Gain	14.0 dB
Circuit Loss	-2.0 dB
Output Power Reduction	-1.8 dB
EIRP	50.6 dBm
Space Loss	-187.8 dB
Observatory Antenna Gain (Assumed - Not Measured)	40.8 dB
Circuit Loss	-1.0 dB
Polarization Loss	-0.2 dB
Off-beam and Pointing Loss	-3.0 dB max.
Total Received Power	-100.6 dBm
Receiver NPD (28.9 dB°K)	-169.7 dBm/Hz
C/NPD (Ground)	69.1 dB/Hz
C/NPD (Satellite)	64.2 dB/Hz
C/NPD (Resultant)	63.0
C/N in 60 kHz Bandwidth	15.0 dB

3.4 Analysis of L-band Ranging Precision

Mr. R. T. Milton of General Electric's Space Division prepared a theoretical analysis of the precision achievable with the tone-code ranging technique. His analysis is presented as Appendix I. He investigated the following topics:

1. The precision attainable with a tone of a given frequency and specified duration when accompanied by noise of a given level. This provides an upper limit on the precision.

2. The precision attainable when the tone-code frequency modulates a carrier. Included are an evaluation of trade-offs of modulation index and tone frequency and the possibilities of FMFB demodulation.

3. PSK modulation with both derived-carrier-synchronous and differential detection.

Milton concluded that phase modulation techniques can give very good range measurement precision when used in the tone-code technique, much better than that possible with FM techniques. Some slight modification of the present circuitry is required because of polarity ambiguity. Also, a somewhat more complicated demodulator, compared to the FM discriminator, is required.

Frequency modulation, a poorer theoretical choice than PSK, was selected for the L-band/VHF transponder to make it compatible with the equipment used in the other transponders and at the Observatory.

For the FM case and the modulation parameters of the L-band/VHF transponder, Equation 11 of Appendix I can be put in more easily interpreted form through the use of the following identities:

QUANTITY	DESIGNATION IN MEMORANDUM	NEW DESIGNATION AND VALUE
Peak Frequency Deviation	ΔF	ΔF = 20 kHz
Carrier-to-Noise Density at IF	$(E_s^2/2)/w(f_s+f_m)$	C/N_o
Tone Duration	T	$T = 30 \times 10^{-3}$ seconds
Standard Deviation of Delay Measurement	σ	σ = to be determined, seconds

Equation 11 of Appendix I can then be rewritten as:

$$\sigma = \frac{1}{2\pi\Delta F[T(C/N_o)]^{1/2}}$$

The value of 20 kHz for ΔF is estimated from a modulating frequency of 10 kHz and a 60 kHz RF bandwidth. The theoretical ranging resolution at L-band is presented in Table 4 for several values of signal-to-noise ratio.

TABLE 4

THEORETICAL RANGING RESOLUTION AT L-BAND

SIGNAL-TO-NOISE	C/N_o IN 60 kHz BANDWIDTH	σ
6 dB	54 dB Hz	0.092 μs
10 dB	58 dB Hz	0.056 μs
15 dB	63 dB Hz	0.032 μs

If the distribution of the measurements were gaussian, as expected when noise is the only cause of the variability in the measurements, 68% of the range measurements would be within ± 1 sigma, 95% within 2 sigma, and 99.7% within 3 sigma.

Time may be converted to range by the factor 984 feet per microsecond, or approximately one foot per nanosecond. The theoretical ranging resolution of single L-band measurements with the L-band/VHF transponder is thus between 32 and 92 feet for signal-to-noise ratios between 15 and 6 dB. Resolution can be improved by the square root of the signal averaging time. Increasing the averaging time by a factor of ten to 0.3 second will improve the range resolution by approximately three times. Averaging one hundred measurements can thus improve resolution by a factor of ten to approximately 3 to 10 feet.

Diurnal changes in ionospheric propagation delay at L-band are expected to be approximately 20 to 50 feet.

Resolution of the L-band measurements is adequate to observe the diurnal changes provided that one hundred measurement averages are used. Accurate measurement of ionospheric propagation delay is accomplished best at VHF, where the effect is one hundred times greater. The L-band measurements can be used to verify the $1/f^2$ relationship of the propagation delay.

3.5 L-band/VHF Transponder Arrangement

The L-band/VHF transponder is designed to receive at L-band or VHF and to respond automatically at either frequency or to respond at both frequencies simultaneously with coherent baseband signals. The arrangement of the transponder is shown in Figure 4. The VHF portion is like the transponders used in the GE network and described in the Final Report on Phases 1 and 2. The L-band portion is similar to the VHF portion, except that L-band employs a higher modulating frequency. The connections to the L-band receiver are shown as dashed lines in Figure 4 because VHF interrogations were used throughout the experimental program. Reception on L-band is an alternative mode that is provided by making connections as shown.

Response of the transponder is initially like that of other tone-code transponders except that it has two address code correlators. The timing circuits were added to adjust the internal delay of the response and to initiate, time, and count one hundred one responses when the transponder is interrogated with one of the two user address codes.

Response delay is adjustable so that the response can arrive at the ATS-5 satellite during its "window". The response rate is adjustable to match the spin rate of ATS-5. Two response rates are available and are separately adjustable, one for the VHF responses and one for the L-band responses, so that the one hundred one responses can be timed separately for spin rates of two different satellites. Response delay and response rates are adjustable with thumbwheel controls.

The functions performed by each tone-code transponder in the GE net work are described below with added comments pertaining to the L-band/VHF transponder.

1. Phase alignment of its own 2.4414 kHz clock with the received 2.4414 kHz signal prior to receiving the address code. The L-band/VHF transponder can also operate on a tone frequency of 9.7656 kHz.

2. Recognition of its user address code. Each transponder contains a shift register prewired for its own address. The L-band/VHF transponder has two correlators, designated user codes 11 and 12.

3. Measuring a precise time delay of 1024 tone cycles duration, 419,430.4 μs. The L-band/VHF transponder delay is adjustable in 25.6 μs steps from 0.4194304 second to 0.6291456 second by thumbwheel controls.

4. At the start of the delay, switching transceiver from the receive mode to the transmit mode.

5. Supplying the properly phased tone modulation signal to the transmitter during the precisely known time delay. In the L-band/VHF transponder 2.4414 kHz is supplied to the VHF transmitter, 9.7656 kHz to the L-band transmitter.

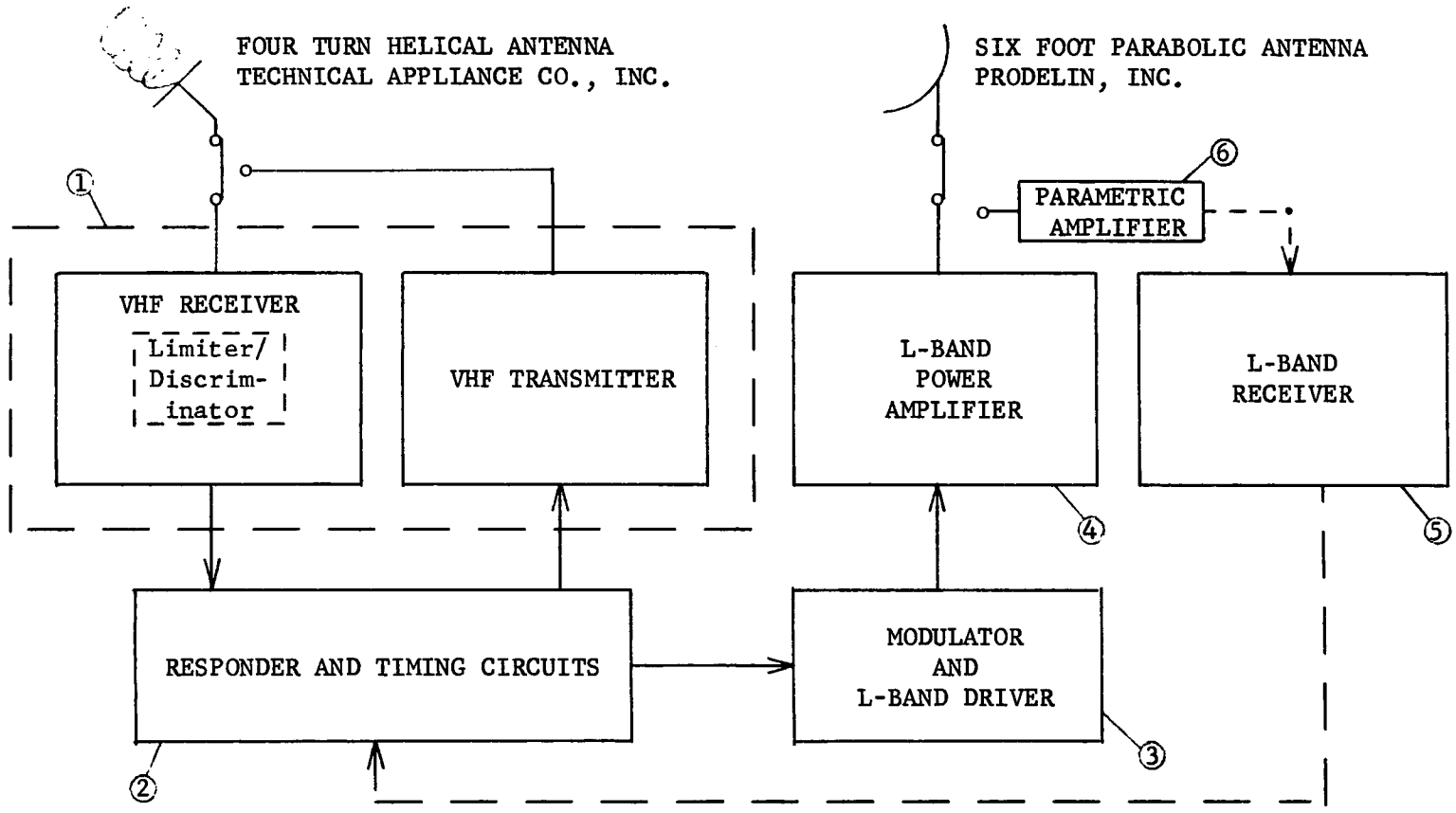

1 - General Electric Mastr Progress Line Base Station DM76LFP55 with Specially Built Balanced Limiter/Discriminator.

2 - Specially Developed Circuits for Platform. Solid-State, Printed Circuit Construction. Physically Located in 1 .

3 - General Electric DM78LAS77 with Applied Research, Inc. Frequency Multiplier.

4 - Specially Developed Solid-State Power Amplifier.

5 - Specially Developed Solid-State Receiver.

6 - S-9821 Sonoma Engineering and Research, Inc.

FIGURE 4. MAJOR COMPONENTS OF L-BAND/VHF TRANSPONDER

6. Transmitting its digital address code starting precisely at the end of the delay.

7. Switching transceiver back to receive mode.

An additional feature of the transponder is a noise inhibit circuit which prevents false correlations on noise during the absence of a received signal. This is achieved by half-wave rectifying, filtering and threshold detecting the output of the narrow band filter. This circuit is designed to respond only to the presence of the continuous synch tone. Once the presence of the tone is detected, the received signal is then allowed to be processed.

Figure 5 is a simplified block diagram of the L-band portion of the transponder. Simplex operation is depicted although duplex could be accomplished by substituting a diplexer for the transmit/receive switch. This is not a requirement for tone-code ranging, however, and results in higher insertion losses. The modular construction provides greater flexibility than an integrated receiver and allows for quick replacement of components if necessary. The receiver is single channel fixed frequency, with provision for changing the received frequency $\pm$ 5 MHz by crystal substitution in the second local oscillator.

The parametric amplifier is centered at 1550 MHz with a 30 MHz bandwidth (3 dB). Fine tuning range is $\approx$ 30 MHz and gain is adjustable from 0 to >25 dB. Total tuning range (internal adjustments) is 1450 to 1750 MHz. The noise temperature is $\approx 100^{\circ}K$ and the unit is weather sealed for ourdoor mounting. Input power is 110V-AC 50-400 Hz at 500 Watts.

The mixer/preamplifier has an rf bandwidth of 1-2 GHz and an IF bandwidth of 16 MHz centered at 30 MHz.

The IF postamplifier has a voltage controlled power gain of 30 to 80 dB and a 10 MHz bandwidth.

The intermediate mixer is a broadband (0.05-200 MHz) double balanced device.

The first LO (local oscillator) is a temperature compensated crystal oscillator with a stability of 1×10^{-6} from 0 to $50^{\circ}C$ and is fixed tuned at 1520 MHz.

The second LO (local oscillator) is a broadband amplifier/crystal oscillator. Stability is 3×10^{-5} and crystal pulling range is $\pm$ 2 kHz. The amplifier range is 20-40 MHz.

The constant phase filter, three stage limiter and discriminator are specially designed and constructed.

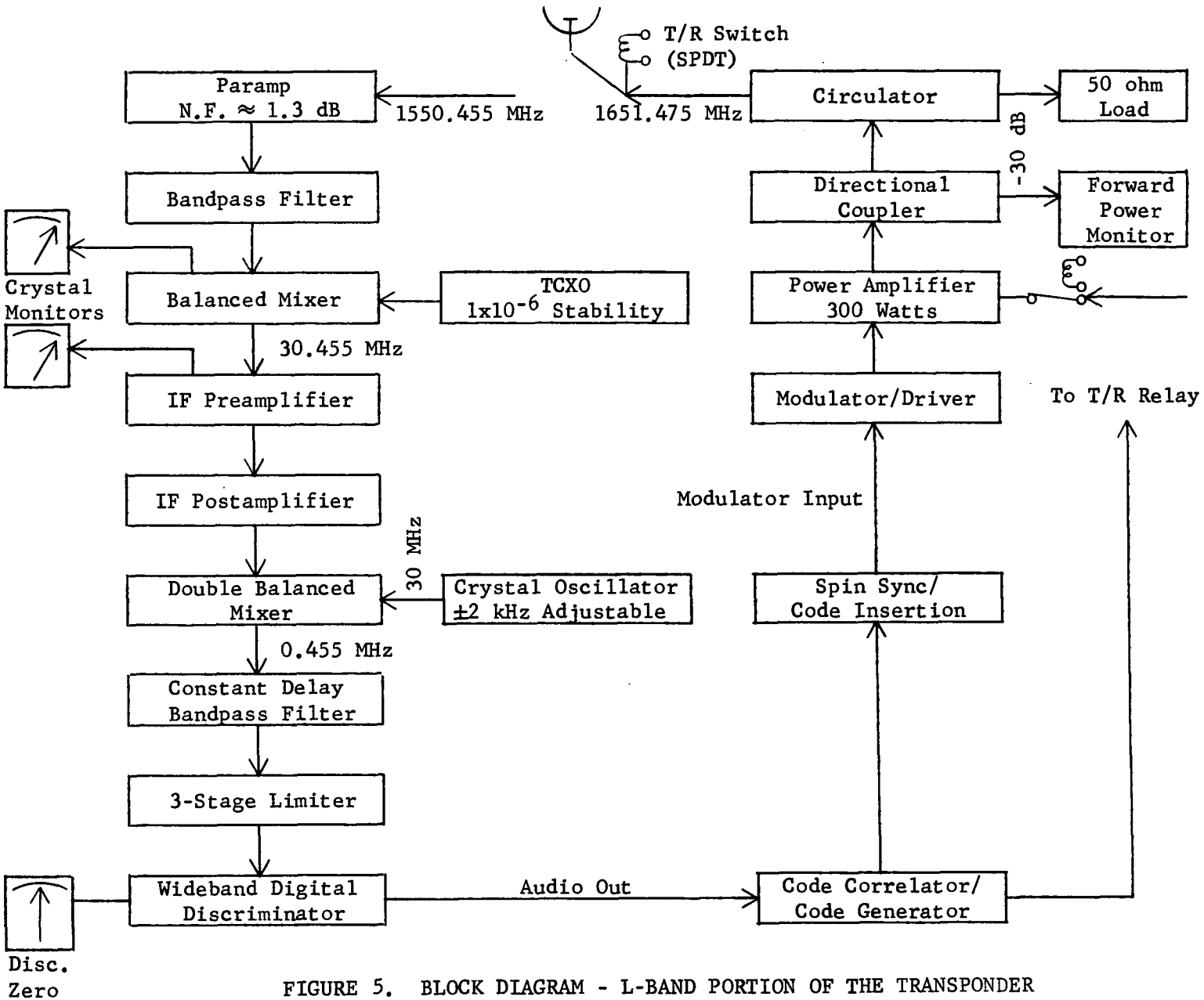

FIGURE 5. BLOCK DIAGRAM - L-BAND PORTION OF THE TRANSPONDER

3.6 L-band 300 Watt Solid-State Power Amplifier

The L-band power amplifier was developed by General Electric's Heavy Military Electronic Systems Products Department at Syracuse, New York. The design of the amplifier was funded in part by Phase 3 of the NASA contract and in part by Heavy Military Electronic Systems Products Department. The amplifier was delivered to the Observatory in January 1972 and used throughout the experimental program, accumulating more than 132 hours of operation.

TABLE 5

300 WATT CW L-BAND TRANSMITTER

P_{out}	300 Watts CW
Frequency	1650 MHz
Bandwidth	~ 50 MHz (1 dB points)
Gain	30 dB Minimum
Efficiency	30% Minimum (DC to RF)
Input VSWR	1.2:1
Load VSWR	Will tolerate short circuit to open circuit
Operating Temperature	40^{o}F to 100^{o}F
Noise Figure	20 dB
19" Rack Mounted	Air Cooled

The 300 Watt solid-state L-band transmitter develops the prescribed gain and power output capability using a total complement of 122 transistors. The individual transistors (conservatively rated at 5 Watts CW output) are initially combined in pairs via -3.01 dB quadratic hybrids. This two transistor module is then combined via series combiners to achieve the required drive level at each interstage and to achieve the final power output.

The quadrature -3.01 dB couplers are fabricated utilizing thin film technology. The required coupling value with good directivity is achieved by connecting two -8.34 dB couplers in tandem.

Higher power levels are achieved by combining appropriate numbers of the dual transistor modules via a series feed/combiner. The series feed/combiner is fabricated utilizing strip transmission line technology.

Protection for the final output stage against inadvertent high VSWR is provided by a circulator. A separate power output monitor port is also provided at -30 dB referenced to the main output.

Figures 6, 7 and 8 are photographs of the overall amplifier assembly.

The basic building block for the overall power amplifier is a module consisting of two transistor amplifiers combined via -3.01 dB quadrature hybrids. The individual amplifiers are capable of 5 Watts CW output at 1.65 GHz. At a supply voltage of 26 Volts the collector current at 5 Watts output is typically < 0.62 ampere. With forced air cooling and the finned heat dissipator provided the individual transistor junction temperature is < 140°C. At the module level the quadrature hybrid coupled transistor pair is conservatively rated at 9 Watts CW power output with a minimum gain of +6 dB. Figure 9 is a photograph of a completed module with typical gain and match characteristics.

Individual amplifiers consist of an MSC 80012 transistor mounted in a Microwave Integrated Circuit (MIC). The MIC consists of a 1.25" x 1" x .040" alumina substrate with thick film circuitry. Discrete chip capacitors are used for tuning and DC blocking components where necessary. Tuning inductors and RF chokes are fabricated as part of the thick film processing.

Transistor chip temperature is a major design consideration for reliable operation. For the MSC 80012, a thermal resistance value of 8.5°C/W is supplied by the manufacturer.

In operation a minimum efficiency of 35% is realized for the individual amplifier. Table 6 shows the junction temperature for various power outputs and case temperatures.

TABLE 6

JUNCTION TEMPERATURE FOR VARIOUS POWER OUTPUTS AND CASE TEMPERATURES

P_o (Watts)	P_{diss} (Watts)	ΔT(°C)	T_J (°C) 40°C Case	T_J (°C) 50°C Case
3	6	51	91	101
4	8	58	108	118
5	10	85	125	135
6	12	101	141	151
7	14	119	159	169

In order to maintain a junction temperature < 150°C the power output is limited to the 5-6 Watt range. The above tabulation does not account for the additional dissipation due to input power. For this reason and the additional fact that gain compression begins at the nominal 5 Watt output level under CW operation, the nominal output per transistor is limited to 5 Watts.

With these constraints the current density should not exceed 2 x 10^5 amp/cm^2 which allows an MTBF value approaching 10^5 hours to be realized at 90% confidence level.

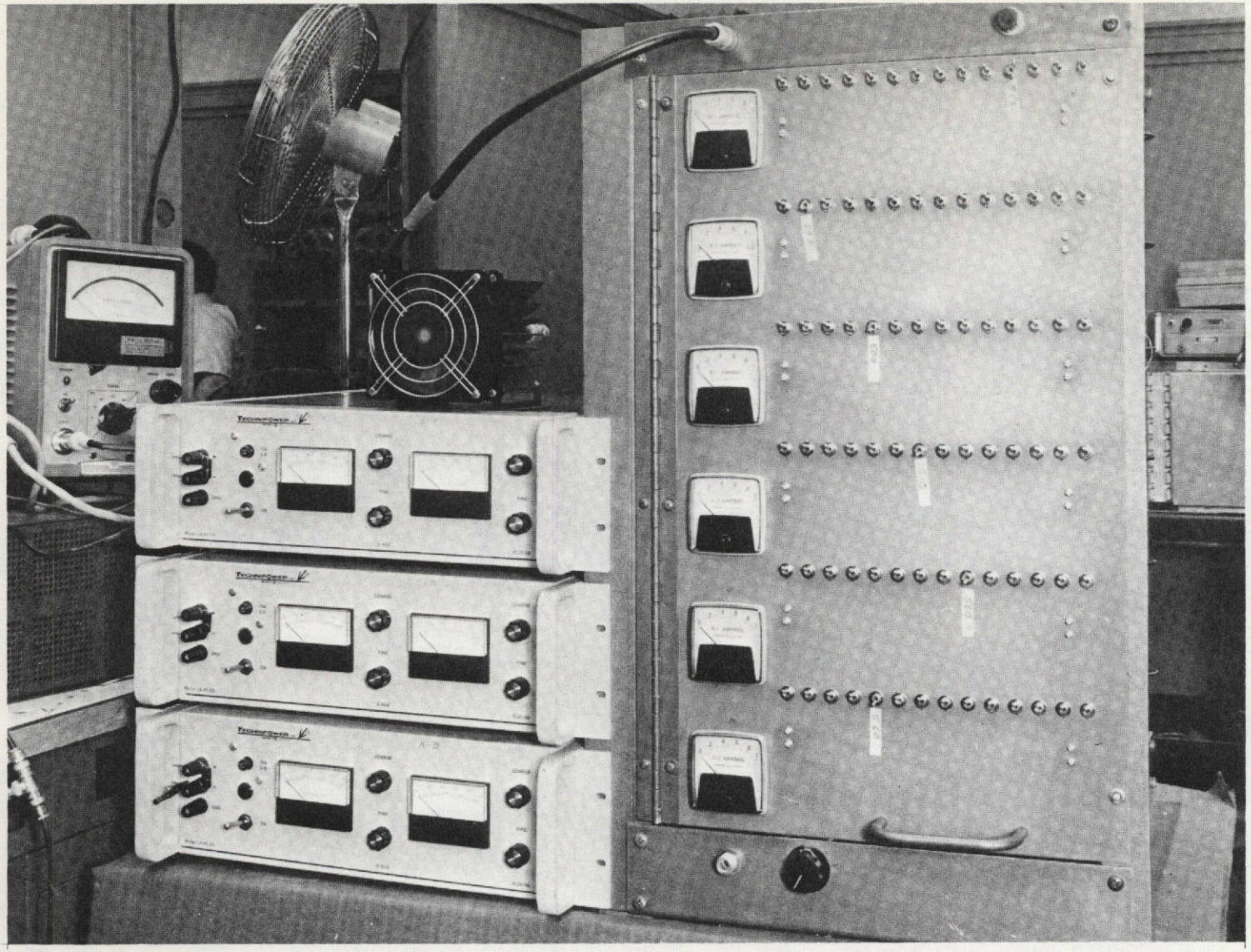

FIGURE 6. AMPLIFIER ASSEMBLY - FRONT VIEW

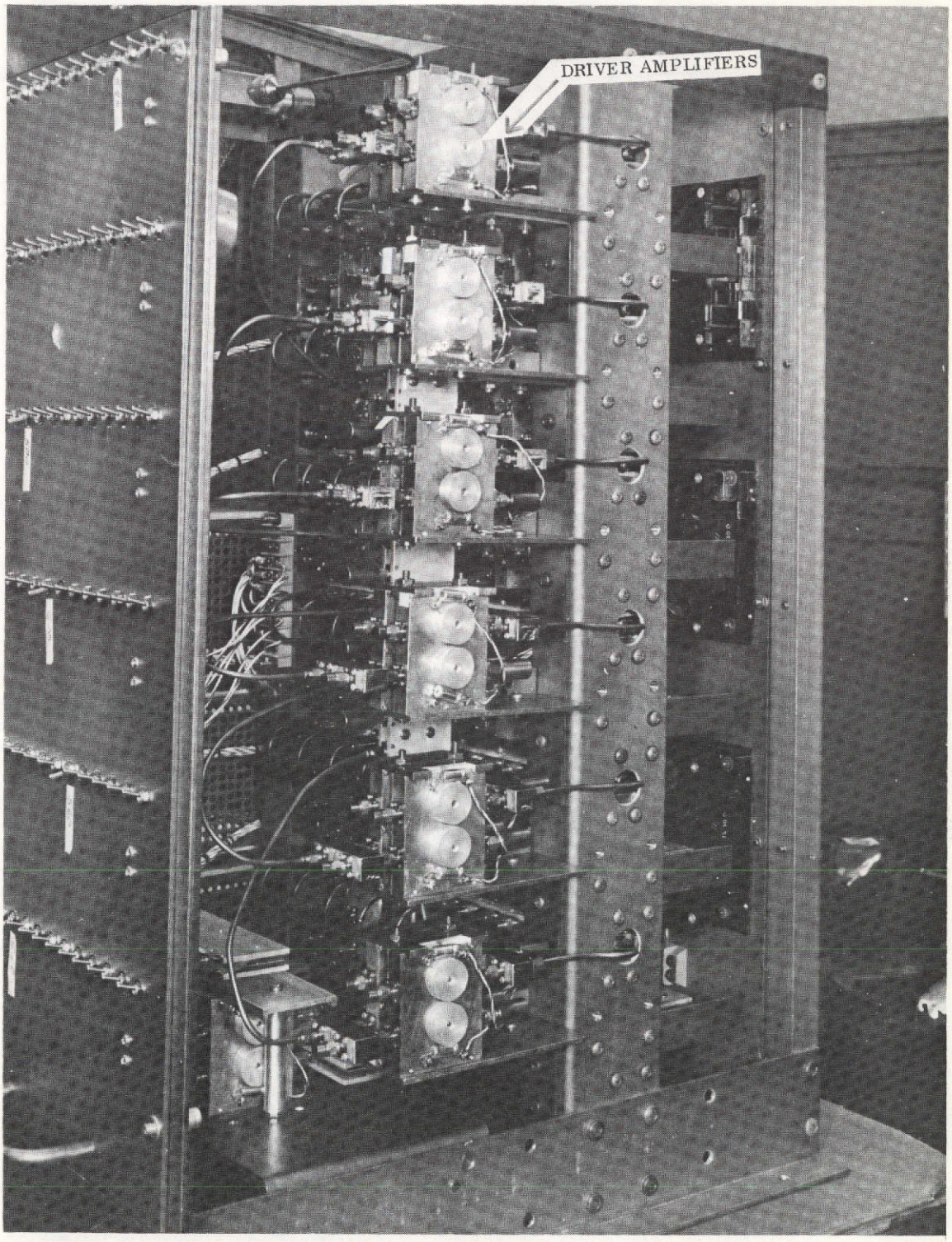

FIGURE 7. AMPLIFIER ASSEMBLY - SIDE VIEW

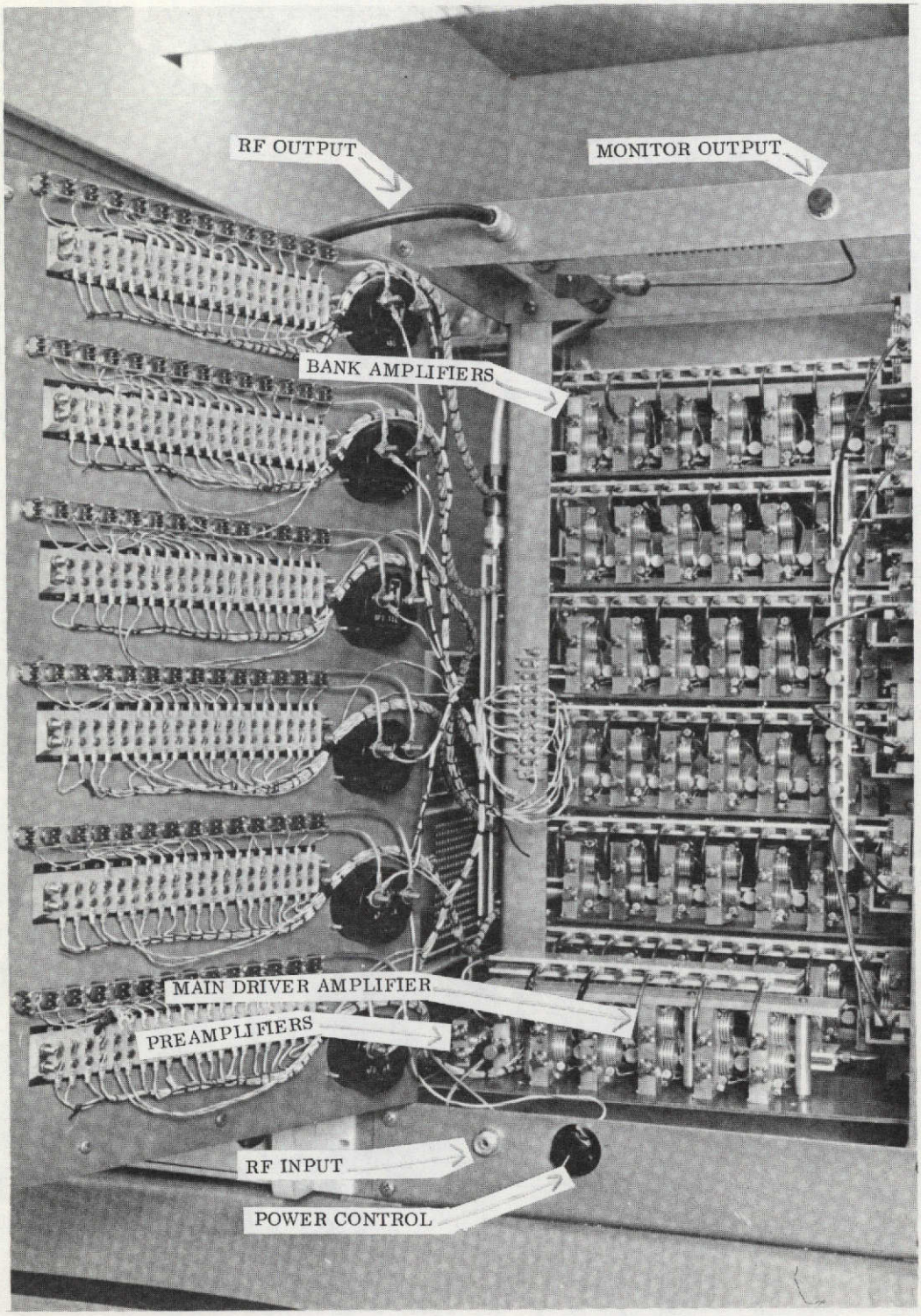

FIGURE 8. AMPLIFIER ASSEMBLY - INTERNAL VIEW FRONT

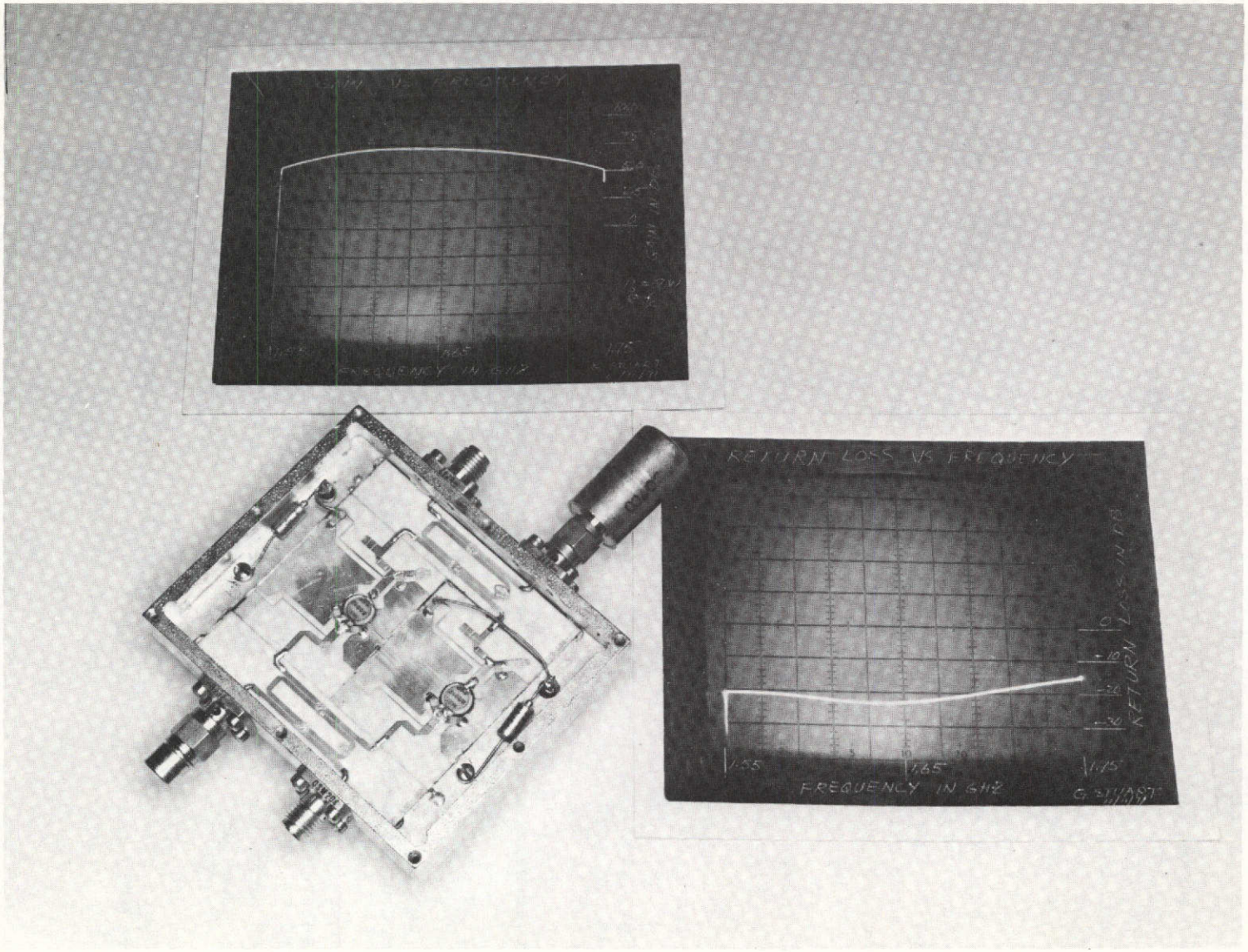

FIGURE 9. COMPLETED MODULE; TYPICAL GAIN AND MATCH CHARACTERISTICS

3.6.1 Power Supply for L-band Power Amplifier

The power supply consists of three 500 Watt Technipower switching power supplies. Each supply is independent of the others. The power distribution is arranged such that should a given supply fail the output power from the ten module main driver decreases. This prevents application of drive power to the final bank amplifiers which could result in unnecessary stress to the final output combiner terminations.

A simplified block diagram with nominal gain and power levels at each interstage is shown in Figure 10. In operation the maximum collector current for any transistor should not exceed 0.620a. The observed range of collector currents is typically 0.350a to 0.620a. This imbalance in collector current is an indicator of variance in efficiency, and/or imbalance in RF input, and less than ideal output load match.

The power amplifier, however, is designed such that with less than optimum performance from each transistor the overall power output specification is readily realized.

It has been observed with the system in operation that the power output tends to increase over approximately a fifteen minute interval after initial turn on. It is, therefore, desirable to initially adjust the power output to approximately 200 Watts. The power output will then increase and stabilize. Once stabilized the power output may then be readjusted to the desired or rated output level. This precaution is necessary to avoid an overdrive situation and the possibility of exceeding transistor ratings for reliable operation.

It is possible to operate the system with isolated inoperative transistors in the final power amplifier at some degradation in power output capability. At the module level, should a failure occur, the power output is decreased 6 dB. Should one of the six output banks of amplifiers become inoperative the overall power output will decrease approximately 30%. It is, therefore, possible to continue operation with isolated failures in the final power amplifier or predriver stages. For a failure occurring in either of the two preamplifier stages, however, RF drive would not be available and immediate repair or replacement is necessary.

This equipment has proven the feasibility of high power, efficient solid-state power generation. The system was designed utilizing existing circuitry where applicable.

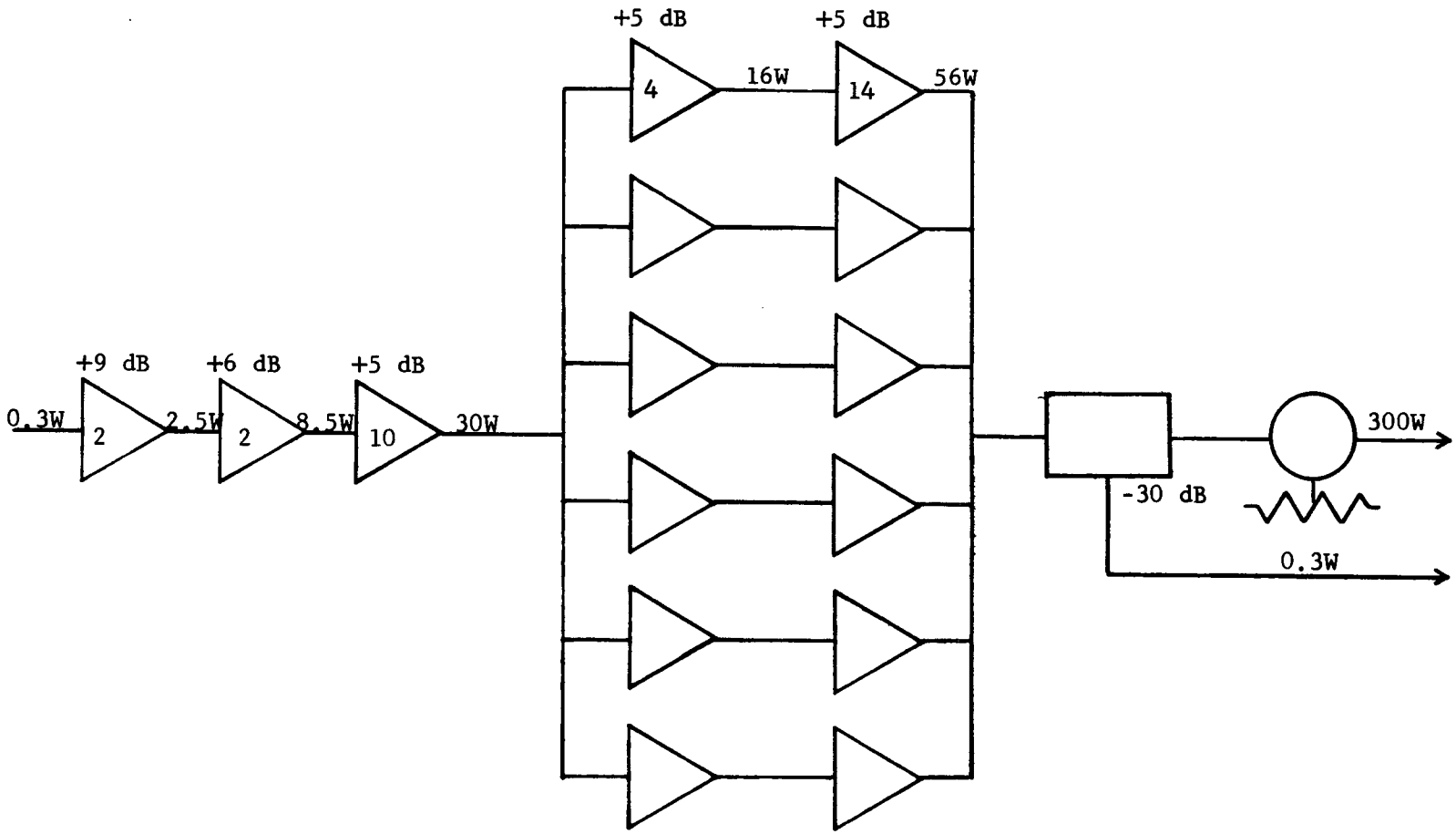

FIGURE 10. 300 WATT CW L-BAND TRANSMITTER BLOCK DIAGRAM

3.7 L-band Receiver

The L-band receiver is of modular construction and is fixed tuned at 1550.455 MHz. Frequency stability is approximately 1 ppm and is obtained by utilizing a TCXO as the first local oscillator operating at 1520 MHz. The second local oscillator is also crystal controlled at 30 MHz. The noise figure (1.6 dB) and RF bandwidth (30 MHz at 3 dB) are determined by the parametric amplifier which precedes the first mixer. The balanced mixer bandwidth is 1-2 GHz, and the second IF bandwidth is selectable 15 kHz or 60 kHz centered at 455 kHz. Provision has been made for injecting an external local oscillator in place of the 30 MHz oscillator contained in the receiver. A tuning range of 1550 MHz ± 5 MHz can then be achieved. If desired, a crystal interchange can be made within the 30 MHz oscillator to offset the same change.

Essential characteristics are as follows:

Received Center Frequency:	1550.455 MHz fixed
Stability:	0.0001%
RF Bandwidth:	30 MHz at 3 dB
First IF Bandwidth:	10 MHz at 3 dB
Second IF Bandwidth:	60 kHz or 15 kHz at 6 dB
Sensitivity:	-173 dBm/Hz
Detection:	FM
Audio Output:	0.06V peak/kHz deviation
Auxiliary Outputs:	30 MHz wideband video (AM) detector 0.455 narrowband AM (envelope) detector (signal level)
Auxiliary Input:	External second local oscillator at 30 5 MHz

Component descriptions are given in Table 7. A block diagram is shown in Figure 11.

TABLE 7

L-BAND RECEIVER COMPONENT DESCRIPTIONS

Transmit/Receive Relay
Model 320-10931-3
Coaxial type, DPST
Insertion loss: 0.2 dB
Isolation: >60 dB
RF power capability: 500 Watts average (cold switching)
DC power: 28 Volts at 180 ma
Manufacturer: Amphenol

Parametric Amplifier
Model 9821
Center frequency: 1550 MHz
Bandwidth: 30 MHz at 3 dB
Gain: 20 dB nominal
Noise temperature: 110°K
1 dB compression: -37 dBm input
Operating temperature range: -30 to +60°C
Input power required: 117 Volts AC at 500 Watts maximum
Manufacturer: Sonoma Engin. & Research, Inc.

Bandpass Filter
Model TBP1550-50-4FF1
Center frequency: 1550 MHz
Insertion loss: 2.8 dB
Bandwidth: 1525 to 1575 at 3 dB
Stopband: 40 dB at 1445 and 1645
Impedance: 50 ohms
Manufacturer: Telonic Industries, Inc.

First Mixer/IF Preamplifier
Model MPX1-2/2C
RF Bandwidth: 1-2 GHz
IF Bandwidth at 30 MHz: 16 MHz
N.F.: 7.5 dB
Gain: 25 dB minimum
L.O. power required: 0 to +3 dBm
DC input required (preamp): +12 Volts DC at 6 ma
Manufacturer: RHG Electronics Labs., Inc.

First Local Oscillator
Model ET-118-2
Temperature Compensated Crystal Oscillator
Frequency: 1520 MHz
Stability: 0.0001 percent from 0 to +50°C
Harmonics: -45 dB
Spurious: -60 dB
Power output: 9 mW
Power Input: +12 Volts DC at 105 ma
Manufacturer: Greenray Industries, Inc.

IF Post Amplifier
Model EVT3010
Bandwidth at 30 MHz: 10 MHz
Gain: 80 dB
MGC: 0-50 dB (0 to -5 V DC)
Input Power: +12 V DC at 210 ma
Manufacturer: RHG Electronics Laboratories, Inc.

Second Mixer
Model MIC
Double balanced diode mixer
Frequency range: .05 to 200 MHz
Manufacturer: Relcom

Second Local Oscillator
Model OT-24
Frequency range: 20-40 MHz with appropriate crystal
Stability: .0035 percent at -40 to +150°F
Output power: 0 dBm
Input power: 9 V DC at 10 ma
Manufacturer: International Crystal Mfg. Company, Inc.

Bandpass Filter
Center Frequency: 0.455 MHz
Bandwidth: ≈ 60 kHz and 15 kHz at 6 dB points
Linear phase filter, equiripple design, 6 tuned circuits
Input impedance: 50 ohms
Hi-Z output impedance: 1000 ohms
Manufacturer: General Electric

Limiter/Discriminator Module
Center frequency: 0.455 MHz
Bandwidth: > 60 kHz
Minimum input for hard limiting: 10 mV RMS
Dynamic range for zero phase shift: 60 dB
Discriminator output 0.06 V per 1 kHz deviation
Input Impedance: 1000 ohms
Manufacturer: General Electric

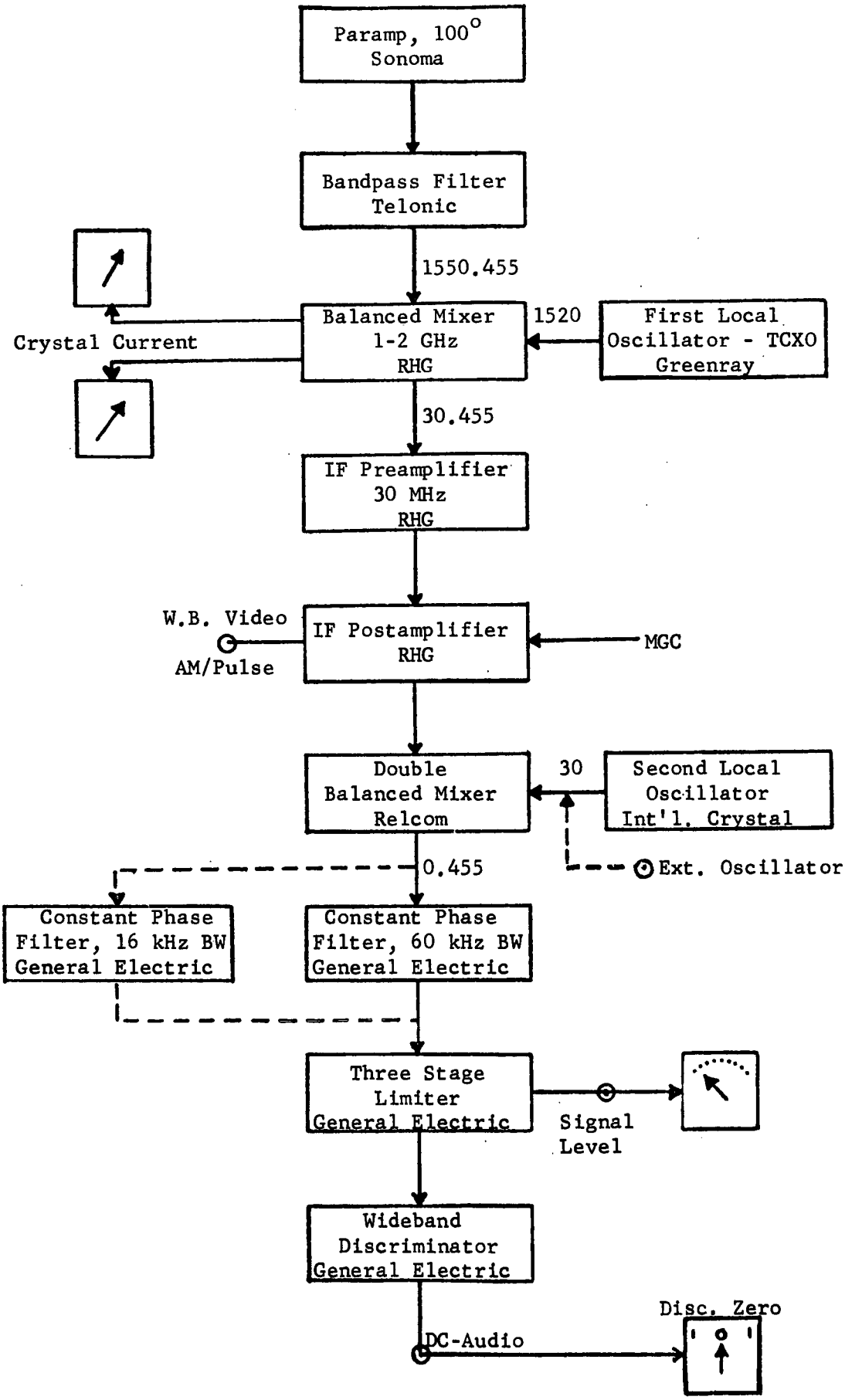

FIGURE 11. L-BAND RECEIVER BLOCK DIAGRAM

SECTION 4

EXPERIMENTAL PROCEDURES

Earth station for experiments with the L-band/VHF transponder was General Electric's Observatory, shown in Figure 12. It is located at 42°50'53" north latitude and 74°05'15" west longitude at an altitude of 1325 feet above mean sea level.

The equipment configuration for the experiments is depicted in the functional block diagram, Figure 13. The automatic address code sequencer at the Observatory was set to interrogate the distant transponders and the L-band/VHF transponder in any desired sequence. Address codes were transmitted once each 1.560 seconds times so that the interrogations were relayed through ATS-3 to the L-band/VHF transponder and initiated replies from the transponder timed so that the transponder's response arrived at the ATS-5 satellite near the peak of its window. The interrogation sequence might be 6, 7, 8, 10, 11, 12, in which case responses were received in order from Kings Point, Shannon, Reykjavik, Buenos Aires, Seattle, followed by a single response simultaneously at VHF and L-band from the L-band/VHF transponder, and then a sequence of 101 responses simultaneously at L-band and VHF from the L-band/VHF transponder. The 101 responses are timed so that there is one for each cycle of the ATS-5 spin. The entire sequence required approximately 90 seconds. The interrogation sequence could be changed to any order and any transponder could be interrogated repeatedly.

A tone-code interrogation was transmitted from the Observatory on VHF through an eight-turn helical antenna to ATS-3 and from ATS-3 to the L-band/VHF transponder where it was received on a four-turn helical antenna. The responder and timing circuits keyed the response of the transponder; a single response if the received address code was GE designated user 11, and 101 responses in sequence if the user address code was 12. The VHF return was through the ATS-3 satellite. The L-band return was through the ATS-5 satellite.

L-band transmissions from the transponders to ATS-5 were made with the 300 Watt solid-state power amplifier and 6 foot dish. With that EIRP the signal-to-noise ratio at the satellite within the total receiver bandwidth in the narrow band frequency translation mode was approximately -1 dB so that the satellite receiver was not saturated by the signal. The signal was received from the satellite using the 30 foot antenna, the circularly polarized feed and a transistor preamplifier. The signal-to-noise power density was 63 dB-Hz, but the signal-to-noise ratio was limited by the uplink. The signal-to-noise ratio in the 60 kHz bandwidth was approximately 15 dB, as shown in Figure 14. The transmitter was frequency modulated with a 9.7 kHz tone with a deviation ratio of 2, yielding an RF bandwidth of 60 kHz.

When the transponder was interrogated with user code 12 for the multiple response, the address code of 30 bits was inserted once per spin cycle of the satellite by suppressing audio cycles for zeros and transmitting audio cycles for ones. Timing circuits initiated the code transmissions at the same rate as the spin cycle, preceeding the window of the satellite by the propagation time so that the 3 ms code occurred

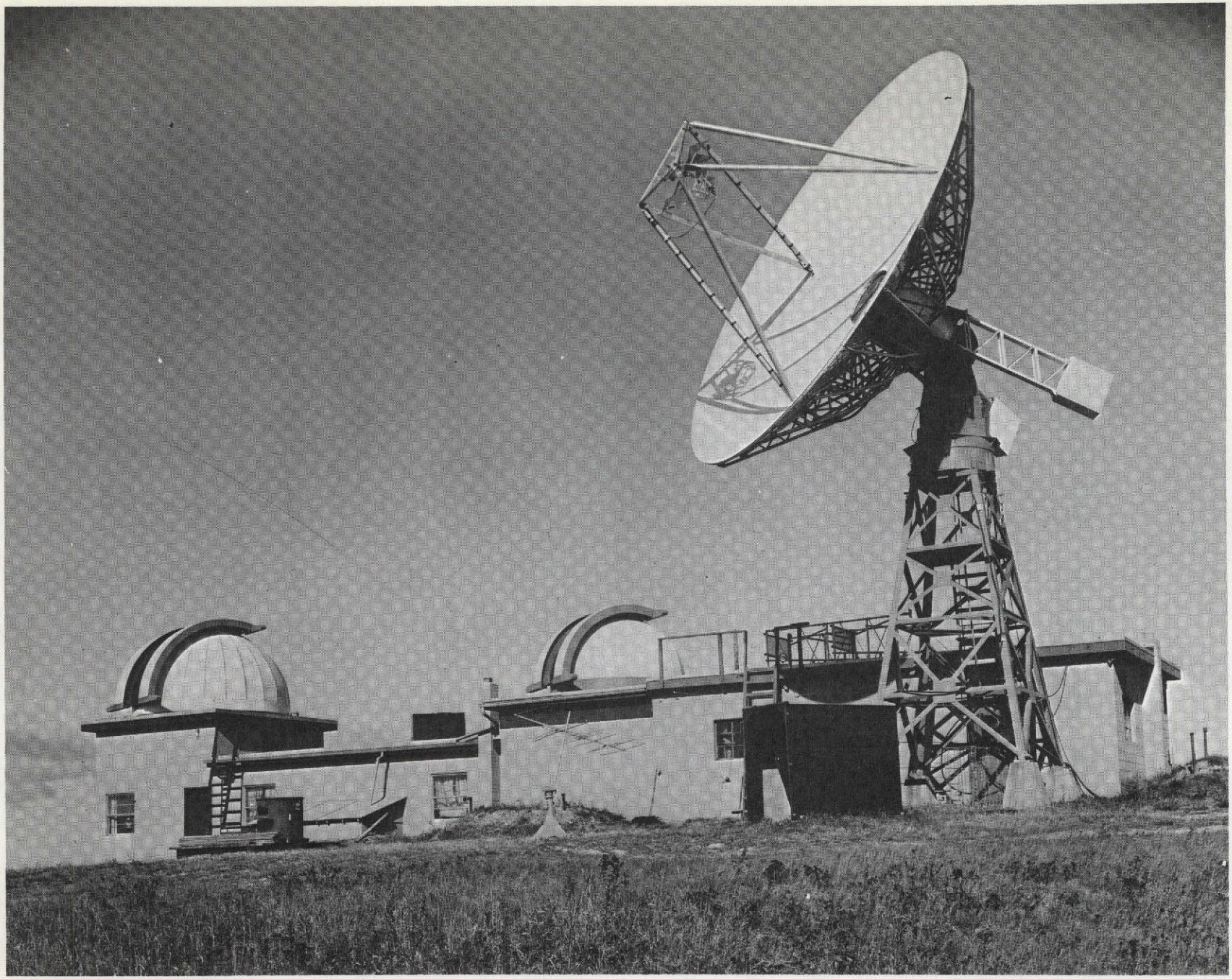

FIGURE 12. RADIO-OPTICAL OBSERVATORY

FOLDOUT FRAME 1

FOLDOUT FRAME 2

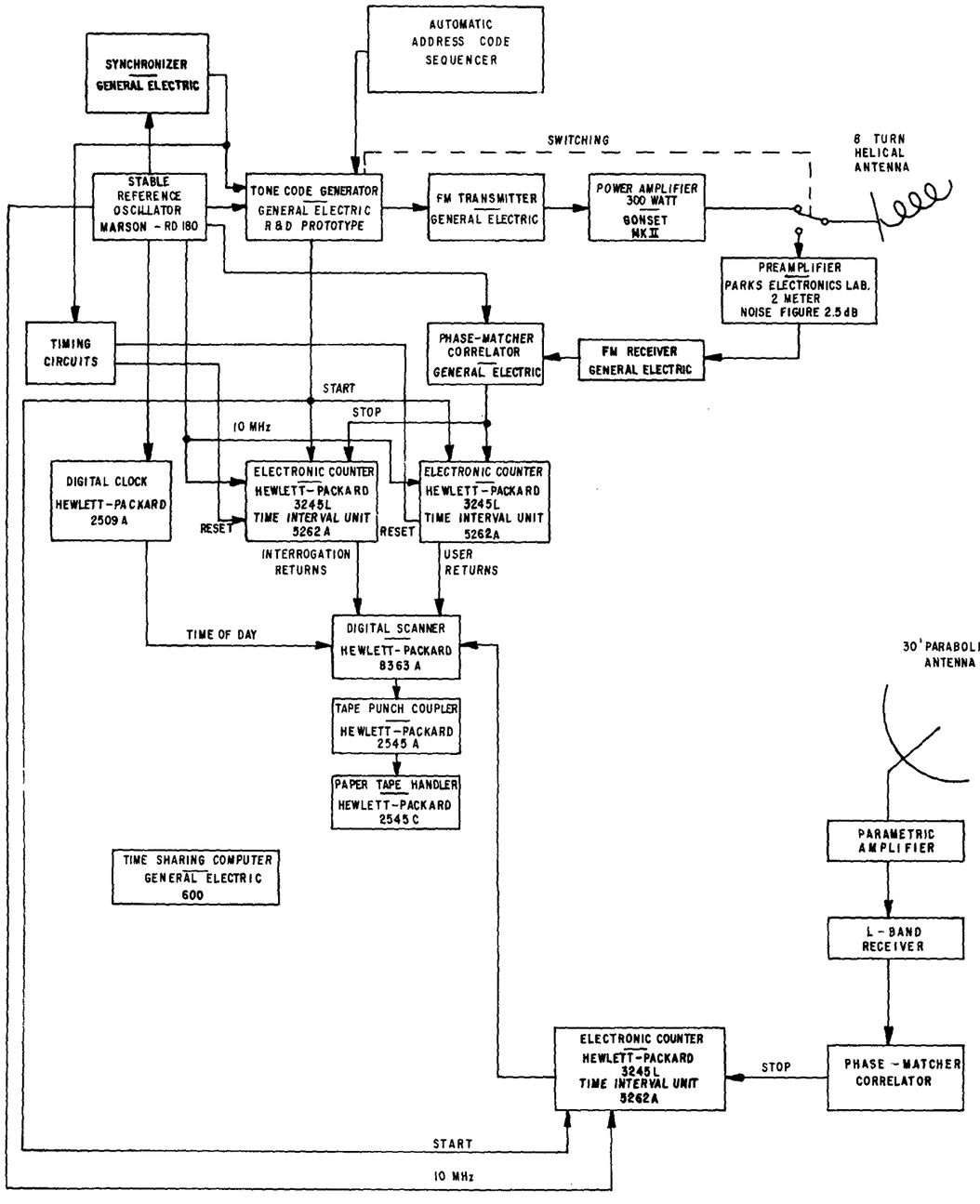

FIGURE 13. EQUIPMENT CONFIGURATION FOR EXPERIMENT

FIGURE 14. L-BAND SIGNAL RETURN FROM SPINNING ATS-5 SATELLITE

just at the end of the window, as shown in Figure 14. The tone-code receiving circuits at the Observatory were gated on to receive 256 cycles of the audio tone from the satellite just prior to the reception of the code so that the ranging measurement was made using a signal duration of approximately 27 ms for the tone and approximately 3 ms for the code, for a total tone-code signal duration of 30 ms.

Figure 15 is a reproduction of the code as received from the satellite and demodulated. The time interval from transmission of the code to correlation of the signal received from the satellite was measured for each rotation of the satellite and recorded on punched tape. At the Observatory the VHF return was received on the same helical antenna that transmitted the interrogation. The L-band signal was received on the 30 foot parabolic antenna, applied to the parametric amplifier, and detected by the L-band receiver. Times of reception were measured by the phase matcher-correlator. The time interval between transmission of the interrogation and reception of the signals at VHF and L-band are separately measured by counters with a 0.1 μs timing resolution.

For single interrogations with user code 11, a digital scanner scanned a digital clock and the three time interval units once for each interrogation, converted their digital readings into an ASCII code and applied them to a paper tape punch where they were recorded.

The scanner also scanned digital voltmeters that measured the amplitude of the correlation pulses which were then digitized and included with the data on the punched tape. The value of the digital voltage changed in quantized steps and was thus a measure of the number of bits in error in the address code received at the Observatory.

Several formats have been used for the recording of the data. One format is illustrated in Figure 16. In addition to the ranging data punched on the tape, manual data was inserted about once each fifteen minutes to record the file number, the date, and other significant data about the particular test. A hard copy print-out of the punched tapes was made after each satellite test period and the data was permanently stored on the punched tape and hard copy print-out. Several computer programs are available for the processing of the data. They are described in the Final Report on Phases 1 and 2 on pages 3-20/22.

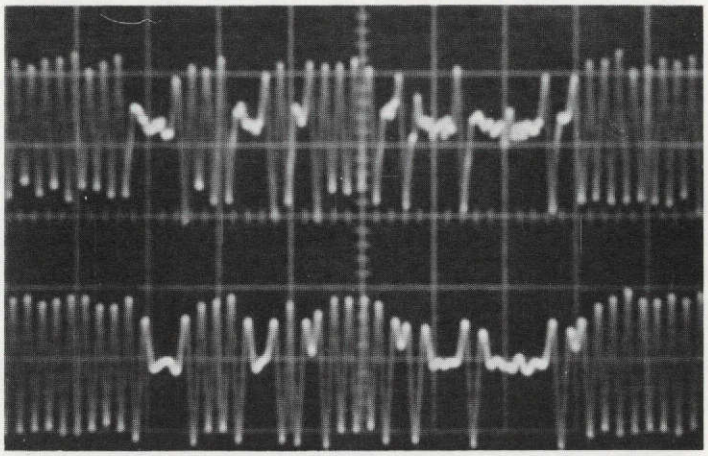

FIGURE 15. REPRODUCTION OF THE CODE AS RECEIVED FROM THE SATELLITE AND DEMODULATED

Time Interval, 0.1 microsecond resolution Observatory-ATS-3-Observatory	User Number	Time, GMT (hours, minutes, seconds)	Time Interval, 0.1 microsecond resolution Observatory-ATS-3-User-ATS-3-Observatory	Time Interval, 0.1 microsecond resolution Observatory-ATS-3-User-ATS-1-Observatory	Word Sync Error Rate	Address Error Rate
02528664	05	045356	09304646	09533611	10065423	10066503
02528659	06	045359	09359837	09588263	10065423	10066503
02528666	05	045402	09304640	09533618	10065423	10066503
02528665	06	045405	09359811	09588253	10065423	10066503
02528668	05	045408	09304674	09533628	10065423	10066503
02528671	06	045411	09359833	09588256	10065423	10066503

FIGURE 16. FORMAT OF DATA RECORDED ON PUNCHED TAPE

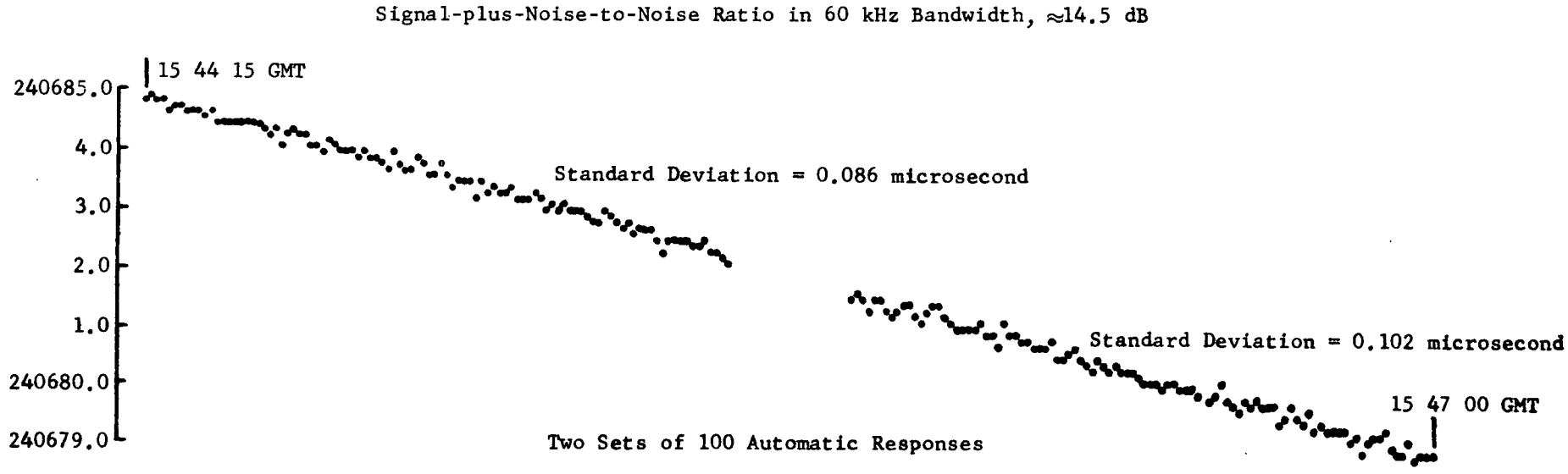

FIGURE 17, L-BAND RANGE MEASUREMENTS - 24 AUGUST 1972

SECTION 5

EXPERIMENTAL RESULTS

5.1 Data Recording Format

Range measurement precision was determined by a computer program that fitted a second order curve to the range data collected during a period of a few minutes. Each individual range measurement was compared with the best fit quadratic curve and the standard deviation of the measurements with respect to the curve was computed. The computer program also produced a histogram of the individual measurements relative to the best fit quadratic curve.

Figure 17 is a plot of range measurements at L-band from the Observatory to the ATS-5 satellite and return. The ordinate is the propagation time interval plus a constant equipment time delay. The abscissa is time. The plot shows that the range measured in microseconds propagation time changed approximately 7 μs between 15 44 15 and 15 47 00. The range rate varies through the day in an approximately sinusoidal manner. Range increases for twelve hours and decreases for twelve hours during the day.

Figures 18 through 23 are sample print-outs of computed standard deviations. Nomenclature used on the print-outs is given below.

Symbol:	Meaning:
TNP (Total Number of Points)	Number of interrogations during the period of the plot
NPU (Number of Points Used)	Actual number of points used in computing the curve and in plotting the histogram
NPE (Number of Points in Error)	Number of points displaced more than the number of μs stated under YMAX, set to reject points due to malfunction
GMTLOW	Time in hours, minutes, and seconds at the start of the best fit curve
GMTHIG	GMTLOW + (TNP-1)
DIFMIN	Largest single deviation of any point in negative direction
DIFMAX	Largest single deviation of any point in positive direction

```
NEXT FILE NAME=F85

L-BAND DATA 4
IDATA     ICFORMATS     IUSER  OBSERVATORY RECORDS     TOTAL RECORDS
  1           1          11          100                   100

IN NI TNP NPU NPE GMTLOW GMTHIG  YMAX  DIFMIN DIFMAX    SD       ERRORATE
 I  1 100  95   0 154908 155047   2.5   -0.30   0.31 1.283E-01 9.99E+02
OV  1 100  95   0 154908 155047         -0.30   0.31 1.283E-01 9.99E+02

      THATDIINT THATDIFIN DIFCHANGE
       240913.8  240911.7       2.1

                  HISTOGRAM FOR OBSERVATORY

      0 POINTS OVER + 2.0 AND LESS THAN +   2.5 MICRO SECONDS
 2.0
 1.9
 1.8
 1.7
 1.6
 1.5
 1.4
 1.3
 1.2
 1.1
 1.0
 0.9
 0.8
 0.7
 0.6
 0.5
 0.4
 0.3 X
 0.2 XXXXXXXXXXXX
 0.1 XXXXXXXXXXXXXXXXXXXXXX
 0.  XXXXXXXXXXXXXXXXXXXXXXXXX
-0.1 XXXXXXXXXXXXXXXXXXXXXXX
-0.2 XXXXXXXXX
-0.3 XX
-0.4
-0.5
-0.6
-0.7
-0.8
-0.9
-1.0
-1.1
-1.2
-1.3
-1.4
-1.5
-1.6
-1.7
-1.8
-1.9
-2.0
      0 POINTS LESS THAN - 2.0 AND OVER -   2.5 MICRO SECONDS
```

FIGURE 18. HISTOGRAM OF STANDARD DEVIATION

```
NEXT FILE NAME=F4

FILE 377P1.2 6/8/72
L-BAND DATA 4
IDATA     ICFORMATS     IUSER  OBSERVATORY RECORDS     TOTAL RECORDS
  1           2           11           91                    91

IN NI TNP NPU NPE GMTLOW GMTHIG  YMAX  DIFMIN DIFMAX     SD      ERRORATE
 1  1  91  91   0 154912 155042   2.5   -0.09   0.07 3.329E-02 9.99E+02
OV  1  91  91   0 154912 155042         -0.09   0.07 3.329E-02 9.99E+02

     THATDIINT THATDIFIN DIFCHANGE
      240913.7  240911.8       1.9

                HISTOGRAM FOR OBSERVATORY

     0 POINTS OVER + 2.0 AND LESS THAN +   2.5 MICRO SECONDS
 2.0
 1.9
 1.8
 1.7
 1.6
 1.5
 1.4
 1.3
 1.2
 1.1
 1.0
 0.9
 0.8
 0.7
 0.6
 0.5
 0.4
 0.3
 0.2
 0.1 XXXXX
 0.  XXXXXXXXXXXXXXXXXXXXXXXXXXXXXXXXXXXXXXXXXXXXXXXXXXXXXXXXXXXXXXXXXXXXXXX 79
-0.1 XXXXXXXX
-0.2
-0.3
-0.4
-0.5
-0.6
-0.7
-0.8
-0.9
-1.0
-1.1
-1.2
-1.3
-1.4
-1.5
-1.6
-1.7
-1.8
-1.9
-2.0
     0 POINTS LESS THAN - 2.0 AND OVER -   2.5 MICRO SECONDS
```

FIGURE 19. HISTOGRAM OF STANDARD DEVIATION

```
NEXT FILE NA+=F86

L-BAND DATA 4
IDATA     ICFORMATS     IUSER  OBSERVATORY RECORDS     TOTAL RECORDS
  1           1          11          100                   100

IN NI  TNP  NPU NPE GMTLOW GMTHIG  YMAX  DIFMIN DIFMAX    SD       ERRORATE
 1  1  100   98   0 155052 155231   2.5   -0.34   0.30 1.215E-01 9.99E+02
OV  1  100   98   0 155052 155231         -0.34   0.30 1.215E-01 9.99E+02

      THATDIINT THATDIFIN DIFCHANGE
       240905.9  240903.8       2.1

                  HISTOGRAM FOR OBSERVATORY

      0 POINTS OVER + 2.0 AND LESS THAN +   2.5 MICRO SECONDS
 2.0
 1.9
 1.8
 1.7
 1.6
 1.5
 1.4
 1.3
 1.2
 1.1
 1.0
 0.9
 0.8
 0.7
 0.6
 0.5
 0.4
 0.3 XXX
 0.2 XXXXXXX
 0.1 XXXXXXXXXXXXXXXXXXXXXX
 0.  XXXXXXXXXXXXXXXXXXXXXXXXXXXXX
-0.1 XXXXXXXXXXXXXXXXXXXXXXXXXX
-0.2 XXXXXXXX
-0.3 X
-0.4
-0.5
-0.6
-0.7
-0.8
-0.9
-1.0
-1.1
-1.2
-1.3
-1.4
-1.5
-1.6
-1.7
-1.8
-1.9
-2.0
      0 POINTS LESS THAN - 2.0 AND OVER -   2.5 MICRO SECONDS
```

FIGURE 20. HISTOGRAM OF STANDARD DEVIATION

```
NEXT FILE NAME=F5

L-BAND DATA 4
IDATA      ICFORMATS      IUSER  OBSERVATORY RECORDS      TOTAL RECORDS
  1            1            11            91                    91

IN NI TNP NPU NPE GMTLOW GMTHIG  YMAX  DIFMIN DIFMAX     SD      ERRORATE
 1  1  91  91   0 155056 155226   2.5   -0.07   0.09 3.372E-02 9.99E+02
OV  1  91  91   0 155056 155226         -0.07   0.09 3.372E-02 9.99E+02

     THATDIINT THATDIFIN DIFCHANGE
      240905.9  240903.9       2.0

                  HISTOGRAM FOR OBSERVATORY

      0 POINTS OVER + 2.0 AND LESS THAN +   2.5 MICRO SECONDS
 2.0
 1.9
 1.8
 1.7
 1.6
 1.5
 1.4
 1.3
 1.2
 1.1
 1.0
 0.9
 0.8
 0.7
 0.6
 0.5
 0.4
 0.3
 0.2
 0.1 XXXXXXXX
 0.  XXXXXXXXXXXXXXXXXXXXXXXXXXXXXXXXXXXXXXXXXXXXXXXXXXXXXXXXXXXXXXXXXXXXXX 78
-0.1 XXXXXX
-0.2
-0.3
-0.4
-0.5
-0.6
-0.7
-0.8
-0.9
-1.0
-1.1
-1.2
-1.3
-1.4
-1.5
-1.6
-1.7
-1.8
-1.9
-2.0
      0 POINTS LESS THAN - 2.0 AND OVER -   2.5 MICRO SECONDS
```

FIGURE 21. HISTOGRAM OF STANDARD DEVIATION

```
NEXT FILE NAME=F87

L-BAND DATA 4
IDATA     ICFORMATS     IUSER  OBSERVATORY RECORDS     TOTAL RECORDS
  1           1           11          100                   100

IN NI  TNP NPU NPE GMTLOW GMTHIG  YMAX  DIFMIN DIFMAX     SD      ERRORATE
 I  1  100 100   0 155304 155443   2.5   -0.32   0.33 1.249E-01 9.99E+02
OV  1  100 100   0 155304 155443         -0.32   0.33 1.249E-01 9.99E+02

      THATDIINT THATDIFIN DIFCHANGE
       240895.2  240893.1       2.0

                  HISTOGRAM FOR OBSERVATORY

      0 POINTS OVER + 2.0 AND LESS THAN +   2.5 MICRO SECONDS
 2.0
 1.9
 1.8
 1.7
 1.6
 1.5
 1.4
 1.3
 1.2
 1.1
 1.0
 0.9
 0.8
 0.7
 0.6
 0.5
 0.4
 0.3 X
 0.2 XXXXXXXXXXX
 0.1 XXXXXXXXXXXXXXXXXXXXXXX
 0.  XXXXXXXXXXXXXXXXXXXXXXXXXXXXX
-0.1 XXXXXXXXXXXXXXXXXXXXXXX
-0.2 XXXXXXXXXX
-0.3 XX
-0.4
-0.5
-0.6
-0.7
-0.8
-0.9
-1.0
-1.1
-1.2
-1.3
-1.4
-1.5
-1.6
-1.7
-1.8
-1.9
-2.0
      0 POINTS LESS THAN - 2.0 AND OVER -   2.5 MICRO SECONDS
```

FIGURE 22. HISTOGRAM OF STANDARD DEVIATION

```
NEXT FILE NAME=F6

L-BAND DATA 4
IDATA      ICFØRMATS      IUSER  ØBSERVATØRY RECØRDS      TØTAL RECØRDS
  1            1            11            91                    91

IN NI  TNP  NPU NPE GMTLØW GMTHIG  YMAX  DIFMIN DIFMAX     SD       ERRØRATE
 1  1   91   91   0 155308 155438   2.5   -0.07   0.07 3.641E-02 9.99E+02
ØV  1   91   91   0 155308 155438         -0.07   0.07 3.641E-02 9.99E+02

     THATDIINT THATDIFIN DIFCHANGE
      240895.1  240893.3       1.8

                    HISTØGRAM FØR ØBSERVATØRY

      0 PØINTS ØVER + 2.0 AND LESS THAN +   2.5 MICRØ SECØNDS
 2.0
 1.9
 1.8
 1.7
 1.6
 1.5
 1.4
 1.3
 1.2
 1.1
 1.0
 0.9
 0.8
 0.7
 0.6
 0.5
 0.4
 0.3
 0.2
 0.1 XXXXXXX
 0.  XXXXXXXXXXXXXXXXXXXXXXXXXXXXXXXXXXXXXXXXXXXXXXXXXXXXXXXXXXXXXXXXXX 76
-0.1 XXXXXXXXX
-0.2
-0.3
-0.4
-0.5
-0.6
-0.7
-0.8
-0.9
-1.0
-1.1
-1.2
-1.3
-1.4
-1.5
-1.6
-1.7
-1.8
-1.9
-2.0
      0 PØINTS LESS THAN - 2.0 AND ØVER -   2.5 MICRØ SECØNDS
```

FIGURE 23. HISTOGRAM OF STANDARD DEVIATION

SD (Standard Deviation)	Standard deviation of the series of data points with respect to the best fit curve. Numbers -01, -02, etc. indicate number of places decimal point should be moved to left.
THATDIINT	Value of best fit curve at time GMTLOW
THATDIFIN	Value of best fit curve at time GMTHIG
DIFCHANGE	Difference between THATDIINT and THATDIFIN

The histogram plots the points with 0.1 μs resolution between the limits +2 and -2 μs relative to the best fit curve. A number appears at the extreme right of the histograms when they go off the scale of the teletype. As the result of a program error, that number, when it appears, is always one greater than it should be.

5.2 Comparison of VHF and L-band Range Measurement Standard Deviations

Comparisons of standard deviations at VHF and L-band were made by interrogating the VHF/L-band transponder with a user 12 code interrogation through ATS-3. The transponder then responded with 101 tone-code ranging responses at VHF and at L-band, transmitting these responses coherently, and timing them to pass through the windows of the spinning ATS-5 satellite. The time duration of 101 measurements than was approximately 78 seconds.

Table 8 summarizes the results of many measurements of standard deviation on sets of 101 sequential responses for VHF and L-band. Each value under the column "VHF Individual Responses" represents the standard deviation of approximately 101 independent range measurements, each response made with the 2.4414 kHz tone in the 15 kHz RF bandwidth. The averaging for the phase measurement was over 256 audio cycles representing an averaging time of 0.105 second. The ten response averages are the standard deviation of a few less than 100 data points, each data point being the average of ten individual responses. The ten response averages were formed by taking the average of individual measurements one through ten, two through eleven, three through twelve, and so forth, then computing a best fit curve to the average-value data points and determining the standard deviation of each data point relative to the best fit curve. The average of individual responses is the average of the values shown in the individual responses column for each day. Signal characteristics changed little from day to day at VHF.

The values under "L-band Individual Responses" are the standard deviations of approximately 101 independent range measurements at L-band with the 9.7656 kHz tone in the 60 kHz RF bandwidth. The phase measurements were averaged over 256 tone cycles for an averaging time of

FOLDOUT FRAME

TABLE 8

STANDARD DEVIATIONS, MICROSECONDS, ~101 SEQUENTIAL RESPONSES

		VHF (15 kHz BANDWIDTH)				L-BAND (60 kHz BANDWIDTH)			
DATE	TIME GMT	INDIVIDUAL RESPONSES	TEN RESPONSE AVERAGES	AVERAGE OF INDIVIDUAL RESPONSES	S + N / N RATIO	INDIVIDUAL RESPONSES	TEN RESPONSE AVERAGES	AVERAGE OF INDIVIDUAL RESPONSES	S + N / N RATIO
8/1/72	15 37 48	.2790		.3245	10-13	.1264		.1412	11 dB
	15 39 21	.3144			dB	.1394			
	15 40 53	.2702			(3 dB	.1383			
	15 42 26	.2412			Spin	.1306			
	15 50 20	.2983			Mode)	-----			
	15 51 52	.2819				.1286			
	15 53 25	.2740				.1396			
	15 55 14	.2908				-----			
	15 56 46	.3027				.1315			
	16 07 22	.2914				.1435			
	16 08 43	.2721	.1027			.1612	.04329		
	16 10 03	.2956	.06293			.1817	.05398		
	16 11 24	.6558				.1929	.04120		
	16 21 41	.3087				.1320			
	16 23 13	.2700				-----			
	16 24 44	-----				-----			
	16 26 11	.3155				.1395			
	16 27 43	.3249				.1386			
	16 29 16	.5113				.1292			
	16 30 48	.3647				.1359			
	16 32 21	.3590				.1343			
	16 33 54	.3185				.1214			
	16 35 50	.4063				.1316			
	16 37 22	.3106				.1321			
	16 40 52	.3046				.1454			
	16 42 25	.3036				.1374			
	16 43 58	.2768				.1457			
	16 45 30	-----				-----			
	16 45 47	.3394				-----			
	16 47 20	.2804				.1539			
	16 48 53	.2979				.1356			
	16 50 25	.2631				.1438			
	16 51 58	.3447				.1428			
	16 53 30	.3332				.1500			
	16 55 03	.4083				.1326			
8/3/72	15 45 37	.4726		.3722	"	.1535		.1461	11 dB
	15 47 26	.3871				.1534			
	15 48 47	.3935				.1390			
	15 50 07	.4388				-----			
	15 52 08	.3316				.1391			
	16 34 41	.3340				.1400			
	16 36 58	.3198				.1645			
	16 38 31	.3907				.1442			
	16 40 01	.3077				.1378			
	16 43 03	.3463				.1435			
8/8/72	15 47 46	.3013		.3228	"	.1414		.1421	12 dB
	15 49 07	.3311	.1122			.1283	.03329		
	15 50 51	.2638	.05584			.1215	.03372		
	15 53 03	.2927	.08915			.1249	.03641		
	16 00 45	.3478				.1322			
	16 04 25	.3454				.1331			
	16 08 33	.3511				.1548			
	16 11 50	.3077	.1169			.1764	.06024		
	16 13 37	.3168	.1502			.1788	.04074		
	16 18 22	.3114	.1295			.1400	.04124		
	16 21 57	.3209	.1475			.1425	.04547		
	16 26 07	.3580	.1763			.1323	.04166		
	16 28 18	.3404	.1859			.1378	.03904		
	16 29 45	.3302	.1585			.1447	.04381		
8/17/72	15 37 39	.4248	.1766	.3571	"	.2475	.07639	.2415	6 dB
	15 39 09	-----				.2380	.07814		
	15 43 56	.3118	.1213			.2511	.07642		
	15 45 43	.3798	.1845			.2318	.05605		
	15 47 03	.3446	.09938			.2471	.08555		
	15 48 45	.3247	.1214			.2092	.04312		
	16 37 16	-----				.2515	.07454		
	16 39 16	-----				.2559	.06024		
8/24/72	15 37 01	.3024	.08886	.2885	"	.1038	.02336	.09957	14.5 dB
	15 37 32	.3390	.09253			.1137	.03175		
	15 39 57	.3011	.08455			.09352	.01851		
	15 41 23	.2846	.1001			.09466	.02619		
	15 42 48	.3550	.1397			.09992	.02379		
	15 44 14	.3163	.05958			.08597	.01827		
	15 45 39	.2744	.07158			.1026	.02691		
	15 47 52	-----				-----			
	15 49 17	.2686	.09202			.09594	.03671		
	15 50 43	.3155	.07365			.1011	.02070		
	16 00 17	.2551	.1162			.1083	.02495		
	16 01 47	.2604	.06229			.1005	.02371		
	16 03 17	.2812	.09790			.09601	.03089		
	16 04 48	.2589	.07888			.1064	.02851		
	16 06 18	.2749	.06457			.09355	.02516		
	16 07 48	.2405	.05542			.09756	.03451		

FOLDOUT FRAME

approximately 0.027 second. The ten response averages and the average of individual responses were computed in the manner described above for the corresponding columns under VHF.

As expected there is a systematic change in standard deviation with signal-plus-noise to noise ratio. The average of the individual responses can be compared with the signal-plus-noise to noise ratio on the day that the measurements were made. Standard deviation varies from 0.24 with a signal-plus-noise to noise ratio of 6 dB to 0.1 with a 14.5 dB signal-plus-noise to noise ratio.

Table 9 compares the measured precision as a function of signal-plus-noise to noise ratio, and the theoretical precision as a function of signal-to-noise ratio as predicted by Milton (see Appendix I).

TABLE 9

THEORETICAL AND MEASURED PRECISION

Theoretical Precision		Measured Precision (L-band)	
S/N	1 Sigma Precision	S+N / N	1 Sigma Precision
6 dB	.092 μs	6.0 dB	.24 μs
10 dB	.056 μs	11.0 dB	.14 μs
15 dB	.032 μs	14.5 dB	.10 μs

5.3 L-Band Standard Deviations

The L-band/VHF transponder was used for L-band range measurements before the receiver of the ATS-5 satellite ceased to function in February 1972. Standard deviations of measurements made in January and February are essentially the same as the standard deviations obtained in the summer months, after the satellite receiver became functional again in June.

Figure 24 is a print-out of the raw data as recorded on February 4, 1972. It is a portion of a seven minute continuous sequence of 538 measurements made between 19 04 00 and 19 11 00 GMT. A useful ranging return was received on every window of the ATS-5 satellite. A computer fitted a quadratic curve to the data, rejecting four points that were more than 2.5 μs displaced from the best fit curve. One of the rejected points is recorded at 16 55 57 in Figure 24.

Later investigation revealed that the errors were due to an incorrect connection on a printed circuit wiring board that caused a quantum jump in phase measurement when signal-to-noise ratio was poor. After the error was located and corrected, the quantum error jumps were eliminated and the distribution of errors was gaussian at all signal-to-noise ratios.

When the four displaced points were rejected, the standard deviation of the remaining 534 points was 0.1569 microsecond. The largest single deviations from the curve were -0.63 and +0.47 microsecond. All of the

Microseconds	User Number Hours Minutes Seconds
02595634	12165530
02595633	12165531
02595633	12165532
02595633	12165533
02595633	12165533
02595632	12165534
02595634	12165535
02595633	12165536
02595633	12165536
02595634	12165537
02595634	12165538
02595635	12165539
02595635	12165540
02595634	12165540
02595633	12165541
02595634	12165542
02595634	12165543
02595633	12165544
02595636	12165544
02595635	12165545
02595634	12165546
02595634	12165547
02595635	12165547
02595634	12165548
02595636	12655549
02595636	12165550
02595636	12165551
02595634	12165551
02595636	12165552
02595636	12165553
02595636	12165554
02595635	12165554
02595635	12165555
02595632	12165556
02595592	12165557
02595634	12165558
02595634	12165558
02595636	12165559
02595635	12165600
02595636	12165601
02595632	12165602
02595637	12165602
02595636	12165603
02595637	12165604
02595636	12165605

FIGURE 24. PRINT-OUT OF RAW DATA - 2/4/72

538 measurements, including the four rejected points, are plotted on the bar graph, Figure 25.

The range measurement made on each window of the satellite was independent of all the others and the signal averaging time was 0.027 second. The precision of range measurement should improve as the square root of the number of points averaged. The computer was programmed to average each sequence of nine points, for example, measurements one through nine, two through ten, three through eleven, etc., and compute the standard deviations of the nine point averages. Each point for the nine point averages represents an averaging time of 0.27 second. A similar computation was made for 99 point averages representing 2.7 second averaging time. For the 534 points the nine point averages produce a standard deviation of 0.0888 μs; the 99 point averages, 0.043 μs. These did not improve in accordance with theory. This might be due to round-off in the computer since the program did not use double precision. The sample length was then limited to the 231 points within the same set of data between 19 06 30 and 19 09 30 GMT. The standard deviation of single points was 0.1385 μs; of nine point averages, 0.0435 μs; and ninety-nine point averages, 0.0096 μs. The numbers do indeed improve in proportion to the square root of the averaging time and are believed to truly represent the results of longer averaging times. The 2.7 second averaging time provides a two-way ranging resolution of about five feet.

A manual plot of data obtained during the test period of February 1 produced results that are in agreement with the computer analysis of the February 4 data. Figure 26 is a sample of a punched tape record showing the time interval measurements with a resolution of 0.1 μs followed by the user address code and the Greenwich Mean Time in hours, minutes and seconds. Samples of the data were plotted manually in the same manner that produced the plot of Figure 17. A histogram showing the deviation of each point from an average value is drawn through the manual plot. Figure 27 displays the histogram of 243 independent measurements made during a 3 minute, 9 second interval. The curve is a mathematical Gaussian distribution with a standard deviation of 0.1 μs. The similarity of the data and mathematical curve suggests that the standard deviation of the range measurements is approximately 0.1 μs which represents 49.2 feet in two-way ranging.

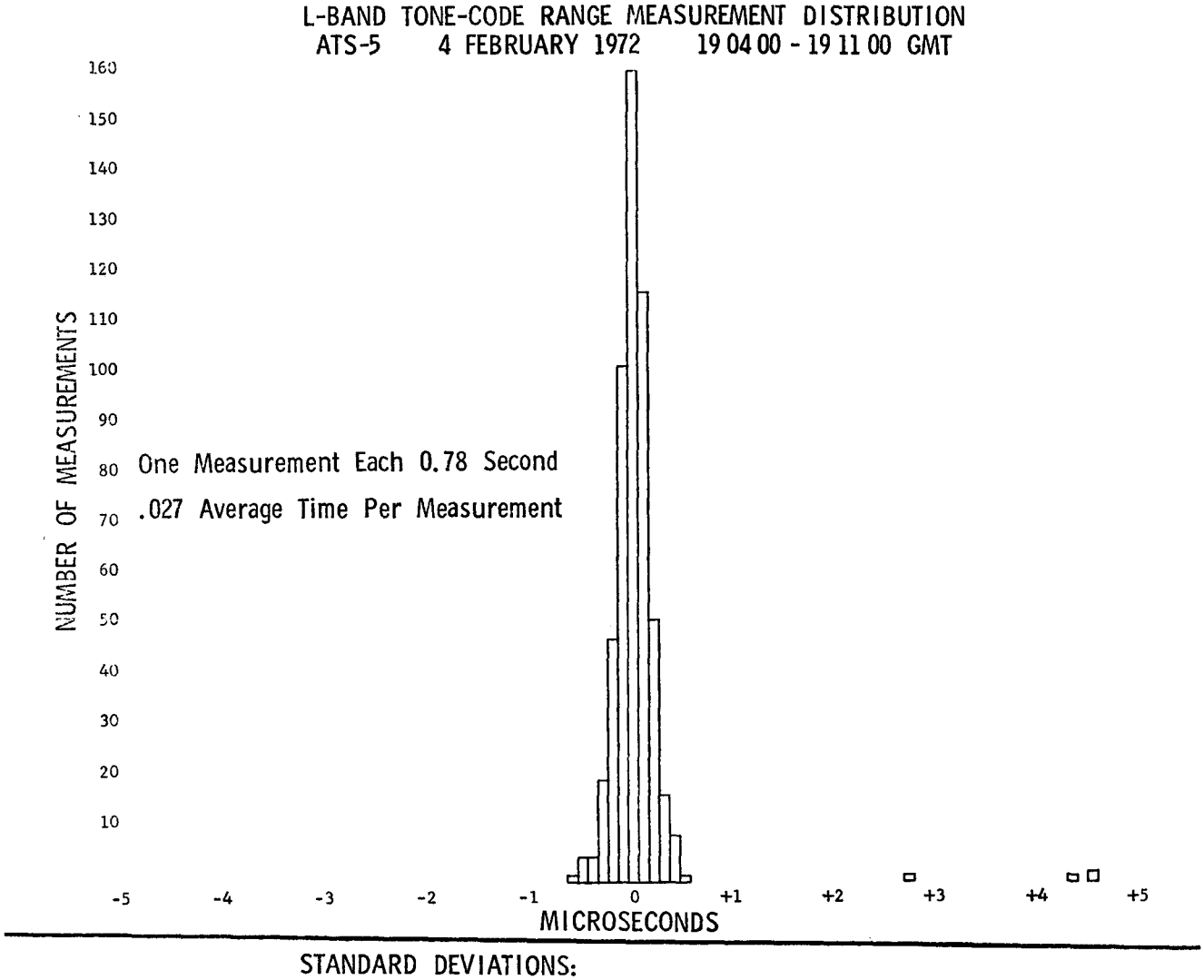

STANDARD DEVIATIONS:
19 06 30 - 19 09 30 GMT

Single Measurements	0.1385 Microseconds,	68 feet
9 Measurement Averages	0.0435 Microseconds,	21 feet
99 Measurement Averages	0.0096 Microseconds,	5 feet

FIGURE 25

Time Interval	Address Number Hours Minutes Seconds
02595629	12165439
02595628	12165440
02595627	12165441
02595628	12165442
02595625	12165442
02595629	12165443
02595628	12165444
02595629	12165445
02595629	12165446
02595625	12165446
02595629	12165447
02595630	12165448
02595629	12165449
02595629	12165450

FIGURE 26. SAMPLE OF A PUNCHED TAPE RECORD

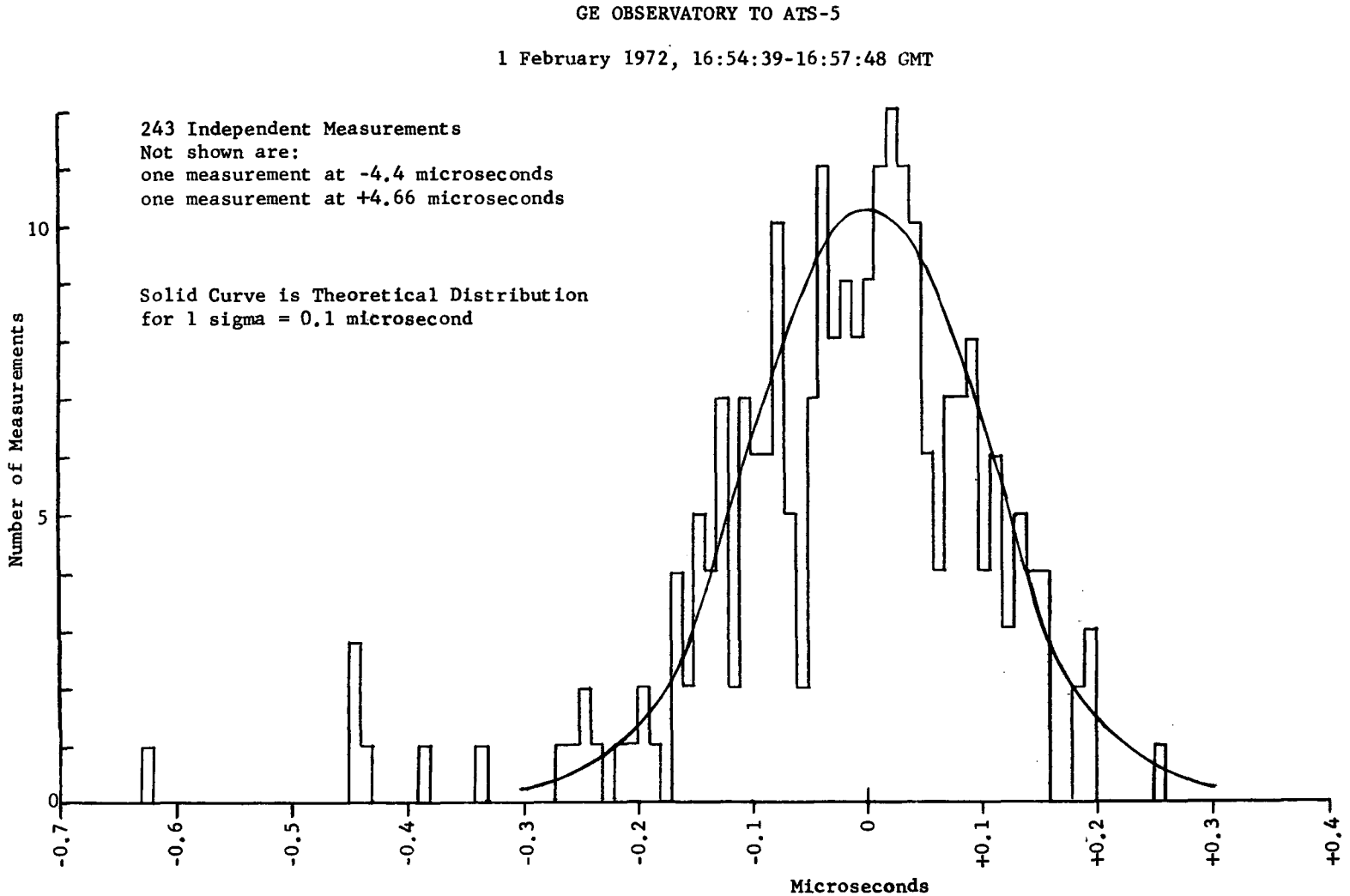

FIGURE 27. L-BAND RANGE MEASUREMENT SCATTER

The digital address codes are formed by suppressing a tone cycle for a digital zero and transmitting a tone cycle for a digital one. The transmission rate at L-band is 9.7656 kilobits per second. The technique of suppressing a cycle for zero is considered to be equivalent to 3 dB worse signal-to-noise ratio than the phase shift keying technique of reversing tone phase. Therefore the technique used in the experiment is less efficient than phase shift keying which we would recommend for an operational system. The measurement of error rates in the experiment can be related to the error rates that would be achieved with other digital keying techniques. Each tone-code ranging response contains 30 digital bits. The chart recordings of the returned signals include a record of the number of bits in error in each response. Although the data were recorded the magnitude of the effort to make a large statistical sampling was considered to be beyond the scope of the contract effort so that bit error rates were not routinely determined. One difficulty in reducing the data taken during the experiment is that the L-band signal-to-noise ratio during the received code is not well defined. The timing of the code is adjusted to be near the trailing edge of the window where the received signal level from ATS-5 is changing rapidly. A small drift in time of the received code relative to the window can therefore result in a rather large change in signal-to-noise ratio.

During a test period on 5 September 1972 care was taken to maintain the code placement in the window so that the signal-to-noise ratio was approximately 15 dB in the 60 kHz bandwidth of the receiver. During that test there were three bits in error in 82,350 received bits.

5.4 VHF Standard Deviations

Under Contract MA2-4066 with the Maritime Administration a series of experiments was conducted to observe the change in standard deviation as a function of signal level with the tone-code transponder located at the National Maritime Research Center, Kings Point, New York. The transmitted power from the tone-ranging transponder at the National Maritime Research Center was 300 Watts. The transmitting antenna was an eight turn circularly polarized helix. Its effective gain when transmitting through the linearly polarized antennas of ATS-3 was 10 dB. Ranging measurements were made with transmitter powers of 300, 30, 10 and 5 Watts. The signal-to-noise ratio when transmitting with 5 Watts from Kings Point and received at Schenectady on a four turn helical antenna was just above the detection threshold for the FM signal, so that it represents the worst standard deviations that would be obtained with the system. Signal levels very much lower would not correlate and would therefore not produce range measurements. Figure 28 shows the change in the standard deviation, the largest single range measurement errors, and plots histograms of the measurements that were between +2 and -2 μs from the best fit curves of the data. The precision of range measurement in the two-way ranging experiment is shown by the scales in microseconds standard deviation, slant range deviation in feet, and the deviation in latitude when the lines of position are projected at Kings Point.

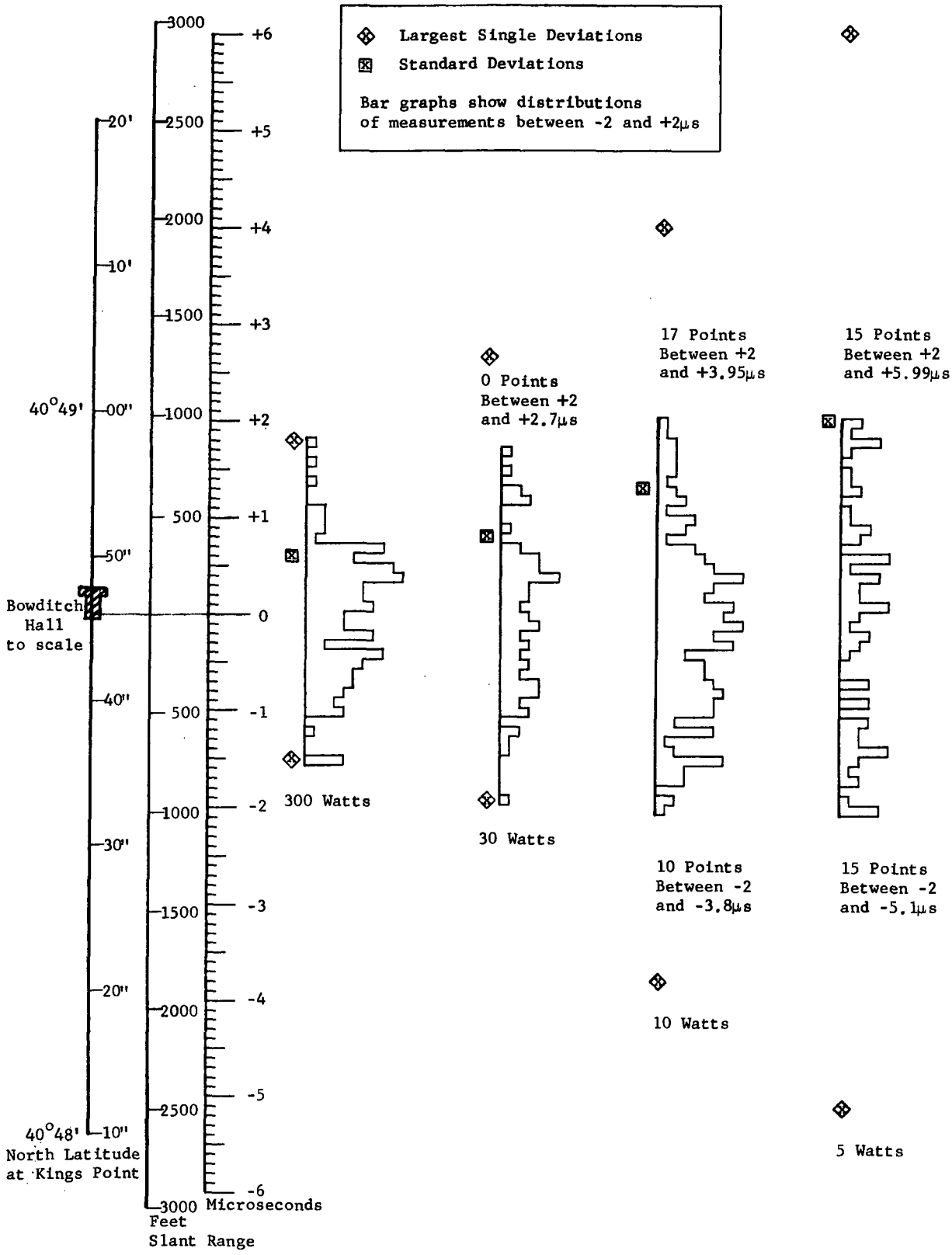

FIGURE 28. SLANT RANGE AND LATITUDE PRECISION VERSUS POWER TRANSMITTED FROM KINGS POINT

5.5 Twenty-four Hour Position Fixing Experiment

A twenty-four hour test using the L-band/VHF transponder was conducted between 1600 GMT on 30 November 1972 to 1510 GMT on 1 December 1972. Test results show the effect of the diurnally changing range errors in the predictions of satellite positions, and demonstrated a position fix precision approaching 0.1 nautical mile for the signalling parameters used with the transponder. Application of independently derived ionospheric propagation delay measurements show the magnitude of ionosphere delay on position fixes for the range measurements at VHF from ATS-3 to the transponder.

Ten minutes of test time each hour were assigned to ATS-5 and ATS-3. The first test period was from 1600 to 1610, the second from 1730 to 1740, and the remaining periods were from the hour to ten minutes after the hour. Except for minor variations, the procedure during each ten minute period was to interrogate in sequence the L-band/VHF transponder with user code 11, the VHF transponders at Shannon, Reykjavik, Kings Point, Buenos Aires and Seattle for approximately eight minutes. The interrogation rate was once each two spin periods of ATS-5, or an interrogation each 1.56 seconds. The L-band/VHF transponder was then interrogated with user code 12 to initiate 101 responses at the spin rate of ATS-5, a procedure that required the remaining time of the ten minute period.

Each ten minute period thus provided about eleven independent two-way measurements of range from ATS-3 and ATS-5 to the L-band/VHF transponder, and approximately the same number of range measurements from ATS-3 to each of the distant transponders. It also provided a sequence of 101 one-way measurements of range from the L-band/VHF transponder to ATS-5 on L-band and to ATS-3 on VHF. The two-way, two-satellite measurements from the L-band/VHF transponder were used to compute position fixes for the transponder based on NASA's predictions of satellite positions. The 101 measurement sequences were used to compute standard deviations of range measurements at L-band and VHF. The range measurements from ATS-3 to each of the distant transponders are available for trilateration computation of ATS-3 locations for comparison with NASA predictions.

A total of 256 position fixes were computed from two-satellite range measurements made during the twenty-four hour test. The number of fixes during each ten minute period are given in Table 10. All interrogations that resulted in range measurements from the two satellites were used to compute fixes. No data were rejected and all of the position fixes are presented.

The transponder failed to respond to eleven interrogations during the twenty-four hour test. They are identified as "missed returns" in Table 10. The missed returns resulted in recorded numbers representing ranges from the satellites to points within the sphere of the earth. The range-time interval counters are set to stop counting after a period of time much longer than expected of any range measurement interval. The counters must stop before the next generation, or they will not be available for the following range measurement. During the test, they were set to stop counting at a limit representing a range within the dimensions of the earth, so that the computer processed them producing false readings

TABLE 10

SUMMARY OF TWENTY-FOUR HOUR TEST RESULTS

11/30/72	16:00:02 - 16:09:33	9 fixes	1 missed return
	17:36:04 - 17:44:40	9 fixes	1 missed return
	18:02:25 - 18:07:08	7 fixes	0 missed returns
	19:00:03 - 19:09:40	12 fixes	0 missed returns
	20:00:39 - 20:09:14	8 fixes	1 missed return
	21:35:03 - 21:43:41	10 fixes	1 missed return
	22:00:03 - 22:09:31	11 fixes	1 missed return
	23:00:09 - 23:09:34	12 fixes	0 missed returns
12/01/72	00:00:01 - 00:09:14	12 fixes	0 missed returns
	01:00:03 - 01:09:30	12 fixes	0 missed returns
	02:00:03 - 02:09:33	12 fixes	0 missed returns
	03:00:08 - 03:09:33	9 fixes	1 missed return
	04:00:27 - 04:09:41	11 fixes	1 missed return
	05:00:26 - 05:09:40	11 fixes	1 missed return
	06:00:36 - 06:09:14	11 fixes	0 missed returns
	07:00:06 - 07:09:32	10 fixes	0 missed returns
	08:00:12 - 08:09:14	11 fixes	0 missed returns
	09:00:01 - 09:09:14	11 fixes	1 missed return
	10:00:03 - 10:09:28	12 fixes	0 missed returns
	11:00:05 - 11:08:43	11 fixes	0 missed returns
	12:00:10 - 12:09:35	12 fixes	0 missed returns
	13:00:26 - 13:09:40	11 fixes	0 missed returns
	14:00:03 - 14:09:28	10 fixes	2 missed returns
	15:00:02 - 15:09:32	12 fixes	0 missed returns

of position fixes on the far side of the earth from the satellites. These fixes were obviously in gross error. This was an occurrence not experienced previously in any experiments, and one easily avoided by lengthening the cutoff time of the time interval counters to make them represent ranges longer than the distances from the satellites to the farthest point of the sphere in space occupied by the earth.

All 256 position fixes for the L-band/VHF transponder are plotted on the mercator projection chart, Figure 29. The actual location of the transponder, 42°50'53" north latitude and 74°04'15" west longitude, is shown as the intersection of the lines forming the encircled cross. One arbitrarily chosen fix from each hourly interrogation period is shown as a small cross and is identified by the exact time it was made. All of the other fixes are shown as dots. The fixes shown as crosses are presented to show the time progression of fix error. For clarity, the fixes shown as crosses are presented without the other fixes in Figure 30.

The time progression of fix error forms an ellipse on the surface of the earth. The ellipse is traced once in twenty-four hours. The ellipse is formed because there are errors in the NASA predictions of satellite locations. The range errors have a twenty-four hour period. Figure 31 presents a simplified illustration for the diurnal period of range error. The satellites are not in perfect geostationary orbit. A slight inclination of a satellite's orbit plane, caused in part by attraction of the sun and moon, causes the satellite to move north and south of the equator. Relative to the earth's surface, it traces a figure eight, completing the figure in one orbit of the earth; i.e., in twenty-four hours. The motion of the satellite relative to the equator and a point at a higher latitude is depicted in Figure 31. If there is a small error in predicting the satellite motion, there is a nearly sinusoidally changing difference between actual range to the satellite and its predicted range. For example, if the positions of the satellite at specified times are as shown by the filled circles in the figure and the predicted positions for the specified times are as shown by the open circles, the actual measured range is longer than the predicted range at time T, while the actual measured range is shorter than the predicted range at T_2. The predicted locations and the measured ranges are used in computing the position fixes. As a result, the computed line of position for each satellite moves sinusoidally with a twenty-four hour period. The amplitude of the sinusoid is proportional to the magnitude of the error in satellite prediction. The magnitudes and phases of the sinusoids of the two satellites are independent, hence the time progression of the position fixes of a stationary transponder traces an ellipse with its major and minor axes depending on the magnitudes and relative phases of the prediction errors of the two satellites.

NASA tracked the satellites by range and range rate measurements at C-band from Rosman, North Carolina and Mojave, California on the day prior to the twenty-four hour test. NASA computed the latitude, longitude, and earth center distance of each satellite and furnished predictions to General Electric for each half hour for the day of the test. General Electric's POSFIX program uses the NASA predictions and makes a third order interpolation of satellite position for the nearest second of

FIGURE 29

ALL THE TWO-SATELLITE FIXES MADE IN TWENTY-FOUR HOUR TEST

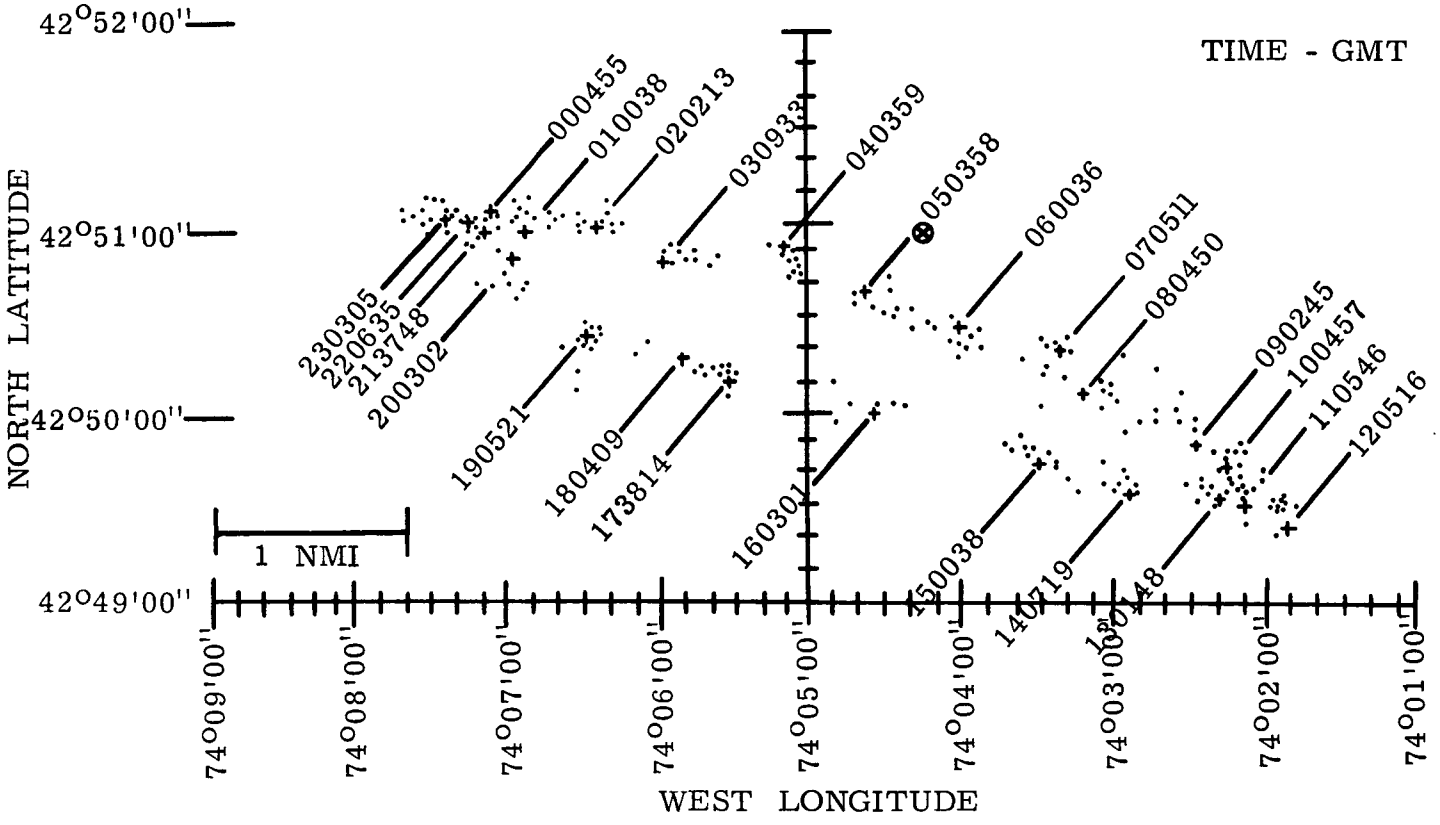

⊗ Location of Transponder

+ · Position Fixes (Fixes plotted as + chosen arbitrarily to show time progression of fix error.)

Twenty-four hour satellite test conducted by the General Electric Company, Schenectady, N. Y. from 1600 GMT on 30 November 1972 to 1510 GMT on 1 December 1972. Interrogations were made at VHF via ATS-3 and responses at VHF via ATS-3 and L-band via ATS-5.

FIGURE 30

DIURNAL PATTERN OF FIX ERRORS

Errors in satellite position predictions caused fixes to trace an ellipse.

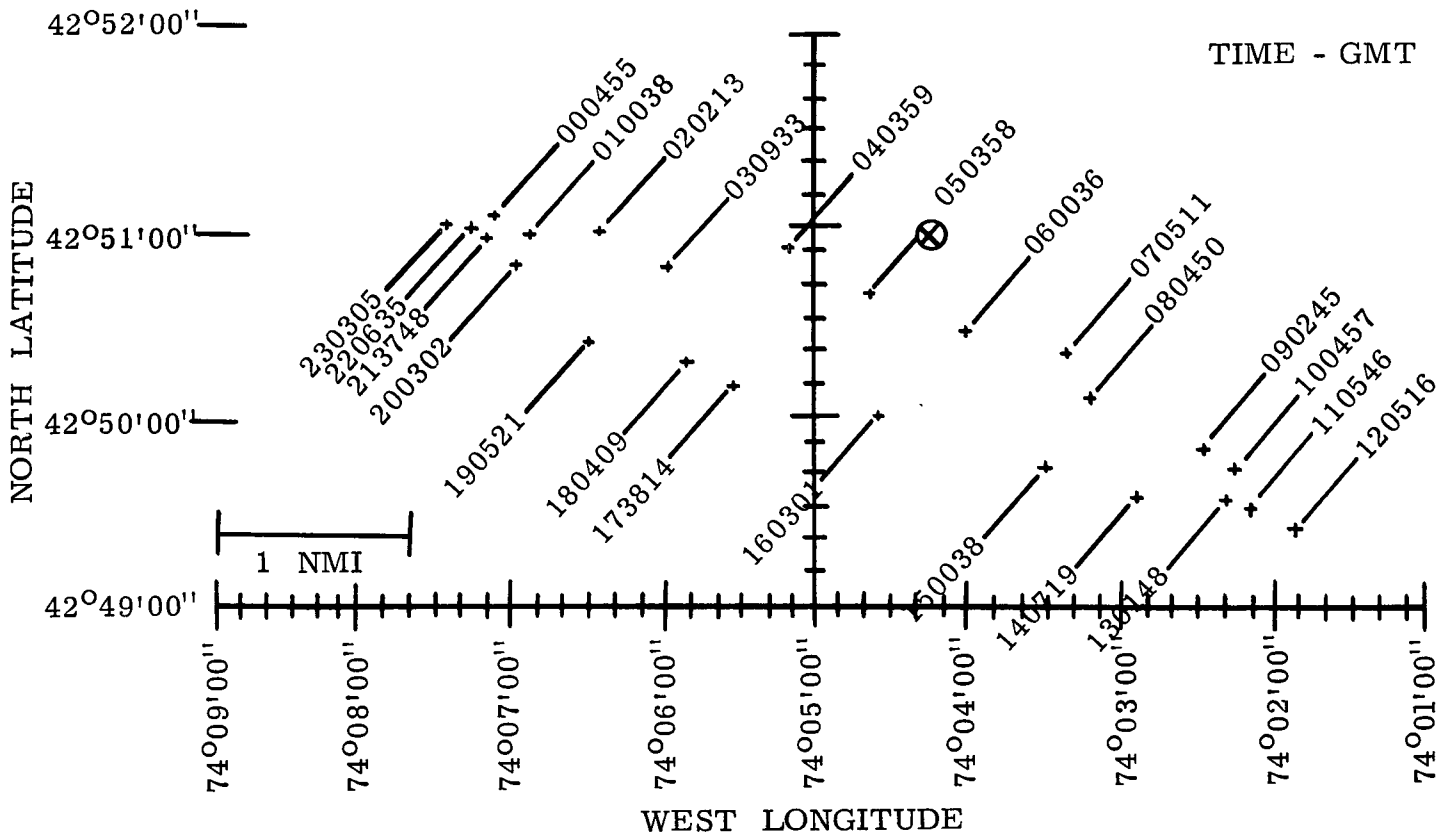

⊗ Location of Transponder
\+ Position Fix (arbitrarily chosen fixes to show time progression of fix error.)

Twenty-four hour satellite test conducted by the General Electric Company, Schenectady, N. Y. from 1600 GMT on 30 November 1972 to 1510 GMT on 1 December 1972. Interrogations were made at VHF via ATS-3 and responses at VHF via ATS-3 and L-band via ATS-5.

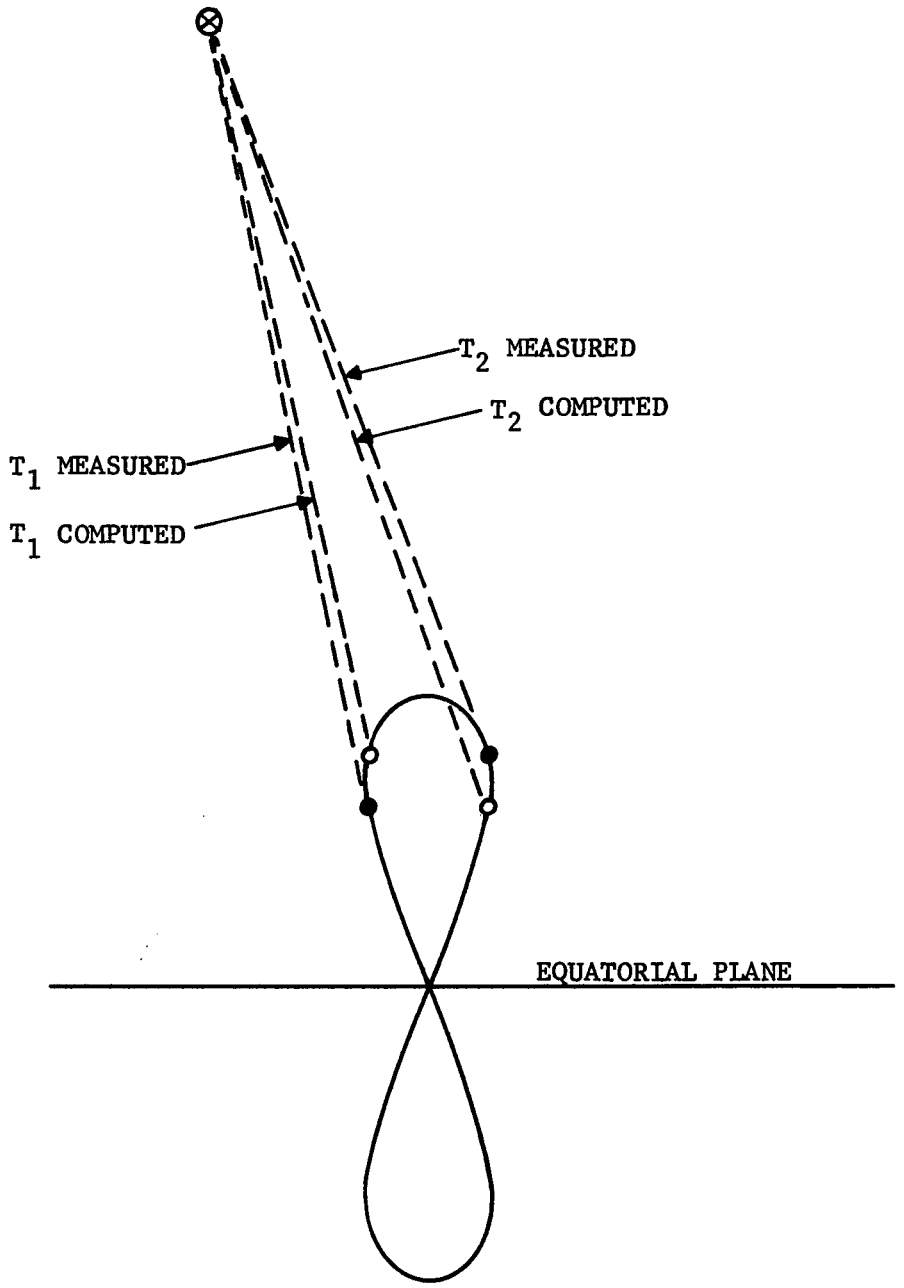

● ACTUAL POSITION
o PREDICTED POSITION

T_1 MEASURED > T_1 COMPUTED
T_2 MEASURED < T_2 COMPUTED

FIGURE 31

CAUSE OF DIURNAL CHANGE IN DIFFERENCE BETWEEN COMPUTED AND MEASURED SLANT RANGES

time to each interrogation of the platform. It uses the interpolated satellite positions as references in computing the transponder location.

On the day of the test ATS-3 moved 3.095° north and south, a distance of 1200 nmi. above and below the earth's equatorial plane. Its earth center distance changed 120.88 nmi. These motions, plus a small east-west excursion, caused a total slant range change of approximately 345 nmi. from Schenectady. The difference between the measured slant range and the slant range computed from the NASA predictions varied sinusoidally through the twenty-four hour period as shown by the solid line curve in Figure 32, where range is expressed in microseconds propagation time. One microsecond is equivalent to 492 feet in two-way ranging. The peak magnitude in slant range error due to NASA's prediction error was +10.5 μs at 0000 GMT and -10.5 μs at approximately 1200 GMT. The peak-to-peak magnitude of the slant range error based on NASA predictions is 21 μs or 1.7 nmi., which is 0.5% of the total slant range change.

The displacement of the axis of the sine wave curve from zero is the bias resulting from error in estimating the equipment time delay. The bias error of -3.6 μs represents a slant range error toward the satellite of 1540 feet.

ATS-5 moved 0.43° north and south of the equator of 170 nmi. above and below the earth's equatorial plane. Its earth center distance changed 79.09 nmi. These motions relative to the earth caused a total slant range change of approximately 105 nmi. from Schenectady. The difference between the measured and computed slant range varied in the sinusoidal manner shown by the dashed curve of Figure 32. The peak error due to the NASA position prediction was +8.1 μs at approximately 0930 GMT and -8.1 μs at approximately 2130 GMT. The peak-to-peak slant range error due to satellite position prediction error was 1.3 nmi., or approximately 1% of the total range change. The slant range bias due to error in the estimate of equipment time delay was 6 μs or 2950 feet.

In addition to the time progression of the position fixes as shown in Figure 30, the fixes are biased away from the true location of the transponder. The center of the ellipse is 0.6 mile from the true location. The most likely cause of the bias error is in the estimate of the time delay within the transponder circuits.

5.6 Ionosphere Effects at VHF

The twenty-four hour test provided a means to evaluate the effect of the ionosphere on the VHF range measurements from ATS-3 to the transponder. Mr. Jack Klobuchar of Air Force Cambridge Research Laboratories provided independent measurements of the columnar electron content to ATS-3 as measured by the Faraday rotation technique. Air Force Cambridge Research Laboratories measures the ionosphere electron content from Sagamore Hill, Massachusetts to ATS-3 at VHF. A twenty-four hour test in March, 1970 compared ionosphere propagation delay derived from range measurements at Gander, Newfoundland and Schenectady, New York with ionosphere propagation delay derived from Air Force Cambridge Research Laboratories electron content measurements. The measurements at Gander, 900

FIGURE 32

ESTIMATED ERRORS IN SLANT RANGE VECTORS DUE TO SATELLITE PREDICTION ERRORS (SINE CURVES)
ESTIMATED EQUIPMENT DELAY BIAS ERRORS (0 AXIS DISPLACEMENT)

Twenty-four hour satellite test conducted by the General Electric Company, Schenectady, New York from 1600 GMT on 30 November 1972 to 1510 GMT on 1 December 1972. Interrogations were made at VHF via ATS-3 and responses at VHF via ATS-3 and L-band via ATS-5.

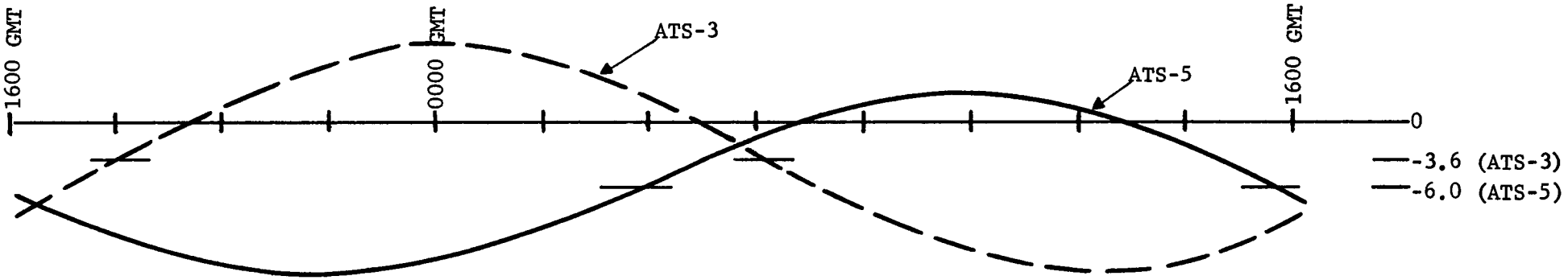

ATS-3 Slant Range Vector Error +10.5μs at ~ 0000 GMT, -10.5μs at ~ 1200 GMT
ATS-5 Slant Range Vector Error + 8.1μs at ~ 0930 GMT, - 8.1μs at ~ 2130 GMT

ATS-3 Error in Estimate of Equipment Delay -3.6 μs
ATS-5 Error in Estimate of Equipment Delay -6.0 μs

FROM PREDICTIONS:

ATS-3	Max. North 3.095°N at 1100, 1 December	Max. South 3.095°S at 2300, 30 November
	Max. Earth Center Distance - 22815.11 nmi. at 1830	Min. Earth Center Distance - 22694.23 nmi. at 0630
ATS-5	Max. North 0.430°N at 1430, 1 December	Max. South 0.430°S at 0230, 1 December
	Max. Earth Center Distance - 22791.68 nmi. at 0600	Min. Earth Center Distance - 22712.59 nmi. at 1800

FROM RANGE MEASUREMENTS:

ATS-3	Max. Range Time Interval - 254772μs at ~ 1000 GMT	Min. Range Time Interval - 250507μs at ~ 2145 GMT
ATS-5	Max. Range Time Interval - 257271μs at ~ 0514 GMT	Min. Range Time Interval - 256002μs at ~ 1710 GMT

miles ENE of Schenectady, and at Sagamore Hill, 150 miles east of Schenectady, were highly correlated with the Schenectady measurements. The 1970 experience, and other data, lead to the conclusion that the ionosphere as measured at Sagamore Hill is very nearly like the ionosphere at Schenectady and that the independent measurements of the ionosphere by Air Force Cambridge Research Laboratories may be applied directly to the range measurements at Schenectady.

The "POSFIX" program contains a model of the ionosphere for correcting VHF measurements. Figure 33 compares the effect of the ionosphere on VHF measurements on 13-14 March 1970, 30 November-1 December 1972, and the model in the "POSFIX" program. The 1970 measurements were made near the peak of the sunspot cycle. The year 1972 is about half-way from maximum to minimum in the eleven year cycle. The model in the "POSFIX" program lies between the values observed on the specific days of the 1970 and 1972 twenty-four hour tests.

The position fixes of Figures 29 and 30 have had the ionosphere effect removed from the ATS-5 lines of position because they were made at L-band where the effect on range measurements is less than 1% of the effect at VHF. The ionosphere model of the "POSFIX" program was used for the ATS-3 lines of position in computing the position fixes of Figures 29 and 30.

The data supplied by Air Force Cambridge Research Laboratories was used to correct the fixes for ionosphere delay as it actually was on the day of the test. Differences between the measured and model ionospheres were used by graphical projection to correct the fixes. Figure 38 shows the computed fixes as crosses and the corrected fixes as circles.

Each position fix computed for the transponder is completely independent of all others. This was insured by the sequence of interrogation that included range measurements to other transponders between each interrogation of the L-band/VHF platform. The scatter of the fixes made within each ten minute period is therefore an indication of fix precision. Within the ten minute periods, there is some time progression along the ellipse - one-sixth of the progression made in the hour. Figures 35 and 36 are sets of fixes made within ten minute periods to convey the magnitude of their scatter. Although no rigorous analysis was made, it is apparent that the standard deviation of the fixes approaches 0.1 nmi., 1 sigma. It is emphasized that the fixes were made with one range measurement at VHF, one at L-band; that the tone frequency was 2.4414 kHz at VHF, 9.7656 kHz at L-band; and the phase measurement averaging time was 0.105 second at VHF, and 0.027 second at L-band. Higher precision could be achieved with longer phase measurement averaging time.

The magnitude of slant range error and its phase through the day can be derived for each satellite from the corrected position fixes by projecting the fixes on the azimuth directions to the satellites and multiplying by the cosine of the elevation angle. Figure 32 presents the slant range vector component of NASA's prediction error as observed by Schenectady.

If it is assumed that the slant range error in the predictions is symmetrical about a mean value that has no bias, and that all of the bias

FOLDOUT FRAME

FIGURE 33

POSFIX MODEL IONOSPHERE VERSUS ACTUAL ON TWO DAYS, APPROXIMATELY 2 1/2 YEARS APART

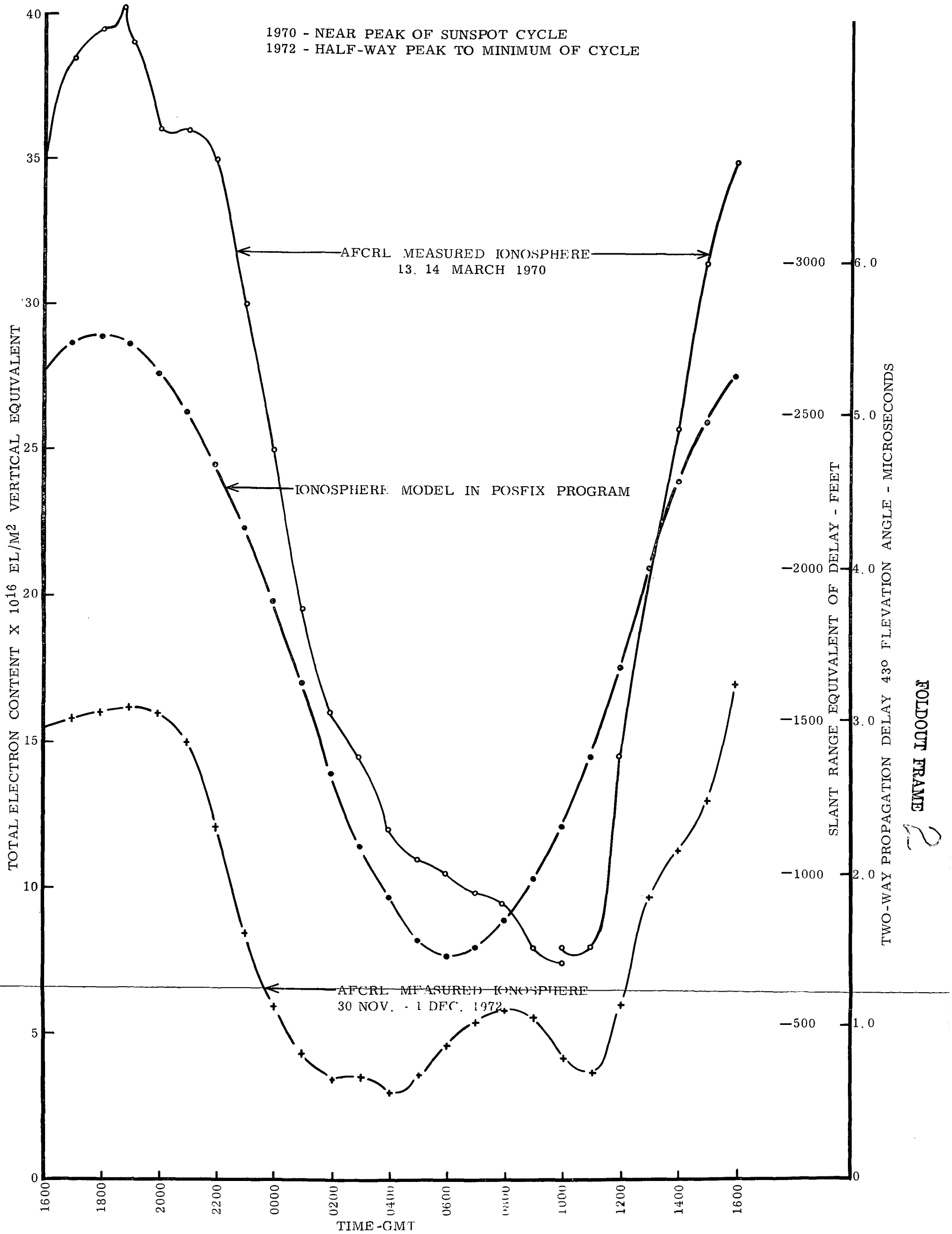

FOLDOUT FRAME

FIGURE 34

DIFFERENCE IN FIXES - ACTUAL IONOSPHERE VERSUS MODEL

Ionosphere affects only VHF ranging from ATS-3.

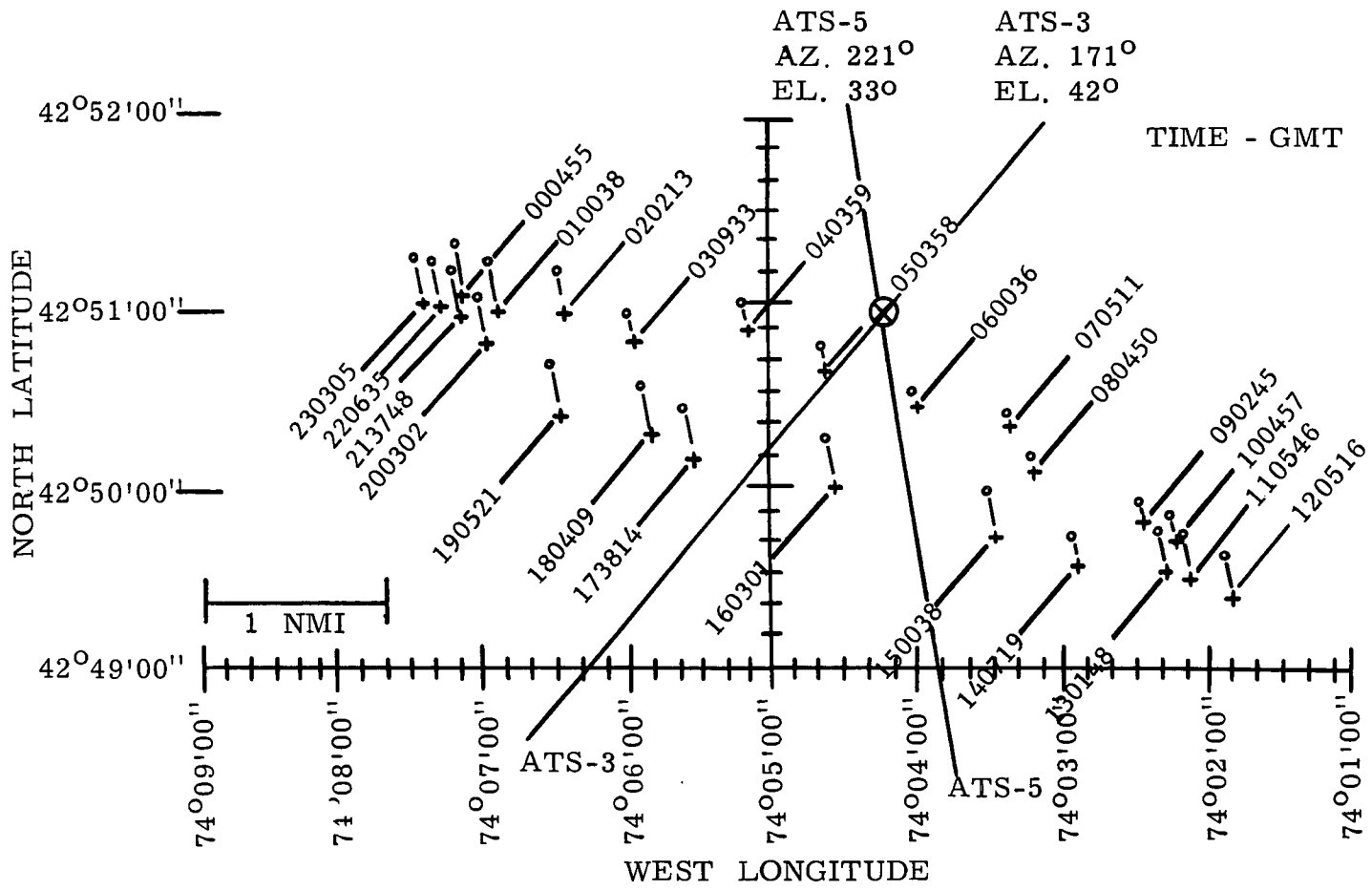

⊗ Location of Transponder
\+ Position Fixes Using Ionosphere Model in Posfix Program
∘ Position Fixes Corrected Using AFCRL Data (Actual Ionosphere)

Twenty-four hour satellite test conducted by the General Electric Company, Schenectady, N. Y. from 1600 GMT on 30 November 1972 to 1510 GMT on 1 December 1972. Interrogations were made at VHF via ATS-3 and responses at VHF via ATS-3 and L-band via ATS-5.

FIGURE 35

SCATTER OF POSITION FIXES

Clusters of fixes made within ten minute periods suggest precision approaching 1 nmi., 1 sigma.

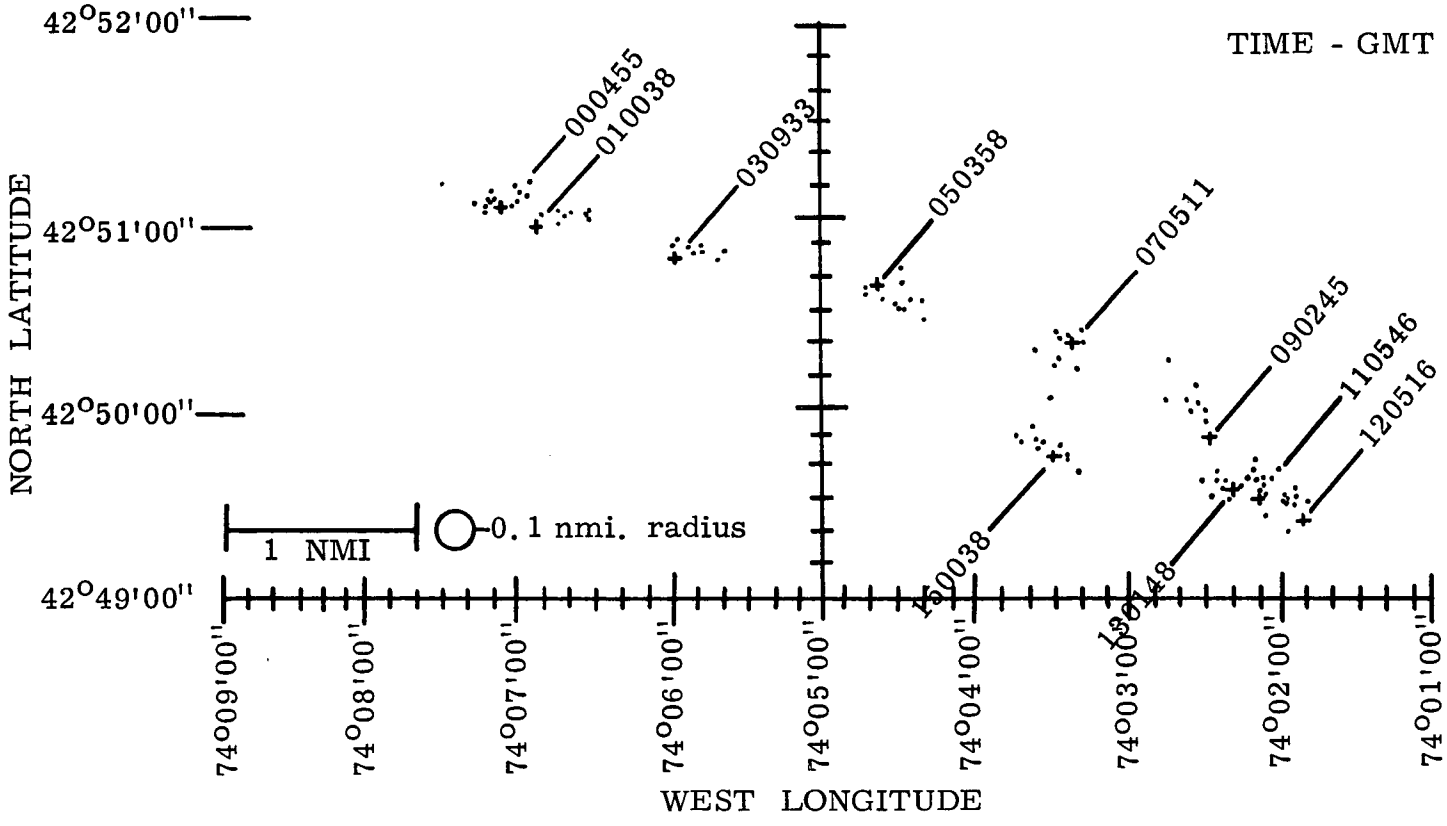

⊗ Location of Transponder

+ · Position Fixes (Fixes plotted as + chosen arbitrarily to show time progression of fix error.)

Twenty-four hour satellite test conducted by the General Electric Company, Schenectady, N. Y. from 1600 GMT on 30 November 1972 to 1510 GMT on 1 December 1972. Interrogations were made at VHF via ATS-3 and responses at VHF via ATS-3 and L-band via ATS-5.

SCATTER OF POSITION FIXES

Clusters of fixes made within ten minute periods suggest precision approaching 1 nmi., 1 sigma.

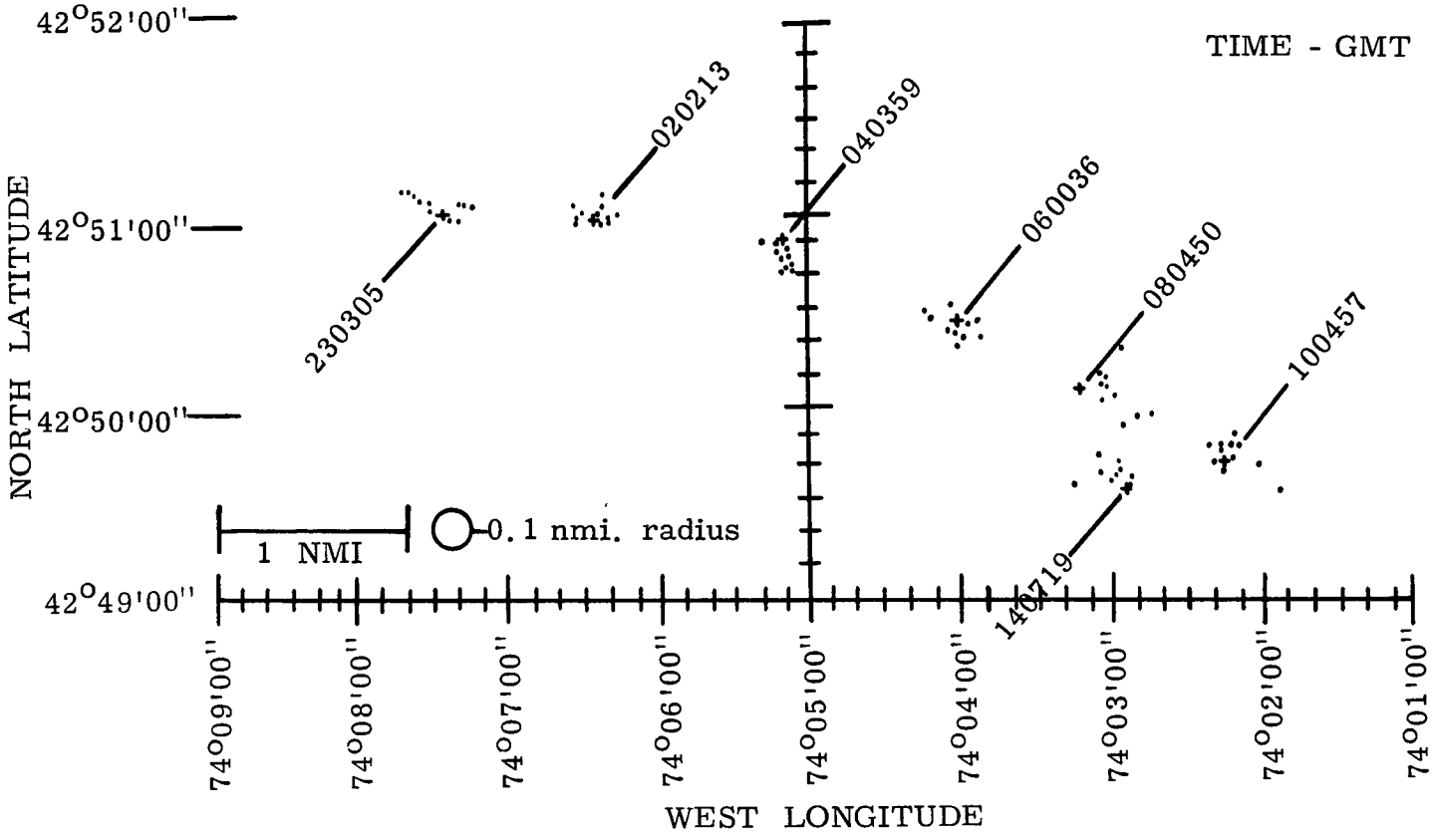

⊗ Location of Transponder

+ · Position Fixes (Fixes plotted as + chosen arbitrarily to show time progression of fix error.)

Twenty-four hour satellite test conducted by the General Electric Company, Schenectady, N. Y. from 1600 GMT on 30 November 1972 to 1510 GMT on 1 December 1972. Interrogations were made at VHF via ATS-3 and responses at VHF via ATS-3 and L-band via ATS-5.

error is due to wrong estimates of equipment delay, the estimate of equipment delay error can be derived by projecting the center of the ellipse onto the azimuth lines and relating it to the time delay correction necessary to move the lines of position to the true location of the transponder. By this means, the error in the estimate of equipment time delay at VHF is -3.6 μs, and at L-band -6.0 μs.

Differences between computed and measured slant ranges to each VHF transponder are shown in Figures 37 through 44. Each difference is the sum of two effects: propagation time delay in the ionosphere, and slant range vector component of the error in the satellite position prediction.

Ionosphere effects are different for each location because of latitude differences, difference in daylight hours, and uncorrelated variations in electron content at the separated locations. Slant range components of satellite prediction error are different because of the satellite-earth geometry.

No attempt was made to separate the ionosphere and prediction error components that contributed to the differences between computed and measured slant range for the distant transponders. The data may be compared with similar data reported in the Final Report on Phases 1 and 2, VHF Ranging and Position Fixing Experiment Using ATS Satellites.

COMPARISON OF DIFFERENCES,
MEASURED MINUS COMPUTED SLANT RANGES AT VHF,
ATS-3 TO EACH TRANSPONDER

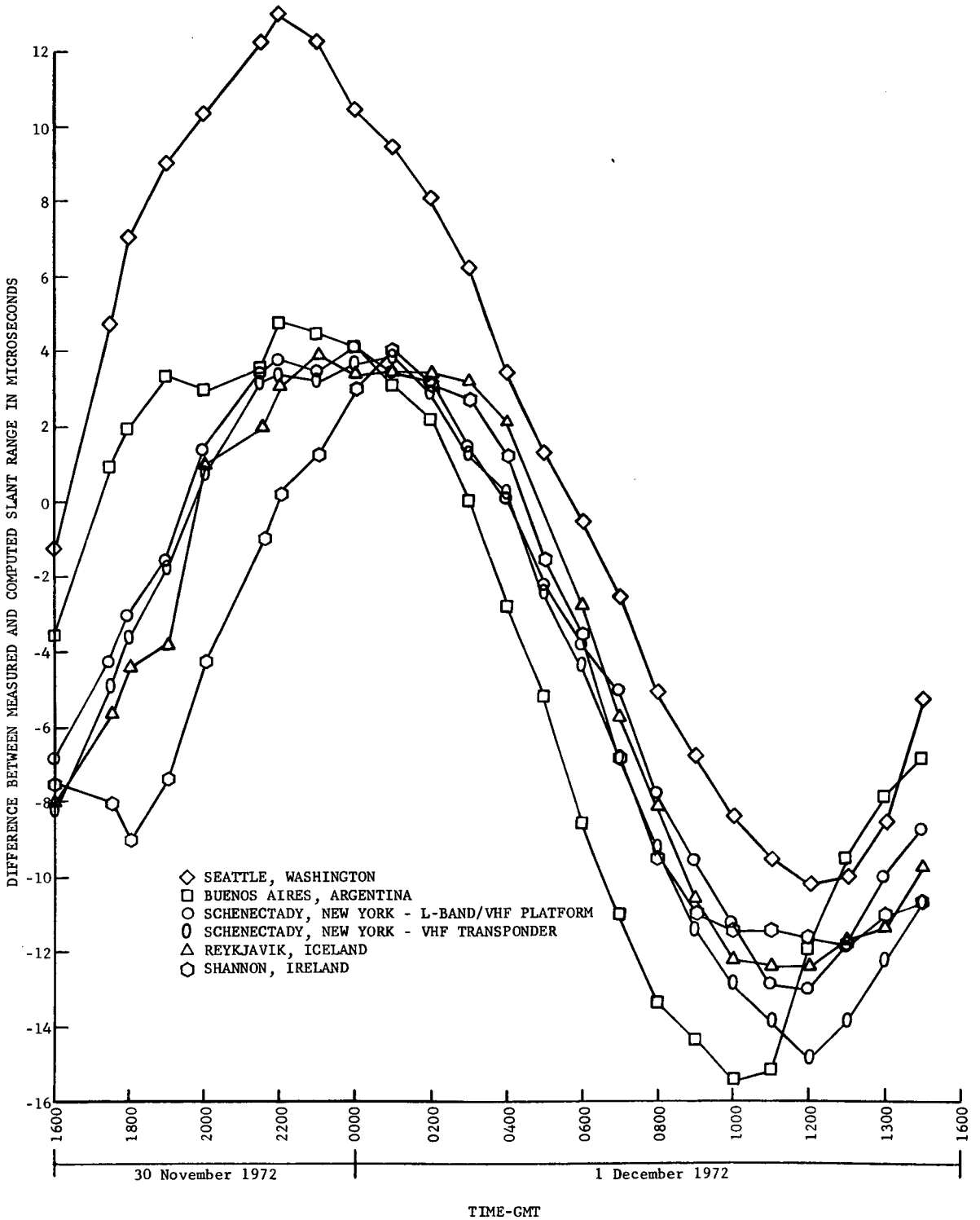

Differences are due to: 1) Ionosphere Propagation Delay; 2) Error in Predictions of Satellite Positions; 3) Error in Equipment Time Delay Calibration. 1 & 2 are cyclic with a 24 hour period; 3 is a fixed bias.

FIGURE 37

COMPARISON OF DIFFERENCES,
MEASURED MINUS COMPUTED SLANT RANGES AT VHF,
ATS-3 TO TRANSPONDER AT BUENOS AIRES, ARGENTINA

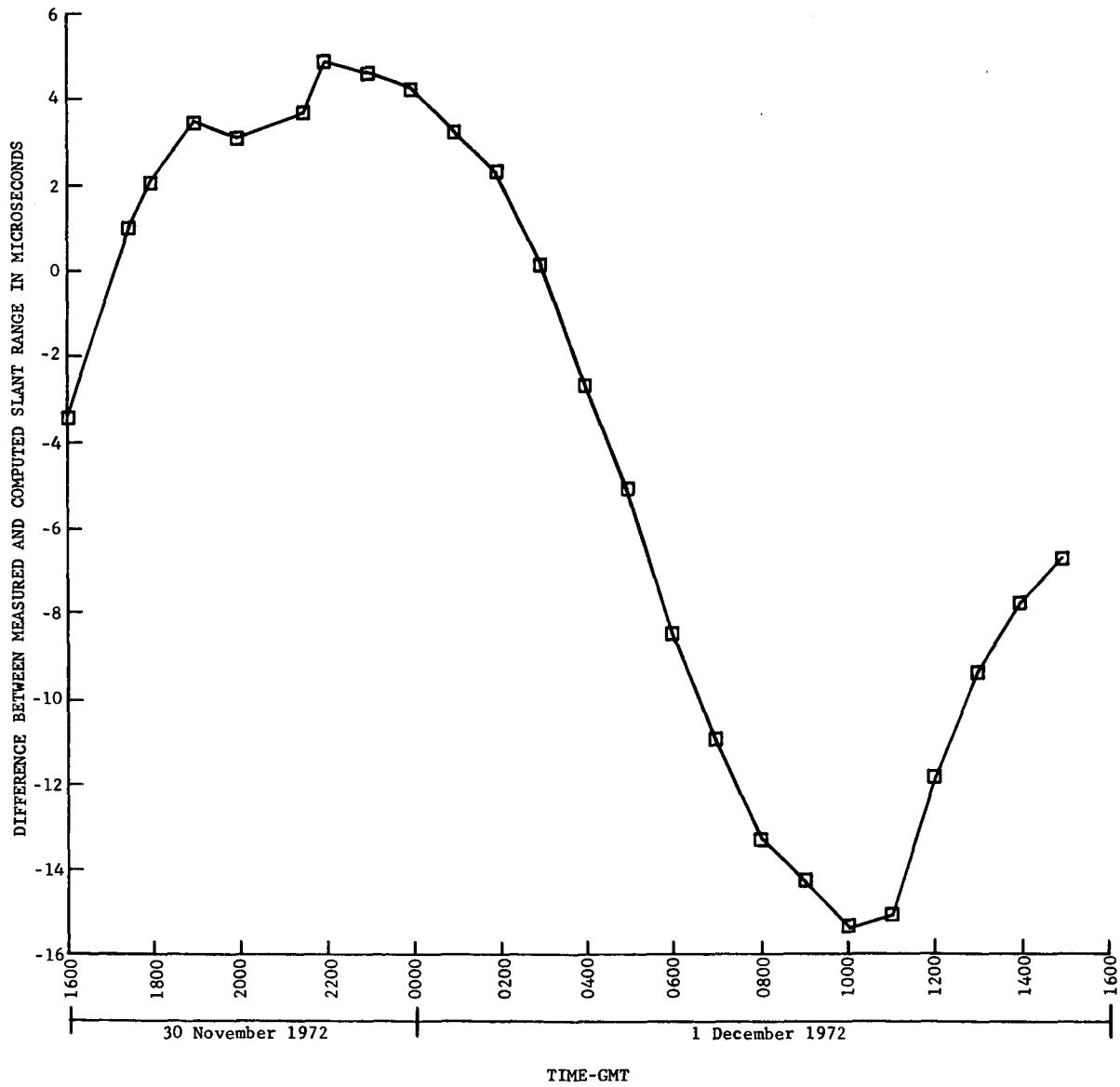

Differences are due to: 1) Ionosphere Propagation Delay; 2) Error in Predictions of Satellite Positions; 3) Error in Equipment Time Delay Calibration. 1 & 2 are cyclic with a 24 hour period; 3 is a fixed bias.

FIGURE 38

COMPARISON OF DIFFERENCES,
MEASURED MINUS COMPUTED SLANT RANGES AT VHF,
ATS-3 TO TRANSPONDER AT SHANNON, IRELAND

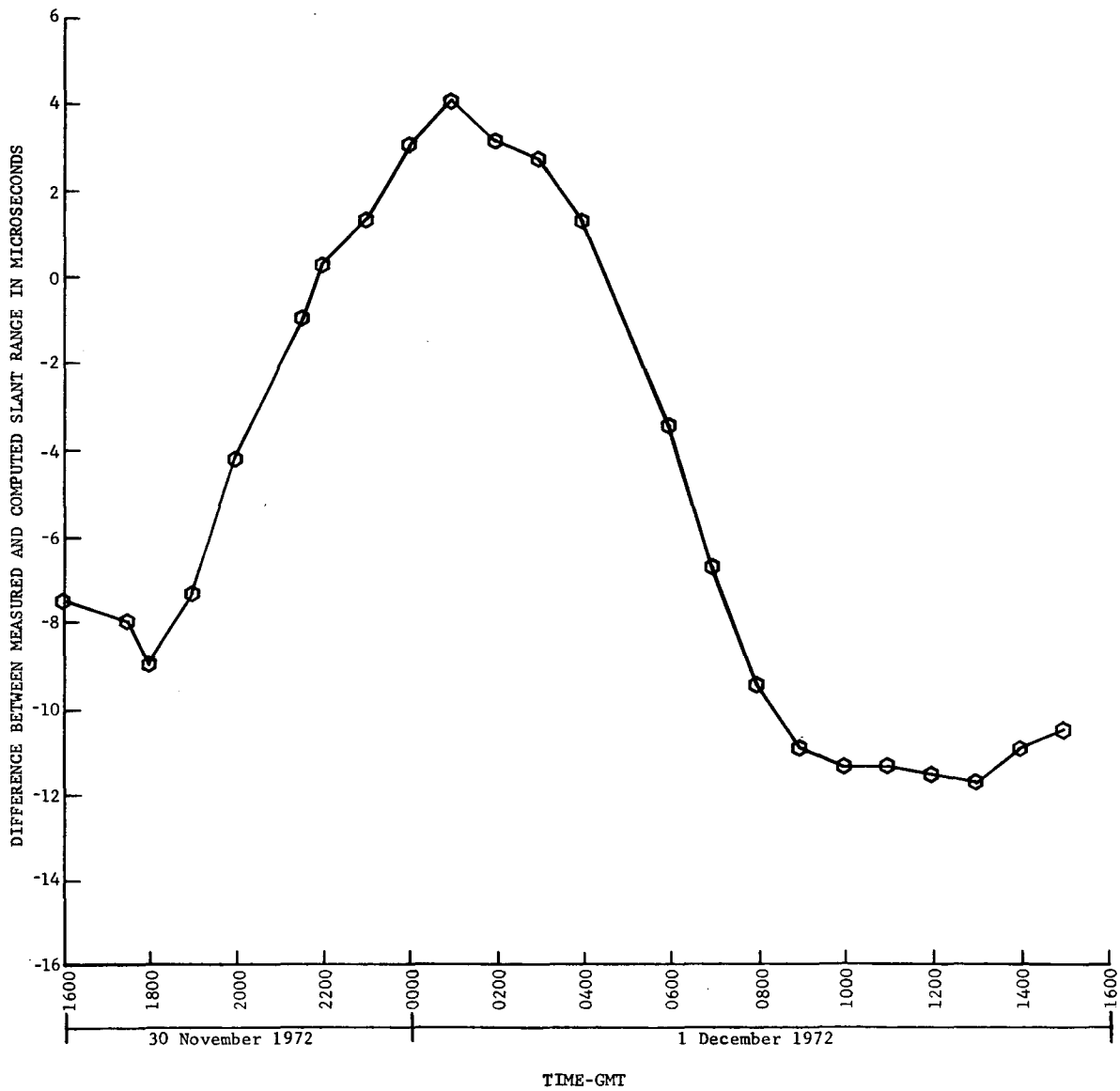

Differences are due to: 1) Ionosphere Propagation Delay; 2) Error in Predictions of Satellite Positions; 3) Error in Equipment Time Delay Calibration. 1 & 2 are cyclic with a 24 hour period; 3 is a fixed bias.

FIGURE 39

COMPARISON OF DIFFERENCES,
MEASURED MINUS COMPUTED SLANT RANGES AT VHF,
ATS-3 TO TRANSPONDER AT REYKJAVIK, ICELAND

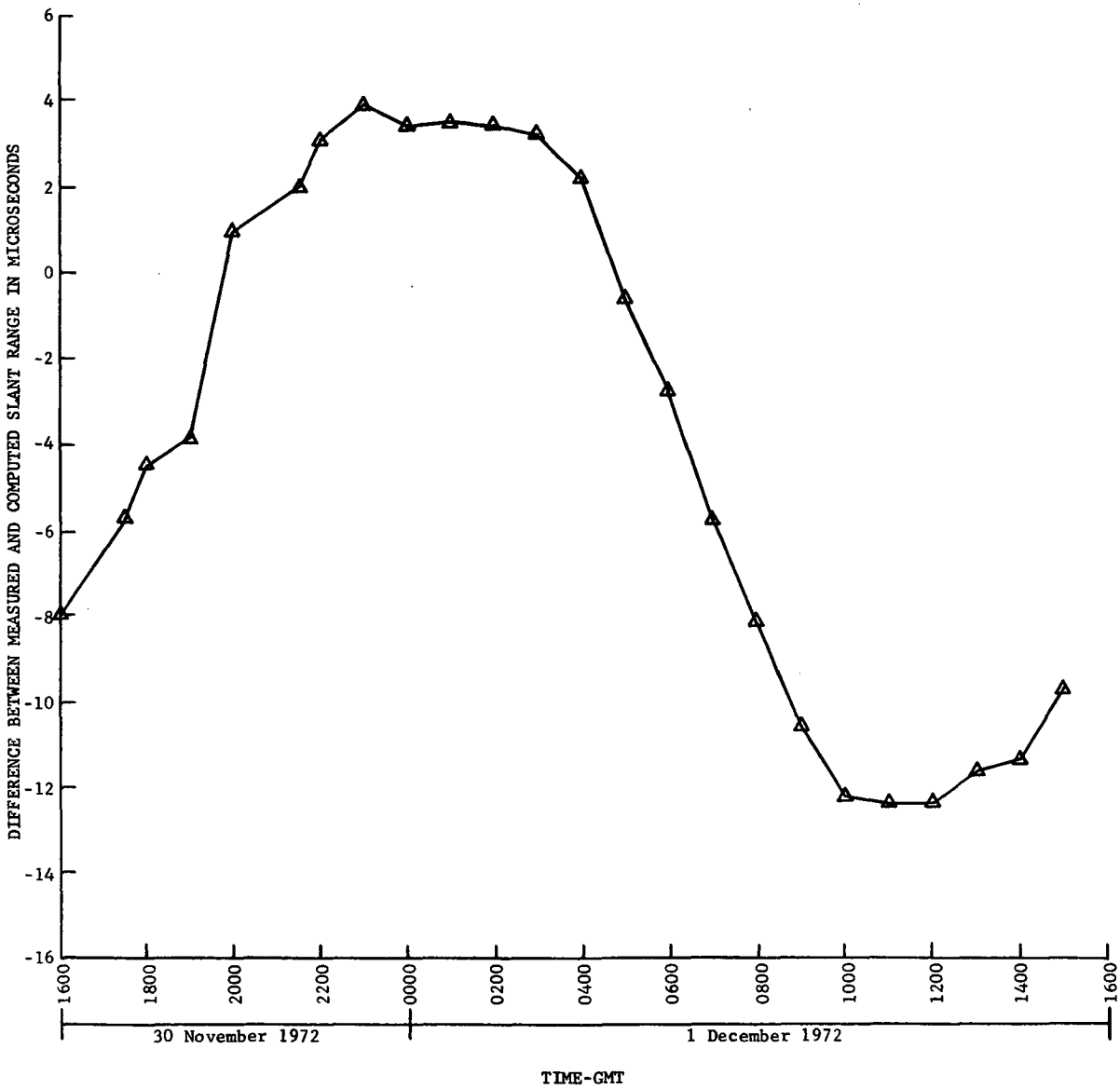

Differences are due to: 1) Ionosphere Propagation Delay; 2) Error in Predictions of Satellite Positions; 3) Error in Equipment Time Delay Calibration. 1 & 2 are cyclic with a 24 hour period; 3 is a fixed bias.

FIGURE 40

COMPARISON OF DIFFERENCES,
MEASURED MINUS COMPUTED SLANT RANGES AT VHF,
ATS-3 TO TRANSPONDER AT SEATTLE, WASHINGTON

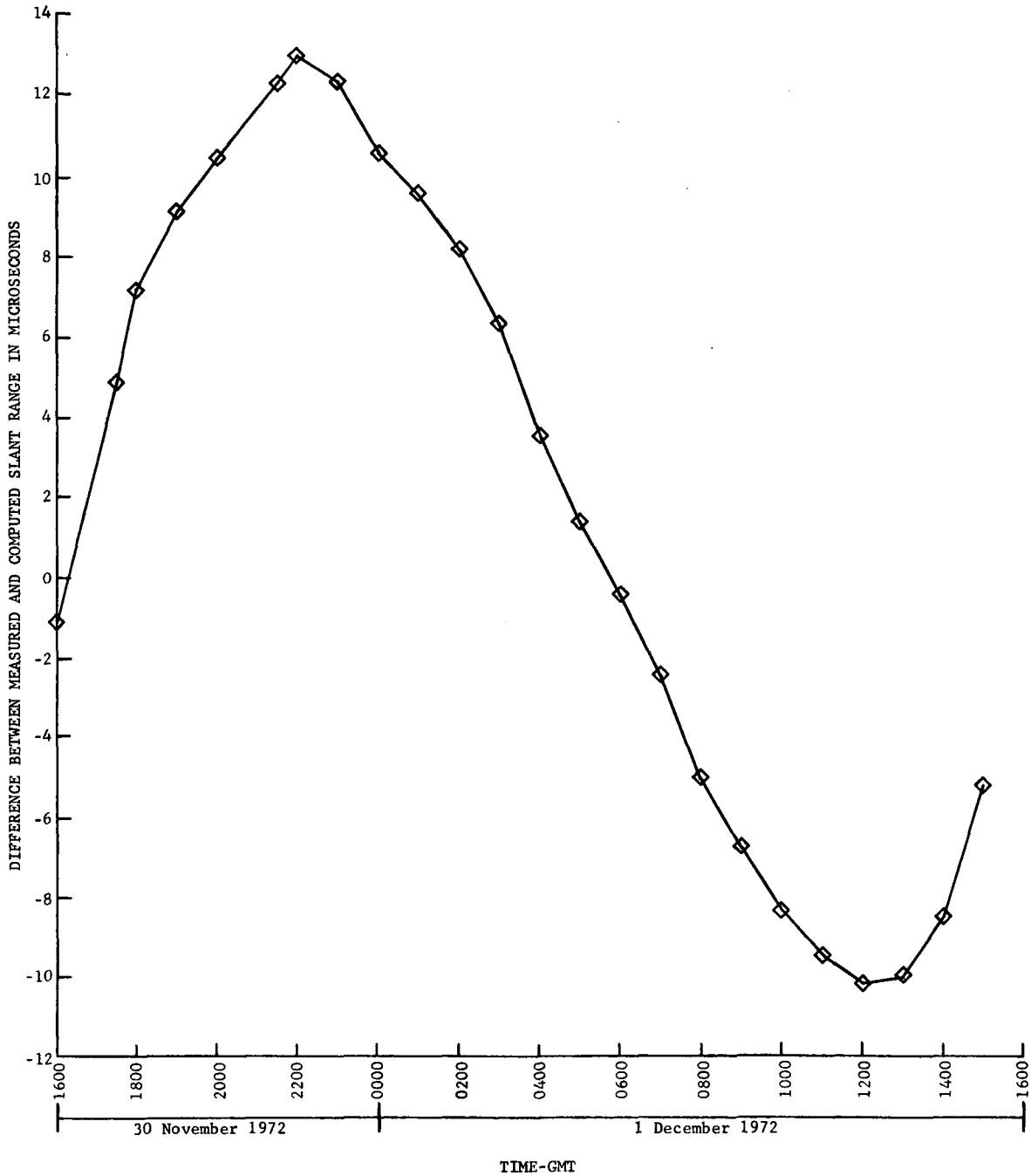

Differences are due to: 1) Ionosphere Propagation Delay; 2) Error in Predictions of Satellite Positions; 3) Error in Equipment Time Delay Calibration. 1 & 2 are cyclic with a 24 hour period; 3 is a fixed bias.

FIGURE 41

COMPARISON OF DIFFERENCES,
MEASURED MINUS COMPUTED SLANT RANGES AT VHF,
ATS-3 TO L-BAND/VHF PLATFORM AT SCHENECTADY, NEW YORK

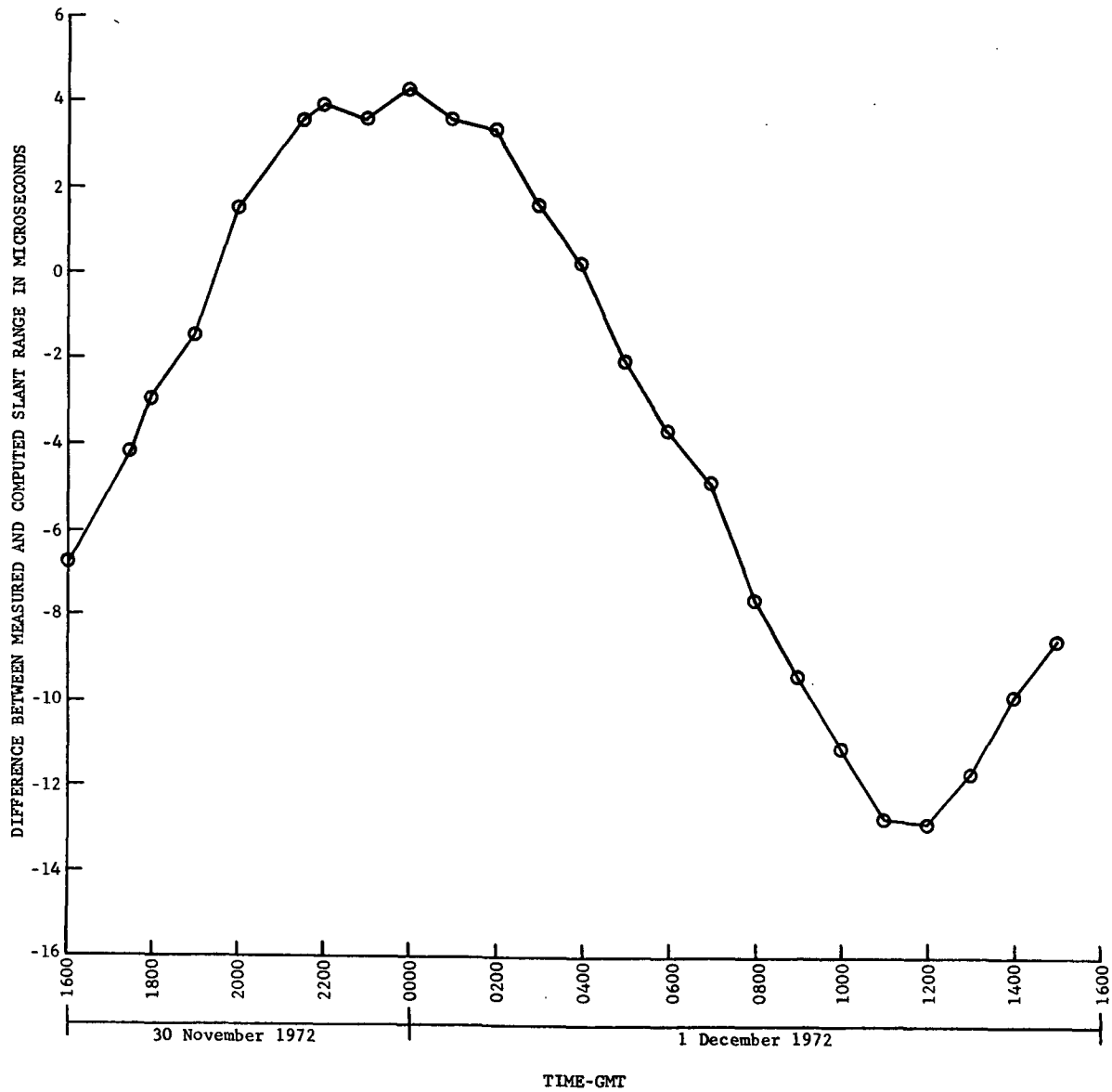

Differences are due to: 1) Ionosphere Propagation Delay; 2) Error in Predictions of Satellite Positions; 3) Error in Equipment Time Delay Calibration. 1 & 2 are cyclic with a 24 hour period; 3 is a fixed bias.

FIGURE 42

COMPARISON OF DIFFERENCES,
MEASURED MINUS COMPUTED SLANT RANGES AT VHF,
ATS-3 TO VHF TRANSPONDER AT SCHENECTADY, NEW YORK

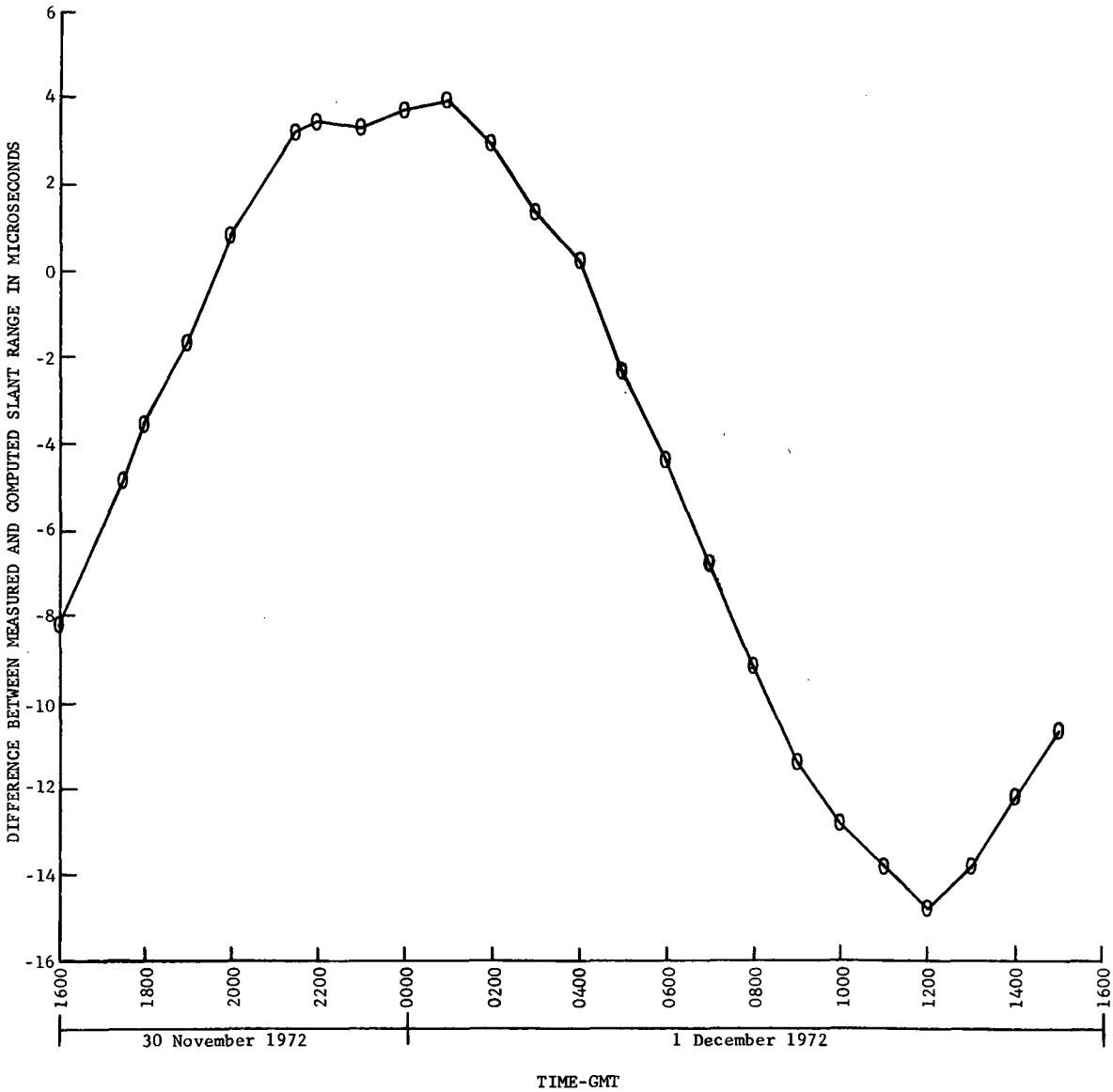

Differences are due to: 1) Ionosphere Propagation Delay; 2) Error in Predictions of Satellite Positions; 3) Error in Equipment Time Delay Calibration. 1 & 2 are cyclic with a 24 hour period; 3 is a fixed bias.

FIGURE 43

COMPARISON OF DIFFERENCES,
MEASURED MINUS COMPUTED SLANT RANGES AT VHF,
ATS-3 TO TRANSPONDER AT KINGS POINT, NEW YORK

The unit at Kings Point, New York was a substitute that was not properly calibrated for equipment time delay.

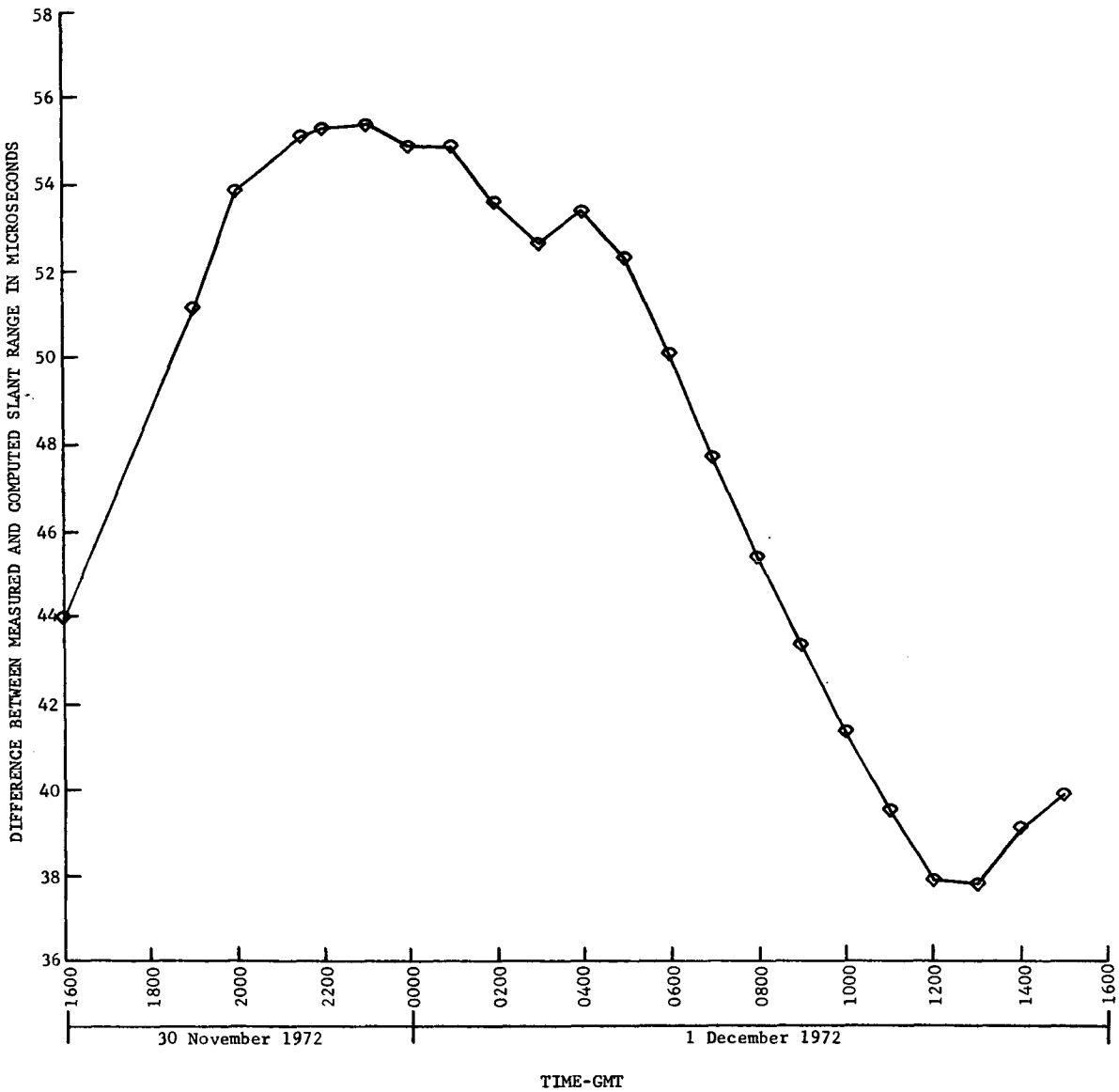

Differences are due to: 1) Ionosphere Propagation Delay; 2) Error in Predictions of Satellite Positions; 3) Error in Equipment Time Delay Calibration. 1 & 2 are cyclic with a 24 hour period; 3 is a fixed bias.

FIGURE 44

5.7 Satellite Location Experiment

The General Electric Company used the transponders at Shannon, Ireland; Reykjavik, Iceland; Buenos Aires, Argentina; and Seattle, Washington to test a satellite tracking concept. The transponders were interrogated from Schenectady, New York where the range measurements were made and recorded in real time. The technique provides range measurements from Schenectady to the satellites as well as to each of the other transponders.

During the experiment, NASA tracked the ATS satellites approximately one day each two weeks by range and range rate measurements at C-band from Rosman, North Carolina and Mojave, California. Range and range rate measurements are used to update the orbit parameters. Acquisition tables are then computed, stating the predicted positions of the satellites in latitude, longitude, and earth center distance for each half hour for several weeks in the future.

NASA estimates that the acquisition tables are correct to approximately one kilometer in each coordinate on the day the satellites are tracked, with the possibility of a deterioration in accuracy with the passage of time beyond the tracking date. General Electric has confirmed NASA's estimate of the accuracy of the acquisition tables by determining the difference between the measured slant ranges from the satellites to accurately located ground reference transponders and the computed slant ranges based on NASA's stated positions of the satellites.

The small inclination of the satellite orbits causes a diurnal motion of the satellites with respect to fixed points on the earth. Error in the satellite position predictions causes a diurnally changing difference between the measured and computed slant ranges to a point on the earth, and a diurnally changing error in a position fix that can sometimes exceed a nautical mile.

The following data plots, Figures 45 through 49, show the differences between the computed slant range measurements based on NASA's statements of the satellite positions and the range measurements made from Shannon, Reykjavik, Schenectady, Seattle and Buenos Aires. The differences between the measured and computed slant ranges to Schenectady and Buenos Aires are in opposite phase due to the diurnally changing error in NASA's statement of the satellite positions relative to those two locations. When the satellite is actually closer to Schenectady than stated by NASA, it is further from Buenos Aires and vice-versa. Figures 50 through 53 show that the locations of the satellite as determined by triads of northern latitude stations have a longitudinal resolution, even at VHF, on the order of 0.001 degree, while any triad employing the Buenos Aires station results in satellite latitude resolution of approximately 0.001 degree. The resolution deteriorates somewhat during times of day when the estimate of the ionosphere delay is less accurate. The stated positions of the satellite by NASA are shown on the diagrams. Disagreement between the position locations determined by General Electric's network and the position locations stated by NASA are shown in Figure 54. The differences show a systematic variation suggesting that the General Electric position determinations have a precision sufficient to make a substantial correction to the NASA predictions.

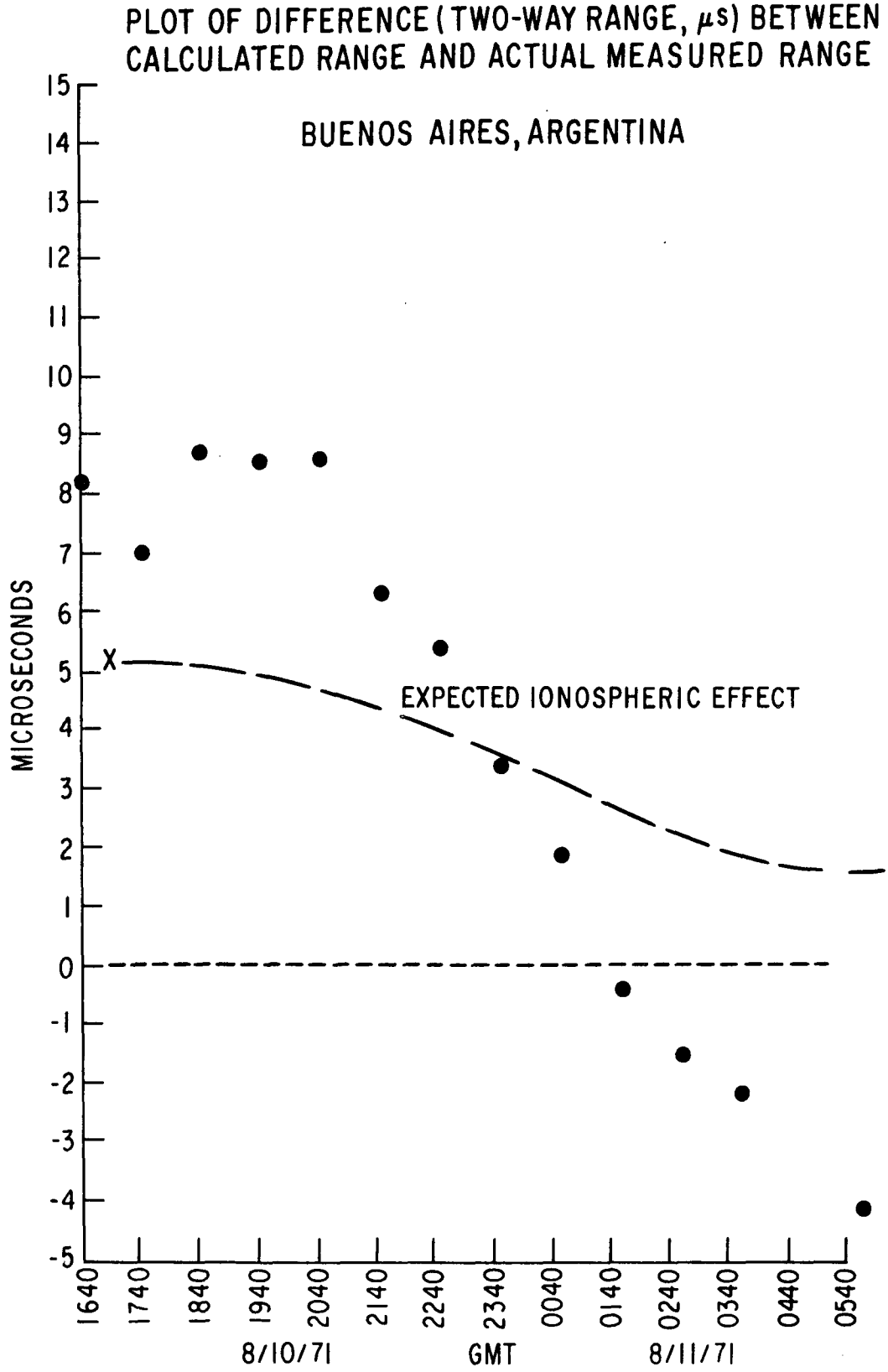
PLOT OF DIFFERENCE (TWO-WAY RANGE, μs) BETWEEN CALCULATED RANGE AND ACTUAL MEASURED RANGE
BUENOS AIRES, ARGENTINA
MICROSECONDS
15
14
13
12
11
10
9
8
7
6
5
4
3
2
1
0
-1
-2
-3
-4
-5
X
EXPECTED IONOSPHERIC EFFECT
1640
1740
1840
1940
2040
2140
2240
2340
0040
0140
0240
0340
0440
0540
8/10/71
GMT
8/11/71

FIGURE 45

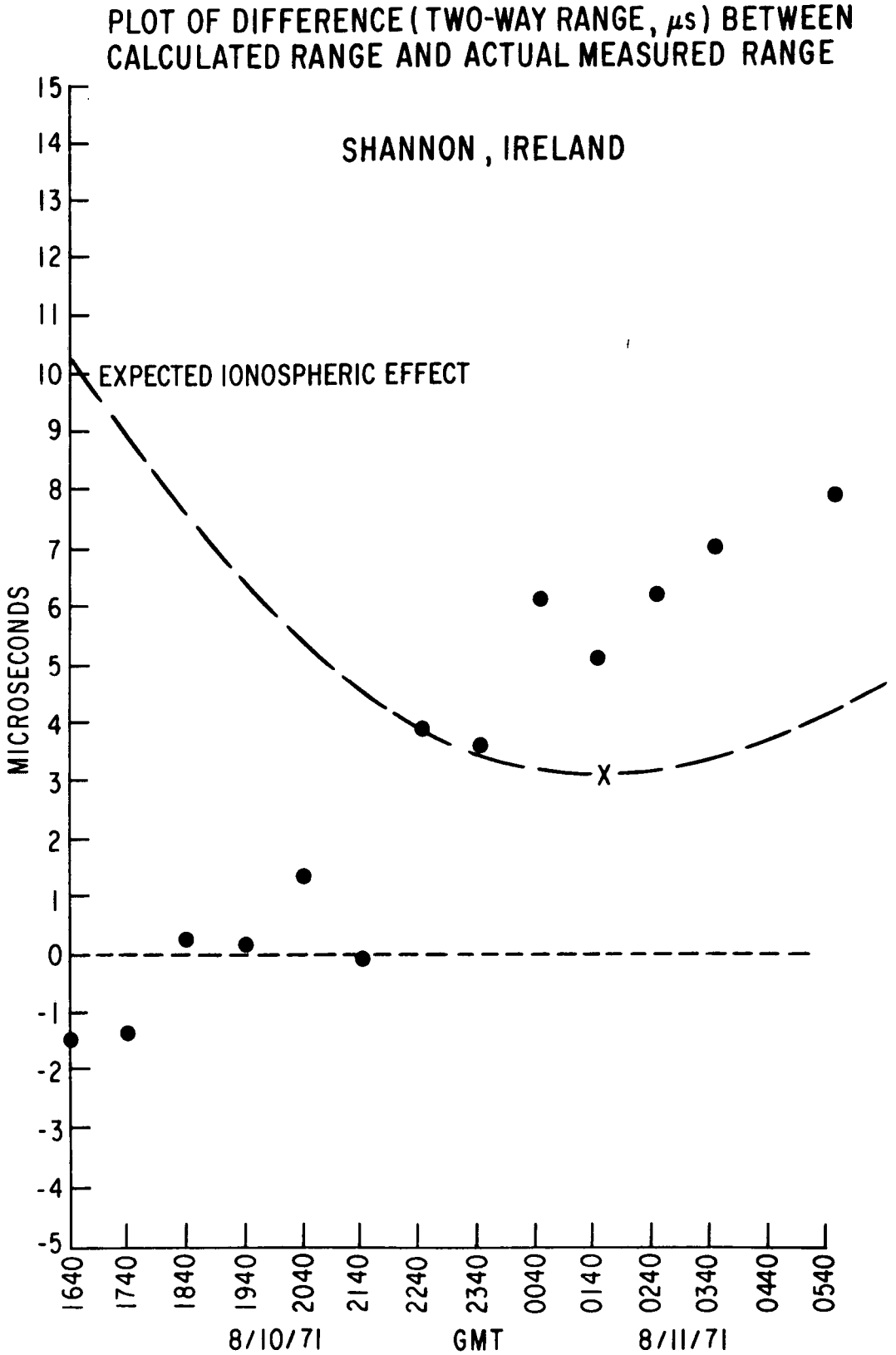
PLOT OF DIFFERENCE (TWO-WAY RANGE, μs) BETWEEN CALCULATED RANGE AND ACTUAL MEASURED RANGE
SHANNON, IRELAND
EXPECTED IONOSPHERIC EFFECT
MICROSECONDS
15
14
13
12
11
10
9
8
7
6
5
4
3
2
1
0
-1
-2
-3
-4
-5
1640
1740
1840
1940
2040
2140
2240
2340
0040
0140
0240
0340
0440
0540
8/10/71
GMT
8/11/71

FIGURE 46

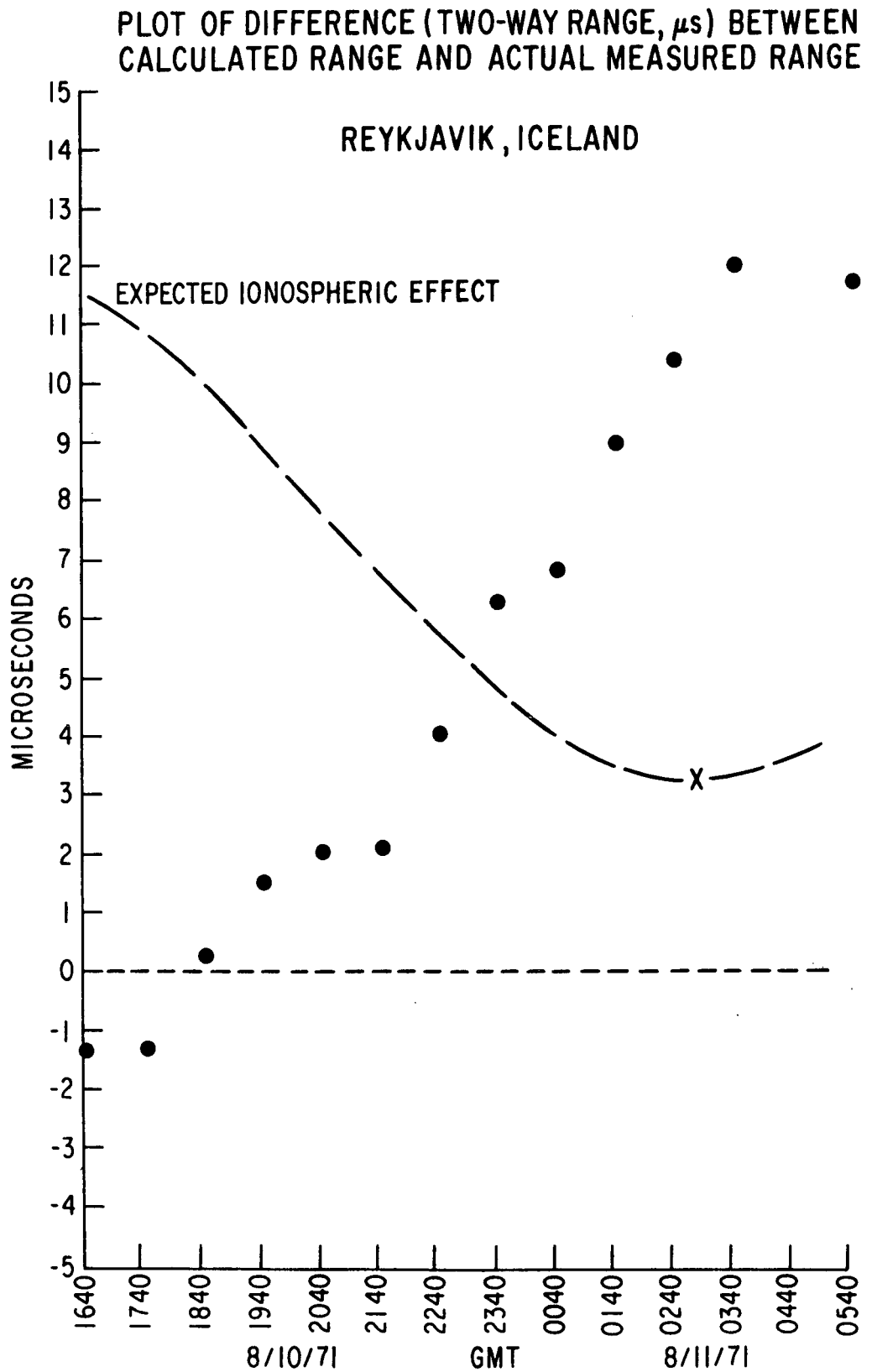
PLOT OF DIFFERENCE (TWO-WAY RANGE, μs) BETWEEN CALCULATED RANGE AND ACTUAL MEASURED RANGE
REYKJAVIK, ICELAND
EXPECTED IONOSPHERIC EFFECT
MICROSECONDS
15
14
13
12
11
10
9
8
7
6
5
4
3
2
1
0
-1
-2
-3
-4
-5
1640
1740
1840
1940
2040
2140
2240
2340
0040
0140
0240
0340
0440
0540
8/10/71
GMT
8/11/71

FIGURE 47

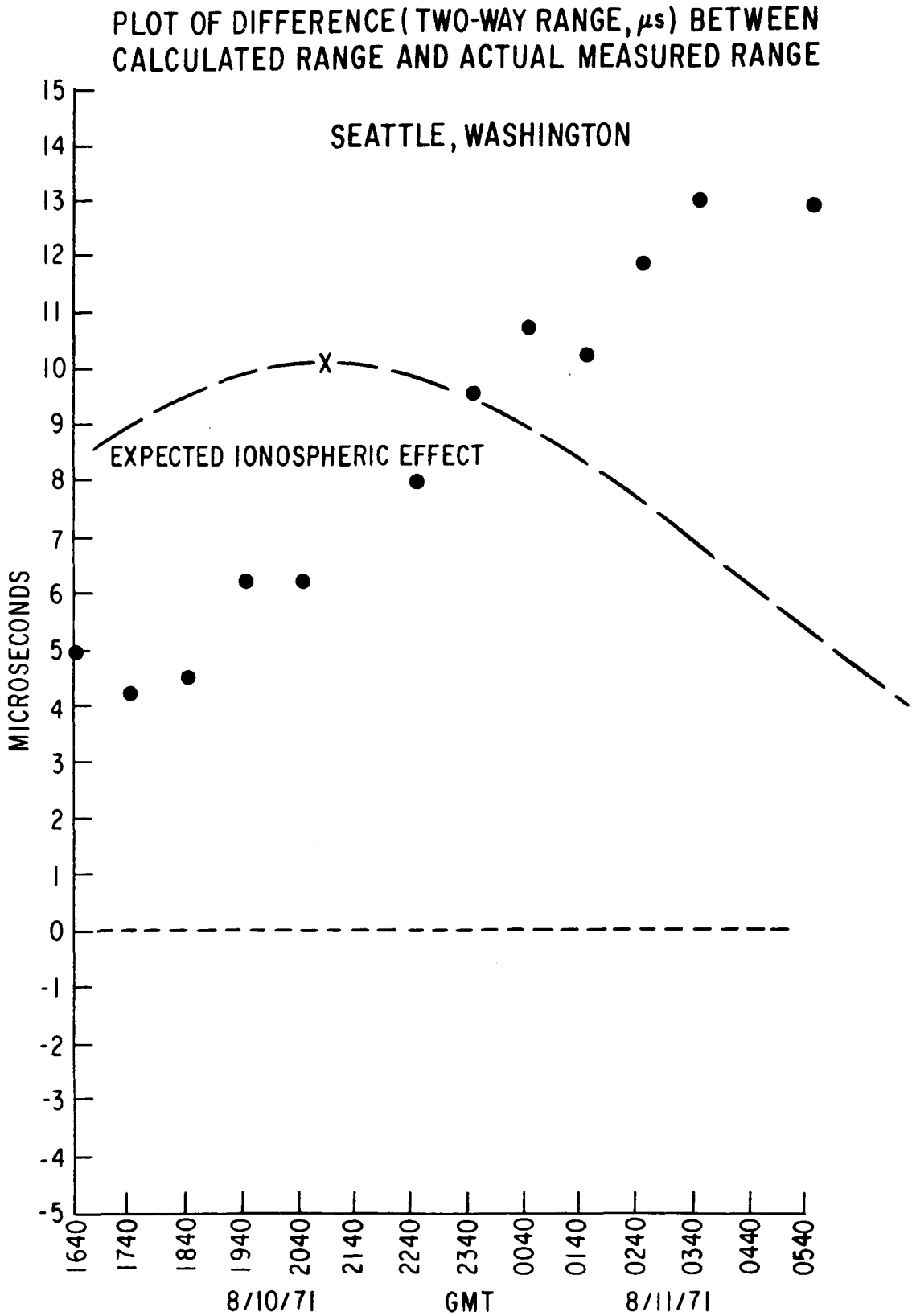
PLOT OF DIFFERENCE (TWO-WAY RANGE, μs) BETWEEN CALCULATED RANGE AND ACTUAL MEASURED RANGE
SEATTLE, WASHINGTON
EXPECTED IONOSPHERIC EFFECT
MICROSECONDS
15
14
13
12
11
10
9
8
7
6
5
4
3
2
1
0
-1
-2
-3
-4
-5
1640
1740
1840
1940
2040
2140
2240
2340
0040
0140
0240
0340
0440
0540
8/10/71
GMT
8/11/71

FIGURE 48

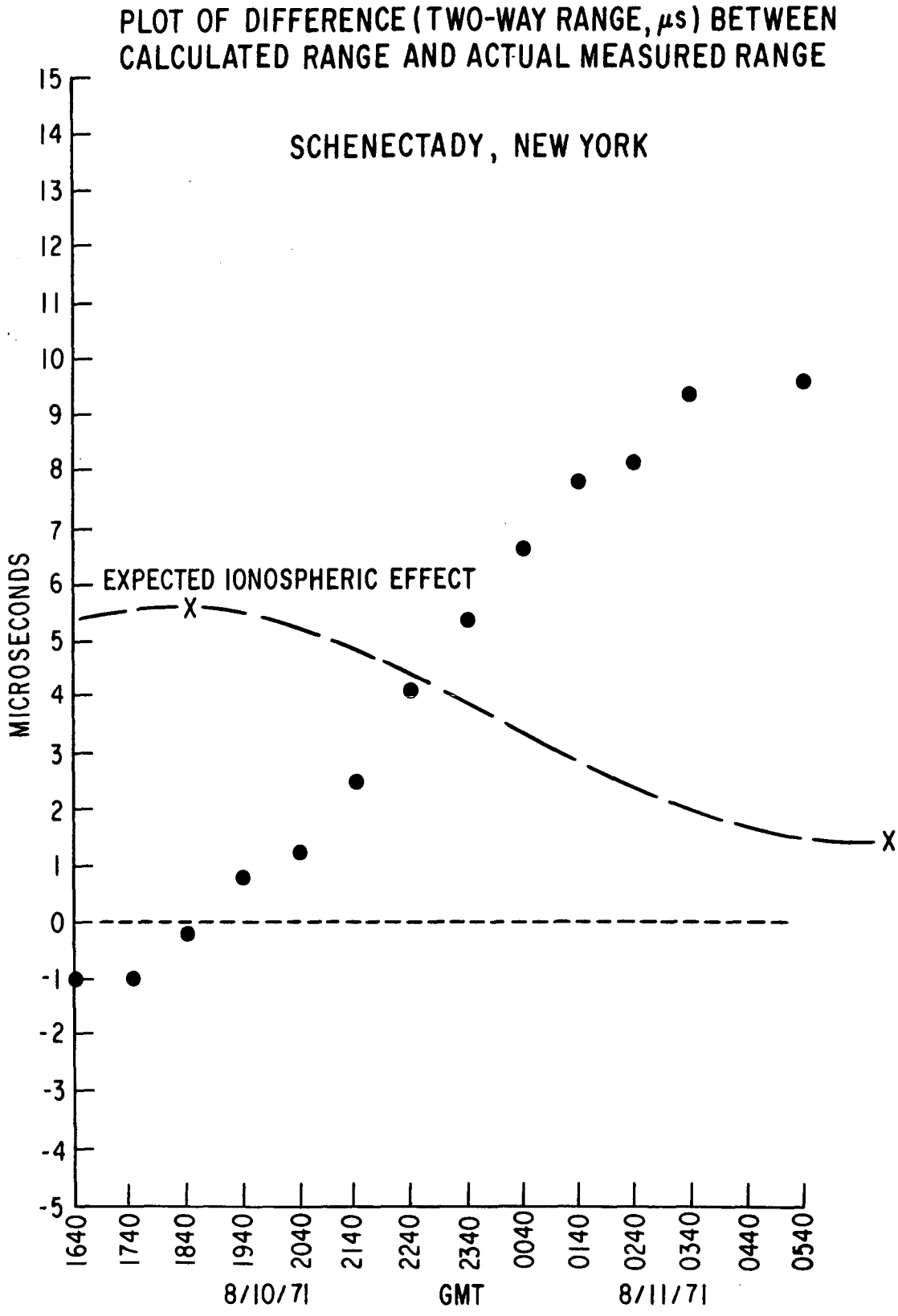
PLOT OF DIFFERENCE (TWO-WAY RANGE, μs) BETWEEN CALCULATED RANGE AND ACTUAL MEASURED RANGE
SCHENECTADY, NEW YORK
MICROSECONDS
EXPECTED IONOSPHERIC EFFECT
X
X
15
14
13
12
11
10
9
8
7
6
5
4
3
2
1
0
-1
-2
-3
-4
-5
1640
1740
1840
1940
2040
2140
2240
2340
0040
0140
0240
0340
0440
0540
8/10/71
GMT
8/11/71

FIGURE 49

FIGURE 50

SATELLITE POSITION AS DETERMINED
BY COMPUTATION FROM GE MEASUREMENTS
USING VARIOUS TRIADS OF TRANSPONDERS
(8/10/71, 0930 GMT)

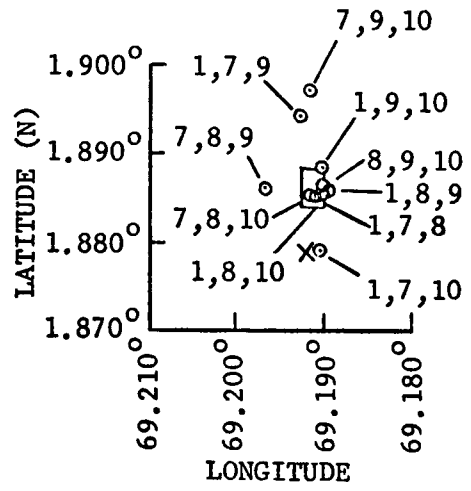

1 - SCHENECTADY, NEW YORK
7 - SHANNON, IRELAND
8 - BUENOS AIRES, ARGENTINA
9 - REYKJAVIK, ICELAND
10 - SEATTLE, WASHINGTON
X - NASA STATED POSITION

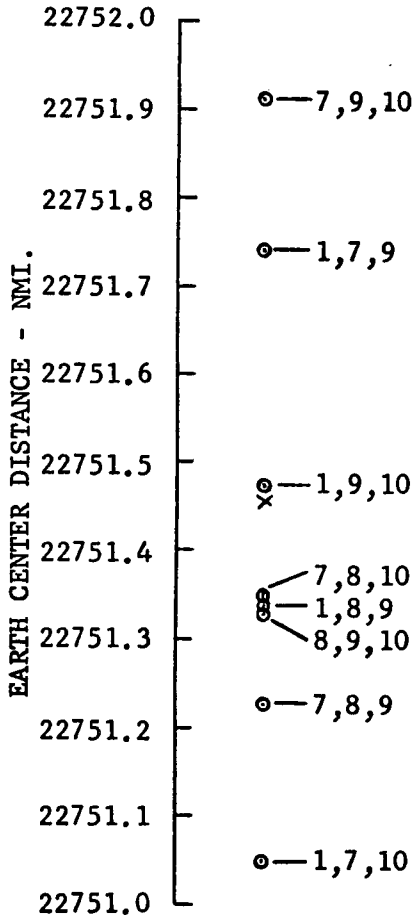

FIGURE 51

SATELLITE POSITION AS DETERMINED
BY COMPUTATION FROM GE MEASUREMENTS
USING VARIOUS TRIADS OF TRANSPONDERS
(8/11/71, 0030 GMT)

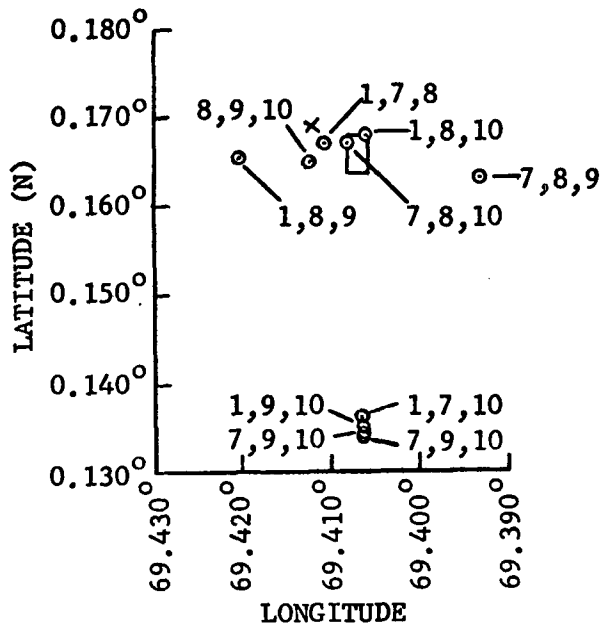

1 - SCHENECTADY, NEW YORK
7 - SHANNON, IRELAND
8 - BUENOS AIRES, ARGENTINA
9 - REYKJAVIK, ICELAND
10 - SEATTLE, WASHINGTON
X - NASA STATED POSITION

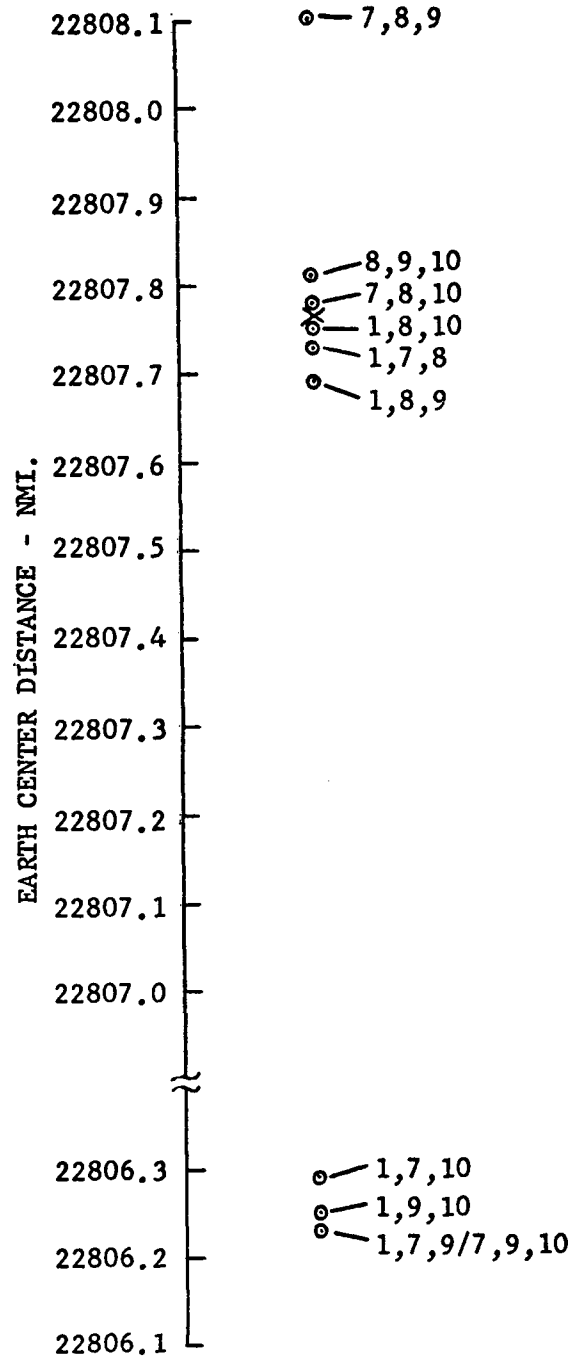

FIGURE 52

SATELLITE POSITION AS DETERMINED
BY COMPUTATION FROM GE MEASUREMENTS
USING VARIOUS TRIADS OF TRANSPONDERS
(8/11/71, 0130 GMT)

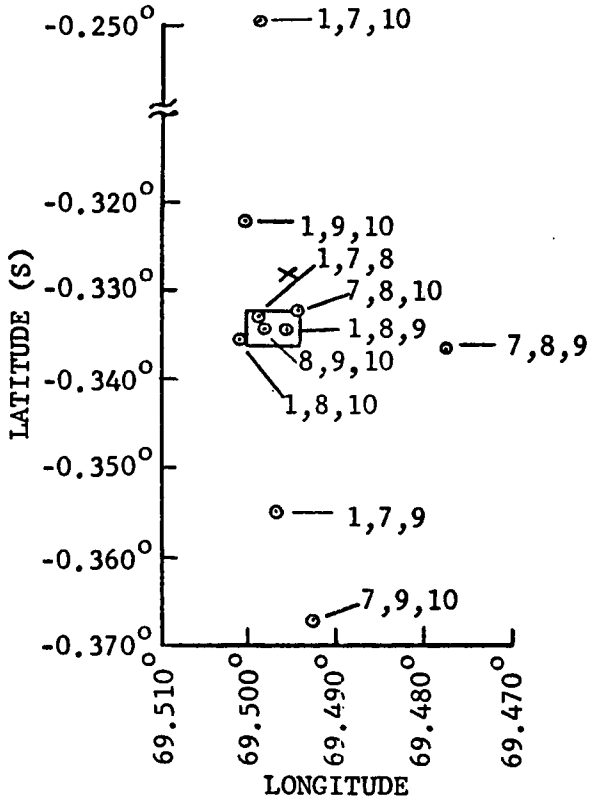

1 - SCHENECTADY, NEW YORK
7 - SHANNON, IRELAND
8 - BUENOS AIRES, ARGENTINA
9 - REYKJAVIK, ICELAND
10 - SEATTLE, WASHINGTON
X - NASA STATED POSITION

FIGURE 53

SATELLITE POSITION AS DETERMINED
BY COMPUTATION FROM GE MEASUREMENTS
USING VARIOUS TRIADS OF TRANSPONDERS
(8/11/71, 0430 GMT)

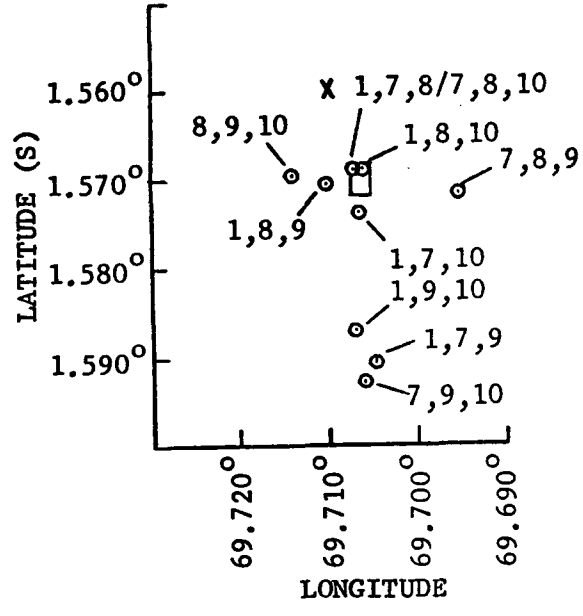

1 - SCHENECTADY, NEW YORK
7 - SHANNON, IRELAND
8 - BUENOS AIRES, ARGENTINA
9 - REYKJAVIK, ICELAND
10 - SEATTLE, WASHINGTON
X - NASA STATED POSITION

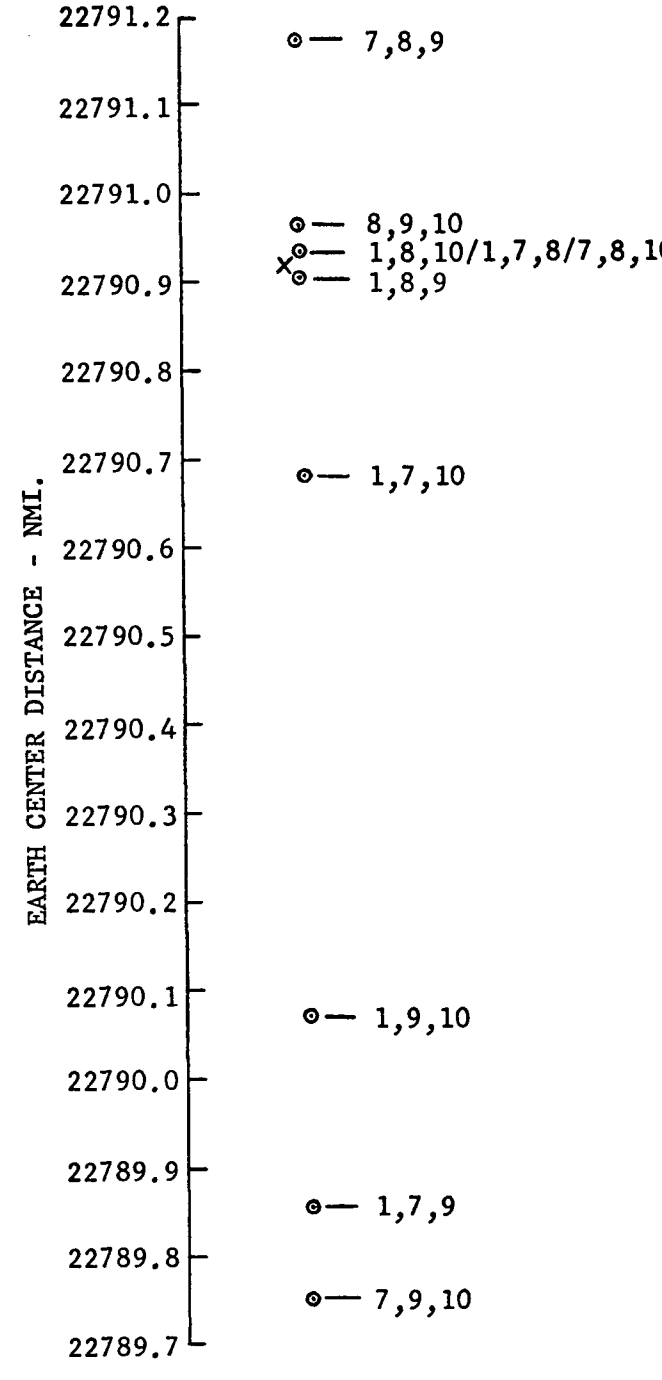

FIGURE 54

DIFFERENCES - NASA AND GE SATELLITE LOCATIONS

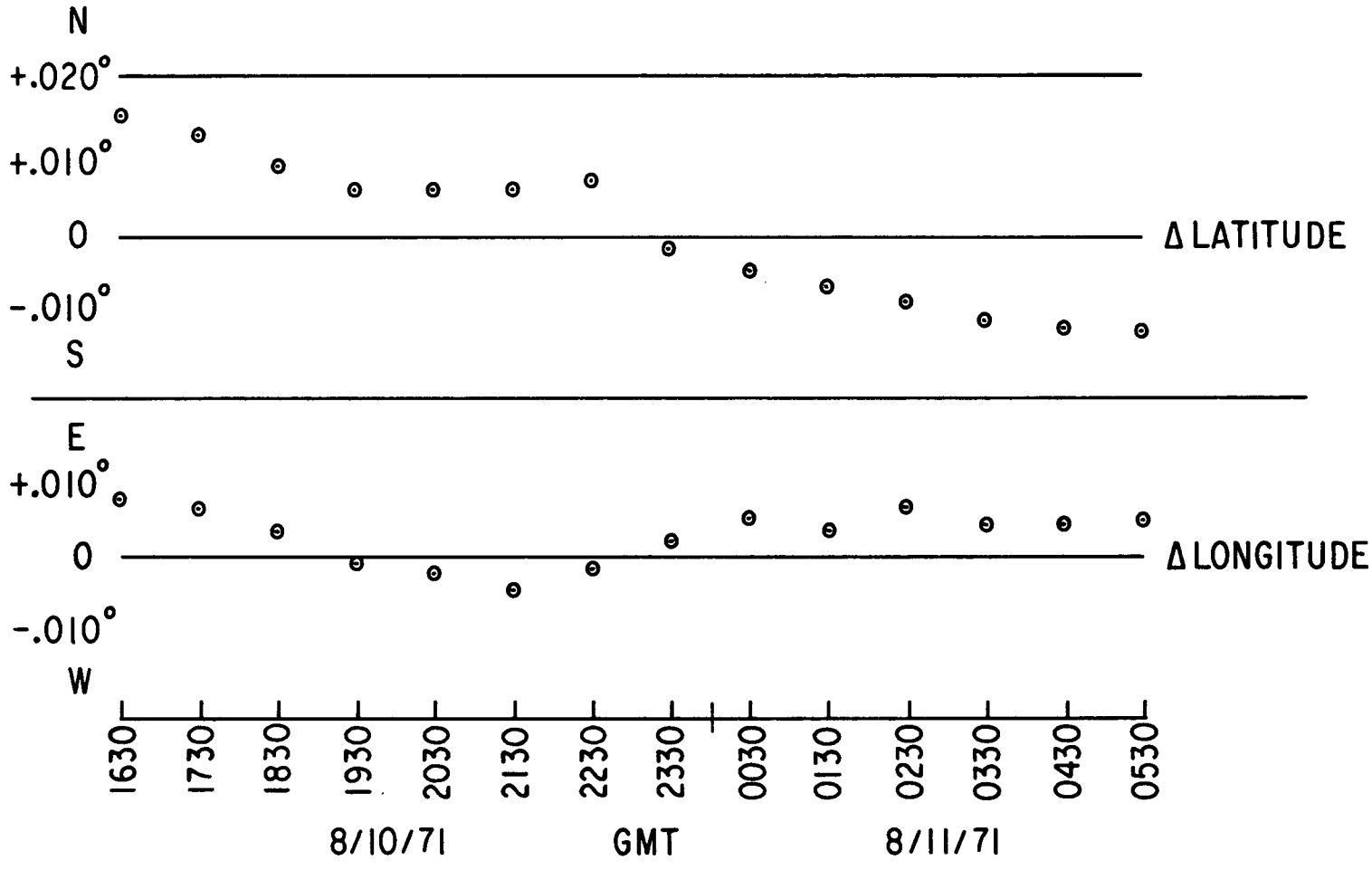

SECTION 6

CONCLUSIONS

1. The L-band/VHF transponder achieved all of its performance objectives.

2. Ranging precision better than 50 feet can be achieved at L-band within the following constraints:
   a. Modulation bandwidth of less than 10 kHz
   b. RF bandwidth less than 60 kHz
   c. The same modulation waveform used for communications and ranging.
   d. Ranging signal duration less than 3 seconds for better than 10 foot range measurement precision; 0.3 second for approximately 15 foot precision; 0.03 second for approximately 50 foot precision (1 sigma, two-way ranging).
   e. Digital data transmission may be used in the range measurement process so that ranging signals can be the digital data clock and the user address code.
   f. No ambiguity in the range measurement.

3. L-band power amplifier design is possible with the following characteristics:
   a. All solid state
   b. Efficiency, DC-RF greater than 35%
   c. Highly reliable, long life
   d. Graceful degradation
   e. Size: 19" wide x 10.5" high x 25" deep (less power supply)

4. Comparison of VHF and L-band ranging was limited in the experiment because the transponders are on separate satellites and the satellite locations are not known accurately.

5. Tone-code ranging with long baselines for computing the positions of satellites by range measurements from simple automatic transponders is practical.

6. The results of the satellite location tests do not prove that the General Electric satellite position determinations are more accurate than those of NASA. An independent check would have to be conducted in order to make such an evaluation. The scope of the effort under the General Electric funding for this initial experiment did not permit such a proof.

7. The results of the experiments conducted in February and during the summer at VHF and at L-band confirm that useful ranging precision can be achieved at both frequencies within the narrow bandwidths used for communications, that the variations in the ranging measurements are randomly distributed and can be improved by the square root of averaging time, and that useful ranging precision is achieved even at signal-to-noise ratios down to the detection threshold of the FM signals used in the tests.

SECTION 7

RECOMMENDATIONS

1. Install L-band/VHF transponder on a ship. Test position fixing with ATS-3 at VHF and ATS-5 at L-band. When ATS-F is in orbit, test position fixing at L-band only with ATS-F and ATS-5.

2. Use the L-band/VHF transponder together with other L-band receiver-transmitters equipped with tone-code responders to locate ATS-5 accurately for L-band position fixing experiments, propagation measurements, comparisons of L-band and VHF ranging precision.

3. Test accuracy of ATS-3 location with GE network.

4. If accuracy determined in (3) is adequate for VHF propagation measurements, use L-band/VHF transponder with ATS-5 and ATS-3 to compare propagation at L-band and VHF.

5. Build operational prototype of L-band power amplifier (the present unit is an engineering model).

6. Design, build and test a modem for combined digital communications and ranging.

NEW TECHNOLOGY

There has been no new technology developed on this contract.

PUBLICATIONS

The following paper was presented by Roy E. Anderson during the course of contract NAS5-11634 and contains results obtained from the work done on that contract:

"A Technique for Synoptic Measurement of Ionospheric Propagation Delays by Ranging from Geostationary Satellites to a Network of Unmanned Transponders", Presented at the International Johannes-Kepler-Symposium on the Future Application of Satellite Beacon Measurements, May 29 - June 2, 1972, Graz, Austria.

The following reports were prepared by Roy E. Anderson during the course of contract NAS5-11634 on related efforts:

"Final Report on Satellite Experiments", Prepared for the Department of Commerce, Maritime Administration, on contract MA2-4066, July 1972.

"Final Report - Evaluation of Maritime Satellite Communications for Inland Waterways", Prepared for the Department of Commerce, Maritime Administration, on contract 3-36216, January 31, 1973.

APPENDIX I

MEMORANDUM - TONE-CODE RANGING PRECISION

by

R. T. Milton
GENERAL ELECTRIC COMPANY
Space Division
Philadelphia, Pennsylvania

August 19, 1971

1.0 INTRODUCTION

This memorandum summarizes a brief investigation of two modem techniques usable with tone-code ranging. That is, a modem such that the demodulator output can be a tone followed by a code. This makes the techniques compatible with the circuitry previously developed for use with the tone-code ranging.

Specifically the following topics are investigated:

1. The precision attainable with a tone of a given frequency and specified duration when accompanied by noise of a given level. This provides an upper limit on the precision.

2. The precision attainable when the tone-code frequency-modulates a carrier. Included are an evaluation of trade-offs of modulation index and tone frequency and the possibilities of FMFB demodulation.

3. PSK modulation with both derived-carrier-synchronous and differential detection.

For a 48 dB-Hz carrier-to-noise density ratio, a 30 ms tone interval and a 10 kHz tone DSB-SC modulating a carrier, the measurement precision is found to be about 0.4 μs, assuming ideal demodulation. The precision increases as the reciprocal of the tone frequency and as the reciprocal of the square root of the number of 30 ms interval measurements averaged.

Under the same carrier-to-noise ratio and measurement time conditions the FM techniques give about 3.7 μs precision.

It is expected that practical PSK techniques would yield precision about 1.5 times worse than those of the optimum technique under the same SNR, tone frequency and tone duration conditions as long as the ratio of carrier power-to-noise power in the IF bandwidth was greater than zero dB.

2.0 ATTAINABLE PRECISION ESTIMATE

It is of interest to estimate the minimum error that could be expected given the carrier power-to-noise density ratio and measurement time. This sets a standard to compare other techniques against.

Helstrom[1] gives as the variance of a time of arrival measurement:

$$\sigma^2 = \frac{1}{d^2\beta^2} \tag{1}$$

Where for our purposes

$$d = \left(\frac{2E}{N_o}\right)^{1/2}$$

$\beta^2 = \overline{\omega^2} - \overline{\omega}^2$ = effective signal bandwidth in radians per second
E = signal energy used in the time of arrival measurement
N_o = noise power density, Watts/Hz
$\overline{\omega^2}$ = mean square value of the modulating signal spectrum

$$= \int_{-\infty}^{\infty} \omega^2 \left|M(\omega)\right|^2 d\omega \Big/ \int_{-\infty}^{\infty} \left|M(\omega)\right|^2 d\omega$$

$\overline{\omega}$ = mean value of modulating signal spectrum

$$= \int_{-\infty}^{\infty} \omega \left|M(\omega)\right|^2 d\omega \Big/ \int_{-\infty}^{\infty} \left|M(\omega)\right|^2 d\omega$$

$m(t)$ and $M(\omega)$ are a Fourier Transform pair
$m(t)$ = modulating signal used for ranging

The energy used in the measurement is:

$$E = PT$$

where

P = power in the modulating signal as delivered to the detection circuit, assumed constant over measurement interval
T = the duration of the signal used for the measurement

From Equation (1) the standard deviation of the range measurement is:

$$\sigma = \frac{1}{\beta d} \tag{2}$$

This equation assumes the use of a matched filter detector and that any ambiguities associated with the ranging waveform, $m(t)$, are resolved.

For a given bandwidth the maximum precision is achieved through the use of a tone modulated carrier, neglecting ambiguities, with the tone frequency equal to one-half the allowable bandwidth. This is because the tone has the spectral distribution that maximizes β. DSB-SC modulation of a carrier produces the required spectrum without any wasted energy in the carrier. For this modulation the bandwidth factor β is:

$$\beta = \omega_m = 2\pi f_m$$

where f_m is the modulating tone frequency.

If T seconds of the DSB-SC waveform are used in the range measurement and the average power of the waveform at IF is P Watts, the energy is E = PT. Letting N_o be the noise spectral density at IF, the signal-to-noise ratio factor is $d = (2\ PT/N_o)^{1/2}$ giving a ranging precision of:

$$= \frac{1}{2\pi f_m} \frac{1}{(2\ PT/N_o)^{1/2}}$$

Taking

$$P/N_o = 10^{4.8}\ (48\ \text{dB-Hz})$$
$$T = 30 \times 10^{-3}\ \text{second}$$
$$f_m = 10 \times 10^{3}\ \text{Hz}$$

gives

$$\sigma = 0.41\ \mu s$$

This precision is about the best that can be achieved under the SNR, measurement interval and modulating frequency conditions given. Averaging N such measurements improves the precision by $N^{1/2}$ and increasing f_m also improves the precision as illustrated in the equation given previously.

Note that the above discussion of the precision implies that some means is provided for synchronously detecting the DSB-SC waveform.

3.0 ACCURACY OF TONE-CODE TECHNIQUE/FM

In this section the precision of the tone-code technique is investigated for the case where the tone is transmitted as a frequency modulation of an RF carrier.

Using results given in Baghdady[2], the SNR from a frequency discriminator is:

$$(S/N)_{out} = (\Delta F)^2 \, E_s^{\,2} \, \overline{m^2(t)} \Big/ \int_{-B_{lp}}^{B_{lp}} f^2 \, w(f_s + f) \, df \qquad (3)$$

where

E_s = peak carrier amplitude

ΔF = peak frequency deviation

$m(t)$ = modulating signal. It is assumed that $|m(t)_{max}| = 1$

B_{lp} = bandwidth of low pass (ideal) filter at output of frequency discriminator

$s(f)$ = IF noise spectral density delivered to discriminator as a function of frequency

f_s = IF center frequency

The noise spectral density around the IF center frequency, f_s, is $w(f_s + f)$. It is a single sided spectral density.

Equation (3) applies when the FM receiver is above threshold. In Equation (3) the signal output is:

$$e_{out}(t) = k_d \, \Delta F \, m(t) \qquad (4)$$

k_d = demodulator constant

and the mean square output is:

$$\overline{e^2_{out}(t)} = k_d^{\,2} \, (\Delta F)^2 \, \overline{m^2(t)} \qquad (4a)$$

The noise power output in the band from 0+ to B_{lp} (excluding dc) is:

$$N_{out} = k_d^{\,2} \left(\frac{1}{E_s^{\,2}} \right) \int_{-B_{lp}}^{B_{lp}} f^2 \, w(f_s + f) \, df \qquad (5)$$

If the noise delivered by the IF to the FM demodulator is white gaussian noise of spectral density N_o Watts/Hz (single sided), the output SNR is:

$$(S/N)_{out} = 3\left(\frac{\Delta F}{B_{lp}}\right)^2 \frac{E_s^2 \overline{m^2(t)}}{2 B_{lp} N_o} \tag{5a}$$

$$= 6\left(\frac{\Delta F}{B_{lp}}\right)^2 \left(\frac{E_s^2/2}{2 B_{lp} N_o}\right) \overline{m^2(t)}$$

For comparison, a DSB-SC modulated waveform has an input SNR, in the signal bandwidth, of:

$$(S/N)_{in} = \frac{E_s^2/2}{2 B_{lp} N_o} \overline{m^2(t)} \tag{6}$$

and, when synchronously detected, the output SNR is:

$$(S/N)_{out} = 2 \frac{E_s^2/2}{2 B_{lp} N_o} \overline{m^2(t)} \cos^2 (\phi_s - \phi_{osc}) \tag{7}$$

where $\phi_s - \phi_{osc}$ is demodulating oscillator phase error. This shows a 3 dB improvement in SNR between input and output when $\phi_s = \phi_{osc}$.

Note that in the equation giving $(S/N)_{out}$ for FM, Equation (5a), the input noise spectral density (to the discriminator) is weighted by f^2 when it appears at the discriminator output. f is measured from zero frequency and is the frequency in the baseband, or modulating signal domain. Thus, if in tone ranging the tone frequency is increased, the noise density in the immediate neighborhood of the tone increases as the square of the frequency. A matched filter for the tone signal is a narrowband filter that has its center frequency at the tone frequency. Thus the noise at the matched filter output increases as the square of the tone frequency. Considering the parameters of the range accuracy equation,

$$\sigma = \frac{1}{\beta \ (2E/N_o)^{1/2}}$$

and the fact that the bandwidth parameter and the noise density at the output of a frequency discriminator are related to the modulating frequency as follows:

$$\beta \propto f_m$$

$$N_o \propto f_m^2$$

it is seen that σ is independent of the modulating frequency in the case of FM, provided that E_s is greater than the threshold value.

The threshold value for E_s is dependent on the FM system bandwidth. Figure 1 shows this dependence for FM and FMFB. In the figure $m = \Delta F/B_{lp}$.

From the above results it is concluded that the lowest modulating frequency consistent with other system requirements should be used for tone-code ranging since this gives the minimum carrier power required to exceed the noise improvement threshold.

This conclusion can be made more precise. Consider a modulating frequency f_m. From Equation (5) it is seen that the discriminator output noise density close to f_m is:

$$\eta = 2\, k_d^2 \left(\frac{1}{E_s^2}\right) f_m^2\, w(f_s + f_m) \tag{8}$$

The signal energy at the discriminator output for the modulating signal $m(t) = \cos \omega_m t$, of which T seconds is used in the measurements, using Equation (4a) is:

$$\begin{aligned} E_t &= T\, \overline{e^2_{out}} \\ &= T\, k_d^2\, (\Delta F)^2\, \overline{m^2(t)} \\ &= \frac{T}{2}\, k_d^2\, (\Delta F)^2 \end{aligned} \tag{9}$$

where the relation $\overline{m^2(t)} = \overline{\cos^2 \omega t} = \frac{1}{2}$ has been used.

Thus the energy-to-noise density from Equations (8) and (9) is

$$E_t/\eta = \frac{T}{4} \left(\frac{E_s^2}{w(f_s + f_m)}\right) \left(\frac{\Delta F}{f_m}\right)^2 \tag{10}$$

This equation can be put in terms of carrier power by recognizing that the carrier power is given by $E_s^2/2$. Doing this and inserting Equations (9) and (10) in the ranging precision equation gives:

$$\sigma = \frac{1}{\beta(2E/N_o)^{1/2}} = \frac{1}{\beta(2E_t/\eta)^{1/2}}$$

$$= \frac{}{2\pi f_m \left[\frac{2T}{2}\left(\frac{E_s^2/2}{w(f_s + f_m)}\right)\left(\frac{\Delta F}{f_m}\right)^2\right]^{1/2}} \qquad (11)$$

$$= \frac{}{2\pi\Delta F \left[T(E_s/2)/w(f_s + f_m)\right]^{1/2}}$$

Equation (11) is seen to be independent of f_m if the IF noise density w(f) is flat out to f_m on both sides of the carrier. Note that

$$\sigma \propto \frac{1}{\Delta F}$$

so that while σ is independent of f_m, it is dependent on the maximum deviation of the carrier from its no modulation value.

To show the accuracy attainable with tone-code ranging/FM, assume w(f) is flat and equal to N_o Watts/Hz and the carrier-to-noise density power ratio is

$$\frac{E_s^2/2}{N_o} = 10^{4.8} \rightarrow 48 \text{ dB Hz},$$

$$T = 30 \times 10^{-3} \text{ seconds},$$

and

$$\Delta F = 1000 \text{ Hz}.$$

The assumption on ΔF gives as the modulation index

$$m = \Delta F/f_m = 1$$

and a carrier-to-noise ratio C/N = 48 - 33 = 15 dB. From Figure 1 it is seen that this C/N places the FM link about 4 dB above the FM noise improvement threshold and about 7 dB above the FMFB threshold.

Inserting the above values into Equation (11) gives:

$$\sigma = \frac{1}{2\pi(10^3)\left[30 \times 10^{-3} \times 10^{4.8}\right]^{1/2}} = 3.65 \times 10^{-6} \text{ sec.}$$

This value for σ can be improved by increasing ΔF, and consequently m, to some extent. However the improvement obtainable is limited by the noise improvement threshold. FMFB might be used to decrease the threshold. As previously, the accuracy can be improved by averaging several 30 ms measurements.

COMPARISON OF OUTPUT SNR's OF FM, FMFB, DSB, SSB AND AM
AS A FUNCTION OF THE RATIO OF AVERAGE CARRIER POWER-TO-NOISE POWER
IN TWICE BASE BANDWIDTH AT RF

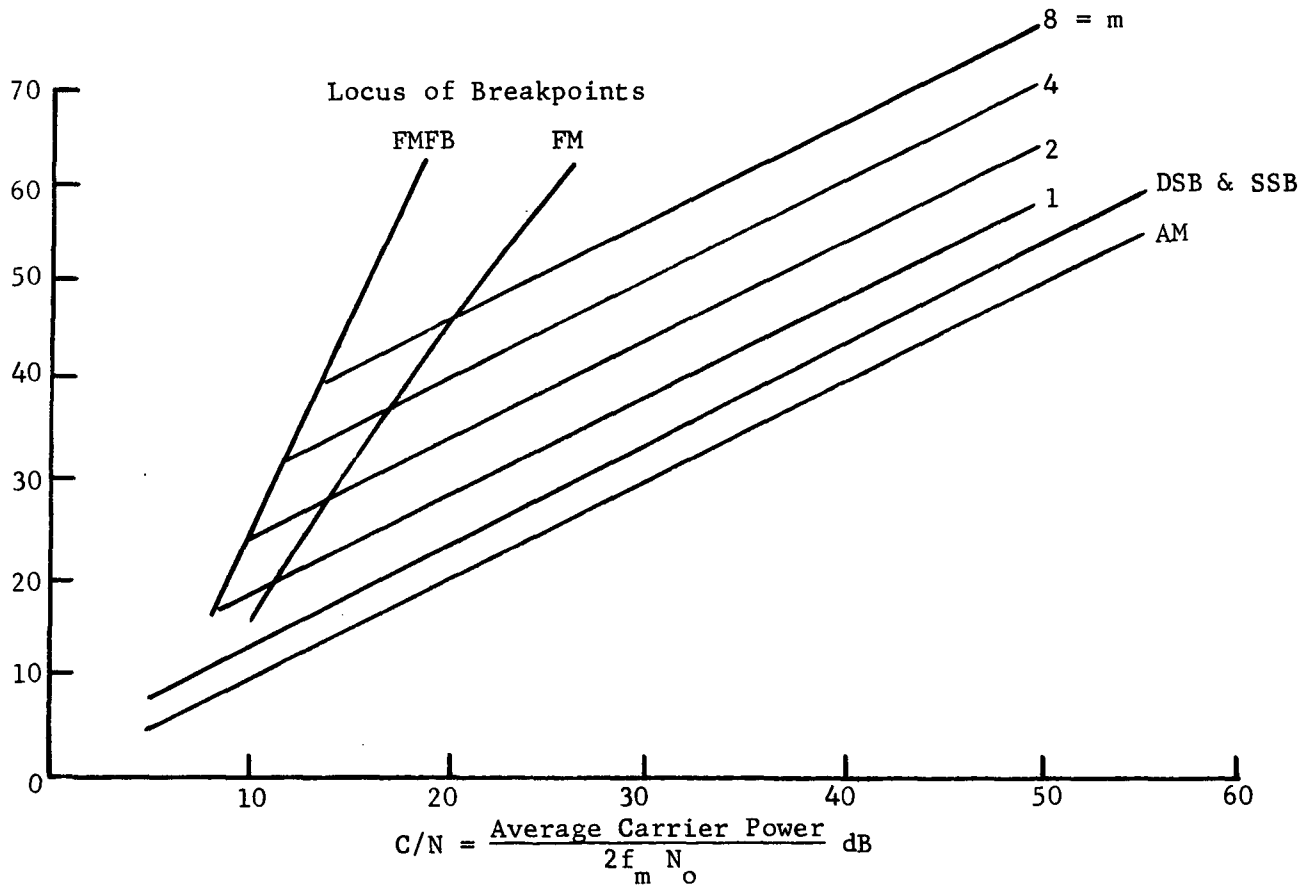

FIGURE 1

4.0 ACCURACY OF TONE-CODE/PSK

This section is concerned with estimating the performance of the tone-code technique when the tone and code are transmitted by phase modulation of a carrier. Considerations are restricted to the tone, since this ultimately determines the accuracy, and means for recovering it.

Two modulation formats and corresponding detectors are shown in Figures 2 and 3. The modulation shown in Figure 2a could be demodulated by means of the detector shown in Figure 3a. However, there is a possible polarity inversion of the demodulated signal due to the 0-180° polarity ambiguity of the tone recovered by means of the squaring circuit. The ranging circuits must be modified to operate with the polarity ambiguity.

Use of differential modulation as illustrated in Figure 2b with the detector of Figure 3b avoids the problem of polarity inversion but would increase the minimum allowable signal-to-noise ratio by perhaps 3 or 4 dB. Since the lowest practical threshold is desired, the differential technique will not be pursued further.

The major difference between the idealized case, considered earlier to provide a bench mark for attainable precision, and the circuit using the squaring circuit to derive a reference signal is that the latter provides a noisy sinusoid to the demodulator. A noisy reference degrades performance. Using the results of Davenport and Root[3] concerning the response of a square law device to a sine wave plus noise, the signal-to-noise ratio from the reference generator circuit can be estimated as:

$$(S/N)_r = \frac{B}{2B_1} (S/N)_{in} \left[\frac{(S/N)_{in}}{1 + (S/N)_{in}} \right] \qquad (12)$$

where

$(S/N)_r$ = SNR of recovered reference signal that provides the demodulator reference

B = RF (and IF) signal bandwidth, Hz ($= \beta/2\pi$)

B_1 = reference recovery circuit bandwidth, Hz

$(S/N)_{in}$ = SNR in bandwidth B at demodulator input

For P/N_o = 48 dB Hz, B = 60 kHz and B_1 = 1 kHz, $(S/N)_{in}$ = 0 dB or 1:1 power ratio, Equation (12) gives $(S/N)_r = B/(4B_1) = 15 \rightarrow 11.8$ dB. This $(S/N)_r$ is expected to increase the phase measurement error of the received signal phase by less than 50 percent. That is the rms phase error of the recovered tone should be less than 1.5 times that in the ideal reference case. Improved performance is possible using a narrower B_1. A phase lock-loop circuit could be used for the filter.

As mentioned the range measurement circuit must be able to handle the ambiguous polarity of the recovered tone-code signal. Perhaps the simplest way to do this is to allow negative responses from the digital matched filter and measuring the time of the negative going zero crossing of the tone to establish timing.

It should be noted that while the technique just discussed is perhaps 50 percent less accurate than the ideal case it can give good accuracy and much better accuracy than FM subcarrier techniques. For $B = 60$ kHz and $P/N_o = 48$ dB Hz, the attainable precision is about 0.1 μs improvable by averaging several 30 ms measurements.

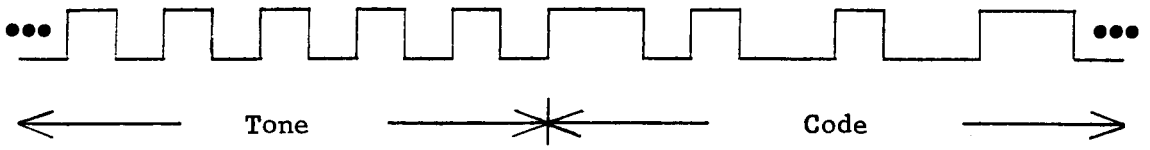

FIGURE 2a. DIFFERENTIALLY ENCODED

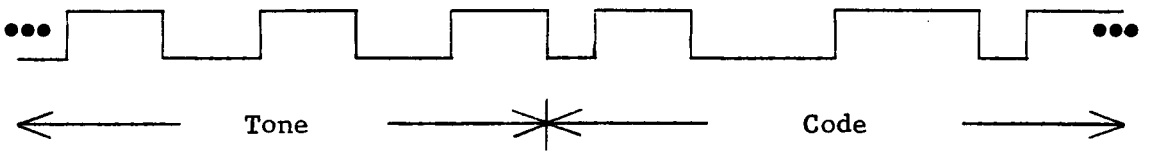

FIGURE 2b. PHASE VERSUS TIME, 180° PHASE SHIFTS

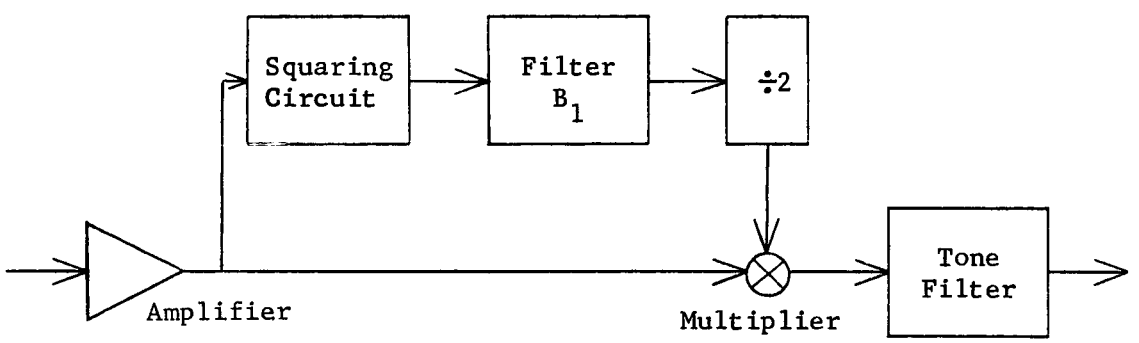

FIGURE 3a. DERIVED CARRIER DEMODULATOR FOR TONE-CODE

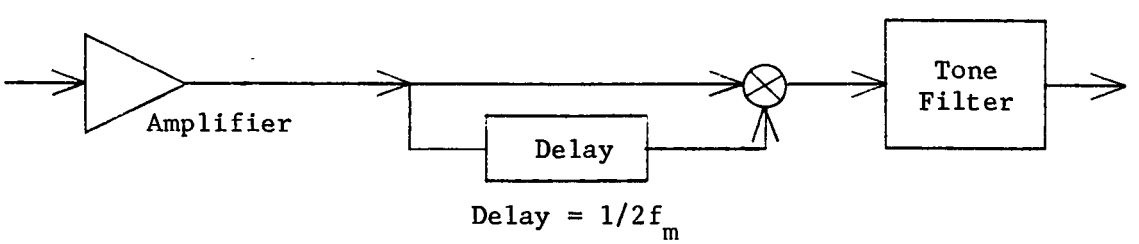

FIGURE 3b. DIFFERENTIAL DETECTOR FOR TONE-CODE

5.0 CONCLUSIONS

Based on the above analyses it appears that phase modulation techniques can give very good range measurement precision when used in the tone-code technique; much better than that possible with FM techniques. Some slight modification of the present circuitry is required because of polarity ambiguity. Also a somewhat more complicated demodulator, compared to the FM discriminator, is required.

6.0 REFERENCES

1. C. W. Helstrom, "Statistical Theory of Signal Detection", Pergamon Press, 1960. (p. 214)

2. E. J. Baghdady (ed.), "Lectures on Communication System Theory", McGraw-Hill, 1961. (pp. 529-540)

3. W. B. Davenport and W. H. Root, "Random Signals and Noise", McGraw-Hill, 1958. (p. 259)